NBSIR 87-3533(R)

Environmental Factors and Mechanisms Controlling Degradation of Tb(III) Chelates: Development of Effective New Tb Phosphors for Postage Stamp Use

E. J. Parks
R. A. Faltynek
F. E. Brinckman

U.S. DEPARTMENT OF COMMERCE
National Bureau of Standards
Institute for Materials Science
and Engineering
Ceramics Division
Gaithersburg, MD 20899

February 1987

Final Report

Issued June 1987

Prepared for
U.S. Postal Service
Research and Development Laboratories
Rockville, MD 20852

CONTENTS

ENVIRONMENTAL FACTORS AND MECHANISMS CONTROLLING DEGRADATION OF Tb(III) CHELATES: DEVELOPMENT OF EFFECTIVE NEW Tb PHOSPHORS FOR POSTAGE STAMP USE

1.0 INTRODUCTION

The United States Postal Service (USPS) operates a high speed mail handling system by which 40 to 50 billion stamped pieces of mail are faced and cancelled automatically each year. Stamp surfaces coated with a tagging phosphor are excited by UV light of a specific wavelength, and emit light of a given wavelength (500 -560 nm) and a minimum decay time (1.5 millisecond). At a speed of hundreds of feet per second, the stamp is scanned in turn by a source of exciting radiation (254 nm) and a phosphorescence detector, transferred to a canceller if phosphorescence specifications are met, or shunted aside if not. Cancellation diminishes the brightness so that a cancelled stamp may not be reused. A defective stamp, however, would have to be cancelled by hand.

Thus, effective tagging phosphors are the essential component of modern stamp coatings. Figure 1 is a schematic diagram showing the cross-section of a typical stamp in current use. The tagged coating consists of an organic varnish loaded with an inorganic phosphor; at present, typically zinc orthosilicate doped with manganese. Just below the coating lie multilayers of pigment (as many as seven) on a sheet of paper; adhesive gum coats the reverse side. The varnish coating (currently 0.0125 mm in thickness, or 0.5 mil) must be transparent to light of 254 nm as well as 500 - 600 nm. It is charged with a phosphor, currently $ZnSiO_4 \cdot Mn$. The concentration of the phosphor in a given varnish is empirically adjusted to obtain a given brightness.

1.1 Advantages and Disadvantages of the Zinc Phosphor

This compound ($ZnSiO_4 \cdot Mn$) displays an emission maximum near 526 nm, whether it is bonded to a ceramic plate [1] or, as shown in Figure 2, bonded to an experimental stamp paper (made by Harrison and Sons, Ltd., U.K.), or scanned as the pure powder; i.e., the emission maximum is not changed in the environment of the stamp coating, although the emission envelope appears to be. The compound has additional advantages. It is relatively inexpensive at the cost of $6.00 per pound, non toxic, and chemically stable [2].

The disadvantage is that the inorganic zincate is immiscible in organic carriers because the chemistry is such that little attractive force exists between the phosphor and the carrier [3], as illustrated in Figure 3. Consequently, the phosphor is easily rubbed off the surface of a stamp. Stamp abrasion during processing results in diminished stamp phosphorescence as well as excessive wear in automated processing and cancelling machinery. The need to hand cancel rejected items is an expensive consequence, having an estimated annual cost of $12 million. The National Bureau of Standards and USPS therefore began a collaborative effort to develop an alternative phosphor, or else a new tagging protocol, that would eliminate the combination of an organic carrier and an inorganic, immiscible phosphor. The available alternatives were to develop a suitable varnish-miscible phosphor and/or a water soluble phosphor.

1.2. Prior Research

Over one hundred organic phosphors had already been tested and found unsuitable [2] for varnished systems. It has long been known that terbium phosphoresces in the green region of the spectrum (500 - 560 nm) after excitation by UV light [4] and that the luminescence is enhanced by ligands other than simple inorganic anions. Accordingly, prior to investigations by NBS, USPS personnel initiated research into the use of terbium coordination complexes as candidate phosphors.

Complexes of terbium(III) with various 2,4-diones have been investigated for many years [5]. Therefore, tris(acetylacetato)terbium(III), $Tb(acac)_3$, initially seemed promising but either failed to display adequate brightness in the green region of the spectrum [6], or reportedly [2] failed to retain the initial brightness in a humid environment. The cost of terbium [approximately $1.00 per gram at present] is such that, to be competitive, a terbium complex used in only trace amounts (preferably less than 0.11 percent by weight as terbium) must produce a phosphorescence intensity equal to that of the current zinc phosphor used in concentrations between 10 percent and 50 percent by weight. Hence, the complex must display initial high quantum efficiency. It must also retain the initial high brightness under anticipated field conditions. Our search of the literature [6] suggested that terbium complexes could be tailored in molecular structure to combine high quantum efficiency with stability if sufficiently bulky chromogenic groups were bonded to the central metal to exclude quenching elements from its coordination sphere [7], i.e., to sequester or "encrypt" the metal.

1.3 Research Objectives.

This report describes the implementation of these molecular concepts over a three-year period, including an experimental plan designed originally to: (1) evaluate the candidate terbium phosphors originally considered by USPS [8]; (2) select candidate phosphors for experimental synthesis and testing; and (3) provide USPS with samples of candidate phosphors for field tests. Details of the initial plan are presented in a contract drawn up by NBS and USPS [8]. The objectives are summarized in a time-line (Figure 3) for parallel testing of the prior candidate phosphors and developing novel materials for USPS to evaluate in small quantities. During the second year of the research, however, one complex emerged as the most promising of all those tested or considered up to that time: the sodium salt of tris(2,6-dipicolinato)terbium(III), or $Na_3Tb(DPA)_3$. This phosphor combines favorable properties demonstrated in NBS and USPS laboratories: it is readily synthesized from water-soluble materials; it is water-soluble in concentrations up to 10 percent (w/v); it can be precipitated as a pure solid from chilled water; and the synthetic method can be used to prepare chelates of rare earths other than terbium. The aqueous solution is so miscible with most of the current organic varnishes that the mixtures are amorphous; or the dissolved phosphor can be applied directly to paper without using a varnish to produce a fine homogeneous coating dispersion (Figure 5). Whether it is used in water or varnish, the excited complex in trace concentrations emits phosphorescent light as bright as that of varnishes tagged with manganese-doped zinc orthosilicate in production runs. At these low concentrations, the terbium phosphor in varnish would be cost effective, considering only the purchase price of raw materials. Accordingly, USPS and NBS drew up amendments

to the original contract [9,10] for the development, pilot-scale production and testing of this complex. Moreover, because of USPS interests in developing advanced postage metering inks, also exploiting chemically tailored fluorescent "tags" for high-speed and high-resolution automated cancelling, NBS was asked to conduct parallel inaugural experiments on potential red-phosphors, i.e., new compatible europium complexes.

We have devoted considerable additional study to the direct application of the aqueous phosphor to paper surfaces (which would eliminate the need for organic varnishes) and particularly to the retention of phosphorescence in harsh aging environments. Since stamp papers are permeable to water vapor, and $Na_3Tb(DPA)_3$ is moderately soluble in water, the phosphor tends to migrate into the body of a stamp coated with the aqueous solution (and no varnish), dried, and exposed to an atmosphere of semitropical high humidity, (e.g., RH>60%). The loss of surface phosphor reduces surface phosphorescence. Thus, an engineering problem remains in the need to immobilize the phosphor through design of a physical or chemical barrier to migration, should USPS elect to discard stamp varnishes.

This final report describes in detail NBS laboratory experiments performed over a three-year period, the results, and recommendations for their future implementation by USPS in the improvement of its high-speed automated mail handling system. Much of the material included here has already been reported to USPS in monthly, quarterly and annual reports. It is restated in this final report in compliance with the terms of the contract [6].

2.0 MATERIALS, INSTRUMENTS, AND METHODS.

2.1. Analytical methods

2.1.1 Spectroscopy.

Phosphorescence measurements were obtained on a U.S. Postal Service Model 4A Phosphor Meter (NCR Postal Systems), calibrated prior to each use with a standard green phosphor [1]. Total luminescence and emission/excitation spectral data were acquired using a Zeiss Universal Microscope equipped with epifluorescence and computer controlled monochromator accessories, data being collected and processed using Zeiss software packages entitled λ-Scan and Manual Photometry Program. Electronic spectroscopy (UV-Vis) was performed on a Hitachi/Perkin-Elmer 330 instrument, using standard 10 mm pathlength quartz cuvettes to contain liquid samples or to support drawdowns of thin varnish films. Infrared spectroscopy was conducted on an Analect AQS-20 Fourier Transform instrument, using appropriate accessories that enabled interrogation of solid samples by diffuse reflectance, and paper surfaces or solutions by attentuated total reflectance. Analyses were also run on paper fibers and small solid aggregates using an Analect XAD microscope attachment that allowed transmission and reflectance FTIR measurements to be made on samples in the 30 - 100 μm size range. Manipulation and reduction of IR data were accomplished using standard Analect software (BIOS version 1.25 or 2.01) in conjunction with a MAP-66 central processing unit.

The single crystal X-ray structural analysis on $Na_3Tb(DPA)_3 \cdot 6H_2O$ was performed by Molecular Structure Corporation of College Station, Texas.

2.1.2. High Performance Liquid Chromatography (HPLC)

Microbore columns were employed (1.0 mm id x 15 cm) packed with particles of strong cation exchange (SCX) or octadecyl (C_{18}) substituted resins, averaging 5 μm in diameter. Effluent: sodium acetate in water (1×10^{-4} M), flowing at the rate of 50 μL min^{-1}. Samples were injected into the LC system by means of a syringe-loaded injection valve that incorporated a 1 μL sample loop (Rheodyne Model No. 7520, Cotati, CA), and transported by means of a ceramic-lined dual piston microbore HPLC pump (LKB Instruments, Bromma, Sweden). Teflon tubing was used to connect the column outlet to a special flow quartz microcell of square cross section (Figure 6).

The detector consisted of a Zeiss universal microscope (Carl Zeiss, West Germany), equipped for epifluorescence operation (schematic diagram shown in Figure 7). A high pressure mercury arc lamp provided UV radiation (254 nm), reflected to the object plane by a dichroic mirror, which also transmitted emission radiation from the excited terbium complex to the photometer for quantitation of emission intensity. A measuring aperture of 2.5 mm diameter was used, producing an image plane of 31.7 μm with a 40x objective lens. Flow injection analysis (FIA) was performed with the same system, with all tubing, injection valves and connectors in place, but without an HPLC column.

Typically, samples were prepared by adding volumetrically varied amounts of Na_2DPA to a constant volume of aqueous terbium nitrate. For a typical experiment, 15 individual samples were prepared containing 2.5×10^{-6} mole of terbium nitrate and sufficient Na_2DPA to obtain molar ratios ([DPA]:[Tb]) ranging from 0:1 to 15:1. Sufficient deionized water was added to make all 15 solutions of equal volume and equal terbium concentration. A 1-μL

injection of each sample contained 2.5 nanomoles of terbium, as the complex. Typically, europium solutions contained 12.5 μmole per injection.

2.1.2.1. Procedures.

For a given series of molar ratios of either [DPA]:[Tb] or [DPA]:[Eu], a series of injections followed a consecutive sequence from the lowest ratio (0:1) to the highest (15:1, for example). The luminescence of the eluent, measured as the photometer output, was sent to an A/D converter and recorded on a strip chart. Peaks were cut out of the paper chart manually and weighed; the weight of each peak was plotted against the molar ratio to show the generation of data illustrated in Figures 27-30, Section 3.13.

2.1.3. Elemental Analysis.

Specific element analysis was routinely performed by Schwarzkopf Microanalytical Laboratory, Woodside, New York.

2.2. Paper Substrate Preparation.

Paper substrates for phosphor testing were provided by USPS. Harrison and Sons, Ltd. of High Wycombe, U.K. produced three phosphor-tagged papers used in NBS studies: one coated with the inorganic phosphor $ZnSiO_4 \cdot Mn$ (3%), and two coated with 0.02% Tb phosphor employing NBS-supplied aqueous $Na_3Tb(DPA)_3$. One of the Tb papers was not inked, while the other was a series of multi-colored "Showboat" trading stamps. The remaining test papers were received containing no phosphor. Table 1 provides compositional information on the nine paper set. Three bear Bureau of Engraving and Printing (BEP)

designations (LP-46, LP-23 and LP-54), while six others were arbitrarily numbered 1 - 6 by NBS.

TABLE 1

Designation of USPS papers used in accelerated aging and luminescence studies

Number	Description
1	Non-filled; non-gummed; plain
2	Non-filled; 50:50 tapioca:vinyl alcohol gum; plain
3	Non-filled; gummed; multicolored "Experimental"
4	Clay-filled; gummed; inked "For Testing Purposes Only"
5	Clay-filled; non-gummed; plain
6	Clay-filled; tapioca-gummed; plain
LP-46	Non-filled; gummed; plain
LP-23	Clay-filled; gummed; plain
LP-54	Clay-filled; gummed; plain; plastic coated

Phosphor solutions or suspensions in water or varnish were applied to the appropriate papers and spread evenly over the surface to depths of 0.5 or 1.0 mil with drawdown bars (Gardner Instrument Co., Sarasota, Florida). Papers were then oven dried for 2 min at 100 ^{o}C, or, where applicable, cured to a tack-free state under 10-60 s irradiation from an unfiltered medium pressure mercury lamp (Hanovia Instruments, Florham Park, N.J.). Unusual sample preparations (for example, the double-coating strategy employing separate solutions of metal and ligand) are described in the appropriate sections of Chapter 3, Results.

2.3. Phosphor Evaluation in Service Environments.

A variety of aging conditions were invoked to establish the useful shelf life of phosphor-tagged stamp facsimiles. Samples were left in air-

conditioned laboratories (23 °C, 50% relative humidity) in the dark; exposed to ambient fluorescent lighting; or exposed to outdoor light filtered through north- and south-facing glass windows. Other tests were run outdoors under ambient daylight conditions in the spring and autumn, and under continuous exposure to round-the-clock 24 hour temperature and humidity fluctuations, both in Montgomery County, Maryland, and at ten USPS field offices in locations of maximum relative humidity. Phosphor-tagged stamps were subjected to intense UV irradiation (Osram 100-watt superpressure Hg Lamp), constant 100% relative humidity (Hotpack Humidity Chamber), ozone exposure, and prolonged storage at 0° - 4 °C. In most cases, the samples were suspended in the existing environment by means of clips equipped with Teflon spacers to avoid paper-to-metal contact. Window-exposed samples were taped directly to glass. Samples stored in desk drawers were laid flat in envelopes.

Variable humidity tests were conducted in a flow cell microchamber with quartz windows, designed and fabricated at NBS specifically for this project. Argon carrier gas, bubbled through deionized water or D_2O under appropriate wet bulb/dry bulb temperatures to deliver the desired relative humidity, was flowed over samples suspended in the microchamber. Total luminescence measurements were made periodically during the experiments on the in-place sample, using the Zeiss epifluorescence system described above.

2.4 Chemicals and synthesis.

2.4.1 Terbium complexes: overview.

Potential phosphors synthesized at NBS in the course of the project were prepared in open containers under ambient conditions, taking the normal safety precautions of hand protection and the use of fume hoods. Although

most of the reagents described in this report are believed to be non-toxic, it is prudent to treat them with respect. Some of the ligands employed, especially 2,6-dipicolinic acid (Figure 8), may be skin irritants. Concentrated solutions of sodium hydroxide (NaOH) and mineral acids are obvious health hazards. Organic solvents should always be handled in a fume hood and disposed of properly. Special precautions are required for the use of tetrahydrofuran (THF). This highly flammable and somewhat toxic solvent can dissolve most plastic gloves, including latex. Neoprene gloves appear to be safer. Observe the safety recommendations of the THF manufacturer with care. THF should not be exposed to the atmosphere for long periods of time since potentially explosive organic peroxides may accumulate in this organic solvent (and many others). If not used immediately, THF should be checked periodically for accumulation of potentially explosive peroxides. A convenient test method is described in the literature [11].

Analytical data on selected compounds are given in the Experimental Section of this report. Where appropriate, the chemical structure of a specific ligand is drawn after the method for synthesis of the complex.

2.4.1.1 Prior candidate ligands.

A variety of terbium coordination complexes containing pi-electron delocalized chelating ligands were synthesized at NBS. Two compounds, tris(acetylacetonato)terbium(III) [2] and bis(anthranilato)acetatoterbium(III) (Atlantic Chemicals, P.O. Box 218, Nutley, N.J. 07110) were supplied by USPS.

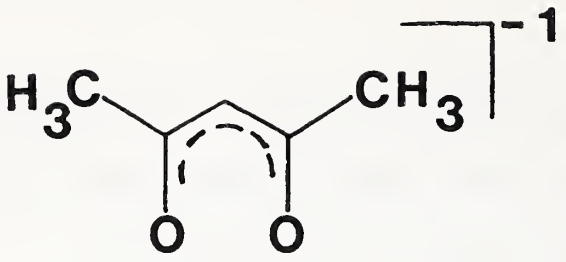

Acetylacetonate (acac)

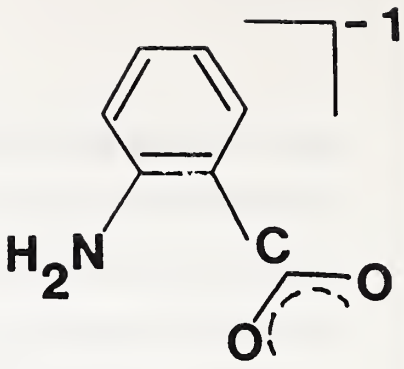

Anthranilate

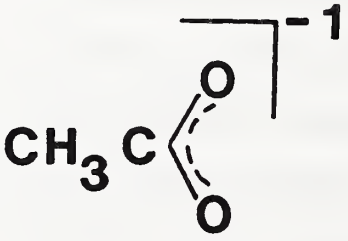

Acetate

2.4.1.2 Pivaloyltrifluoroacetone (PTA) Trioctylphosphine Oxide (TOPO) [12].

Transfer 1.0 mL of a $TbCl_3$ solution (Alfa Research AAS Standard 88110, containing 1095 μg of Tb per mL: another pure source of Tb may be substituted. Bring the acid solution to pH 5 with aqueous 1.0 N sodium hydroxide. Dilute to 10 mL with deionized water. Transfer 3 mL of the terbium solution to a Teflon-capped, Teflon test tube. Add 3 mL of 0.01 M TOPO in methycyclohexane (MCH), and add 3 mL of MCH solution containing 12 μL of 1,1,1-trifluoro-5,5-dimethyl-2,4-hexanedione (PTA). Shake manually for about 15 min and then allow the aqueous and organic phases to separate. Place a few drops of the organic phase on a microscope slide and observe with an excitation by light of 254 nm; measure the intensity of emitted luminescence at 545 nm.

For comparison, examine the luminescence of complexes prepared either without TOPO or without PTA, as well as anhydrous and hydrated $TbCl_3$

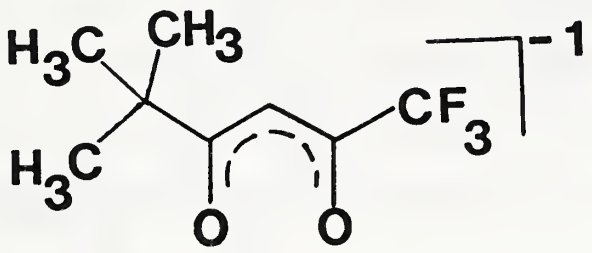

Pivaloyltrifluoroacetonate (PTA)

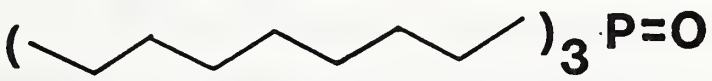

Trioctylphosphine Oxide (TOPO)

2.4.1.3. Aurintricarboxylic Acid (ATC) [13].

Dissolve 0.1940 g of ATC (4.6×10^{-3} mole) in 10 mL of absolute ethanol and add, dropwise, 1.0 mL of a $TbCl_3$ solution containing 0.01824 g of $TbCl_3$ (6.86×10^{-5} mole) to precipitate the complex. Let stand for several days. Filter through coarse filter paper, wash with ethanol, and examine for fluorescence after drying on a microscope slide.

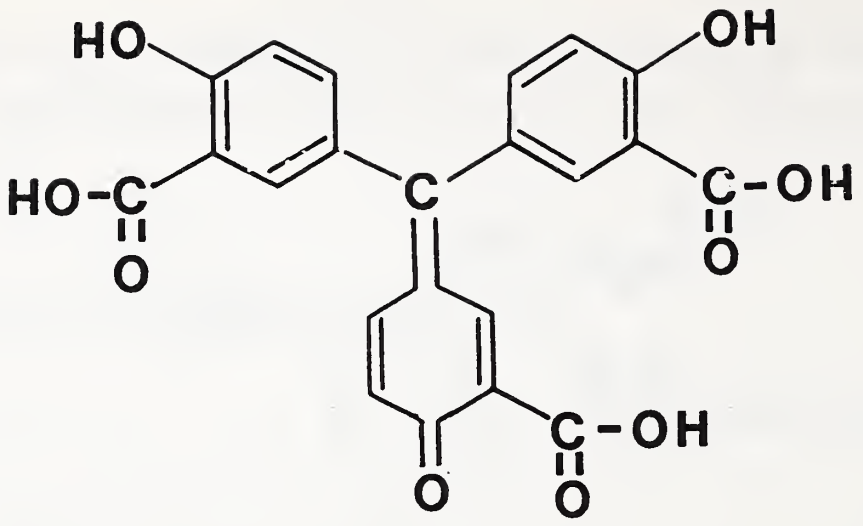

Aurintricarboxylic Acid (ATC)

2.4.1.4. Trifluoro-1-phenyl-1,3-butanedione(TFPB) with TOPO [6].

Dissolve 0.1910 g (0.494 mmole) of TFPB in 10 mL of MCH. Mix a 3-mL solution of TOPO and 3 mL of TFPB (0.2639 millimole) with 1.0 mL of $TbCl_3$ solution containing 0.01854 g (6.86×10^{-5} mole) in a Teflon-stoppered Teflon test tube, shaking 15 min. Measure on a microscope slide luminescence at 545 nm, with excitation at 254 nm.

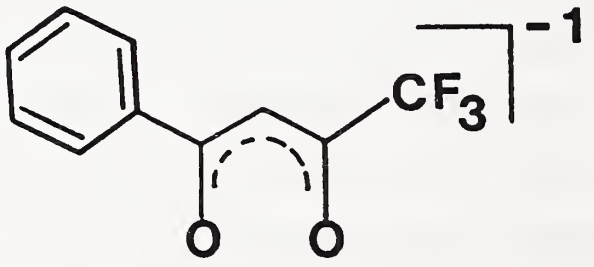

Trifluoro-1-phenyl-1,3-butanedionate (TFP

2.4.1.5. 1,1,1,5,5,5-Hexafluoroacetylacetone(HFA) with TOPO[14].

Dissolve 0.207 g of TOPO (0.535 mole) in 3 mL of MCH, and 0.2 mL (about 0.96 mmole) of HFA in the same solvent. Add 3 mL of each solution to 0.0686 mmole of $TbCl_3$ dissolved in 1 mL of water to give a molar ratio of HFA:$TbCl_3$ of about 5:1, with TOPO in large stoichiometric excess. Shake about 15 min, and place a drop of the organic phase on a microscope slide to examine fluorescence.

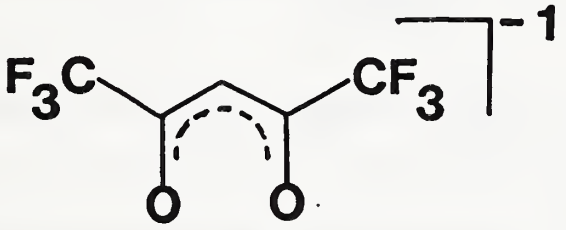

1,1,1,5,5,5-hexafluoroacetylacetonate (HFA)

2.4.1.6. Benzo-15-Crown-5 [15].

Dissolve 0.1354 g (0.5 mmole) of crown ether in 5 mL of acetone in a capped Teflon vial containng a magnetic bar coated with polyethylene. Add 0.0840 g (0.19 mmole) of $Tb(NO_3)\cdot 5H_2O$ in 5 mL of benzene. Stir at room temperature 60 min. Let stand at 4° C for three days or longer.

If precipitation does not occur, evaporate to three mL or less, add a few drops of hexane and permit the solution to stand for a prolonged period of time (e.g., two weeks). Deposit a drop of the solution on a microscope slide to determine luminescence in the usual manner.

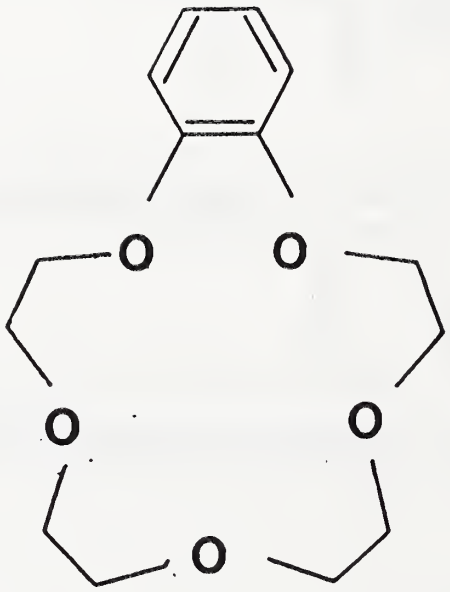

Benzo-15-crown-5

2.4.1.7 Poly(1-pyrazolyl)-Poly(1-imidazolyl)borate [16].

The ligands were prepared from sodium borohydride (Morton Thiokol Inc, Alfa Products Division; Danvers, MA) and pyrazole or imidazole (Aldrich Chemical Co, Milwaukee, WI) according to the method of Trofimenko [17]. As noted in the literature, the degree of substitution on boron during synthesis is temperature dependent, and three ligands of each type were made:

$$BH_4^- + x\ LH \xrightarrow{t} [H_{4-x}BL_x]^- + x/2\ H_2$$

(where LH = pyrazole or imidazole; t = 120 °C, x = 2; t = 180 °C, x = 3; t = 220 °C, x = 4). The B-N ligands thus obtained as sodium salts were very soluble in water and their aqueous solutions were used in subsequent reactions with terbium(III) nitrate: transfer to a small beaker containing a magnetic stirring bar, 10.0 mL of 0.10 M $Tb(NO_3)_3 \cdot 5H_2O$ (Morton Thiokol Inc, Alfa Products; Danvers, MA). Add dropwise 30.0 mL of 0.10 M $Na[H_{4-x}\ BL_x]$ while stirring the mixture. Hold the resulting slurry at 90°-95° for thirty min to form larger precipitate particles by digestion. Filter while still warm through a fritted disk, and wash the white solid with 3 x 20 mL of deionized water. Dry by suction in air.

The complex formed between sodium tris(1-pyrazobyl)borate and terbium nitrate has a complex stoichiometry that is approximated by $Tb_3[HB(1\text{-pyrazobyl})_3]_7$: Calculated (found): %C = 38.45 (37.71), %H = 3.59 (3.75), %N = 29.89 (28.91), %Tb = 24.23 (22.35).

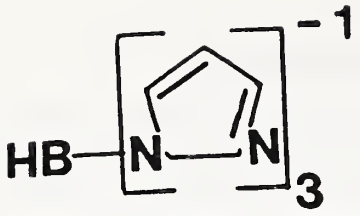

Tris(pyrazol-1-yl)borate

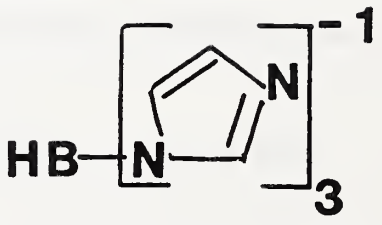

Tris(imidazol-1-yl)borate

2.4.1.8 Sodium salt of pyridine-2,6-dicarboxylic acid (DPA): $Na_3Tb(DPA)_3 \cdot 6H_2O$ [18].

Dissolve 3.2 g (19 mmole) of H_2DPA (Aldrich Chemical Co., Milwaukee, WI) in approximately 50 mL of 1.0 N sodium hydroxide, aqueous. Dilute with deionized water to about 95 mL. Neutralize with dilute acetic acid (1:100 glacial acetic acid:deionized water) and finally dilute to 100 mL with deionized water, to prepare solution A.

Dissolve 2.05 g (4.75 mmole) of $Tb(NO_3)_3 \cdot 5H_2O$ (hydrated terbium nitrate) in 50 mL of deionized water and dilute with 50 mL of deionized water to give solution B. Mix solutions A and B in equal proportions to obtain the phosphor $Na_3Tb(DPA)_3$ (aqueous). Check the pH of the solution and adjust with acid (HOAc or HNO_3) or base (NaOH) as necessary to a final pH between 6 and 8.

This process can be scaled up at least by a factor of 80 in terms of the mass of terbium(III) and DPA. We have routinely prepared enough of the aqueous phosphor *in situ* to yield 5-liter batches containing 1.12% concentrations of Tb (as the DPA complex) by the scaled-up procedure.

Pure solid $Na_3Tb(DPA)_3 \cdot 6H_2O$ can be obtained by cooling the 1.12% terbium solution to 0° - 4°C until precipitation occurs, decanting the supernatant liquid, and collecting the remaining solid on a fritted disk. Yields of the crystals so obtained are routinely 95-100%, a fact confirmed by observing only very weak green phosphorescence in the decantate. Elemental analysis of a typical solid batch established the presence of six molecules of water of hydration per terbium, corresponding to the formula given above:

$Na_3Tb(DPA)_3 \cdot 6H^2O = C_{21}H_{21}N_3Na_3O_{18}Tb$. Calculated (found):

%C = 30.34 (28.86); %H = 2.55 (2.40); %N = 5.05 (4.93); %Na = 8.30 (8.17); %O = 34.64 (37.29, by difference); and %Tb = 19.12 (18.35).

A sample of the hydrated phosphor was recrystallized from boiling deionized water and submitted to the Molecular Structure Corporation, College Station, Texas for single crystal x-ray structural analysis. The solid state structure is reproduced in Figures 9 and 10 and is discussed in detail below (RESULTS, Section 3.1.2).

2.4.1.9. Protonated form of $Na_3Tb(DPA)_3 \cdot 6H_2O$

The sodium salt described can be protonated by aqueous nitric acid, yielding a sodium-free form of the complex $Tb(HDPA)_3 \cdot 2H_2O$. Pass 1 mL of 1 M HNO_3 over each gram of $Na_3Tb(DPA)_3 \cdot 6H_2O$ on a fritted filter disk; wash with 3 x 1 mL/g of deionized water, followed by 3 x 1 mL/g of absolute ethanol.

Dry in a stream of nitrogen or argon at 60 °C. The complex analyzes as $Tb(HDPA)_3 \cdot 2H_2O$: Calculated (found): %C = 36.38 (36.10); %H = 2.33 (2.26); %N = 6.06 (6.07); %O = 32.31 (32.62), by difference; %Tb = 22.92 (22.95).

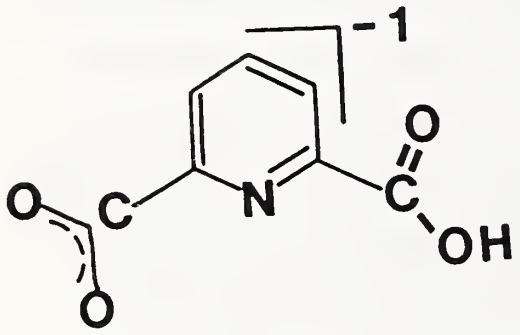

HDPA

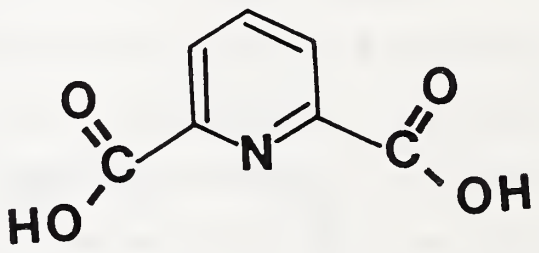

H_2DPA

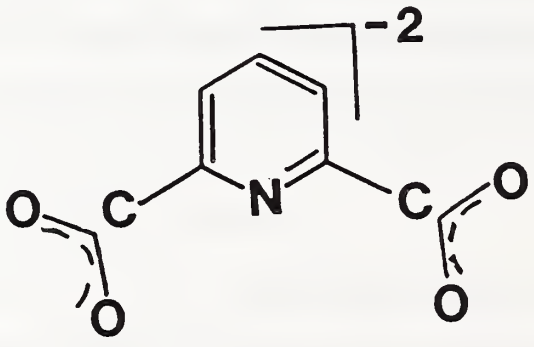

2,6-DPA

2.4.1.10. Preparation of Complex in Tetrahydrofuran.

A complex having unknown stoichiometry is prepared in tetrahydrofuran (THF). Add 3.2 g of DPA (19.1 millimoles) to 500 mL of THF, in which the acid is almost insoluble. Add approximately 50 mL of deionized water with swirling to dissolve all but a trace of DPA. Filter through coarse sintered glass, washing twice with about 5 mL of wet THF (10% H_2O). To the filtrate in an Erlenmeyer flask, add dropwise 2.05 g of $Tb(NO_3)_3 \cdot 5H_2O$ (6.1 millimole) dissolved in 5 to 10 mL of water. Let the mixture stand at least overnight to coagulate the colloidal suspension. Use a pipette to transfer the clear upper phase for filtration through a weighed, sintered glass crucible (medium porosity). When most of the clear solvent has been removed, wash the suspension with additional wet THF, mix the solvent and colloid, and again wait for separation. Repeat three times to remove all of the soluble, excess DPA. Finally, separate the complex by filtration on a coarse sintered glass grit or by ultracentrifugation, decanting supernatant fluids. For final drying, place in a desiccator and subject to partial vacuum overnight.

Elemental analysis indicates that the complex has the stoichiometry $C_{60}H_{81}N_8O_{48}Tb_6$. Calculated (found): %C = 27.3 (27.0); %H = 3.1 (3.1); %N = 4.2 (4.4); %O = 29.1 (29.0, by difference); and %Tb= 36.2 (36.3). This does not correspond to a simple empirical formula, but it is likely that the complex exists as a terbium-DPA cation/nitrate anion pair solvated with water and THF.

2.4.2. Europium Complexes.

In a manner similar to the procedures given for the terbium complexes in (2.4.1.7) and (2.4.1.8), above, the compounds $Eu[H_{4-x}BL_x]_z$ and $Na_3Eu(DPA)_3$

were made from $Eu(NO_3)_3 \cdot 5H_2O$ (Aldrich Chemical Co.) and the appropriate ligands.

2.4.3. Inorganic Complexes.

The insoluble inorganic phosphors zinc orthosilicate doped with manganese ($ZnSiO_4 \cdot Mn$), zinc sulfate doped with copper ($ZnS \cdot Cu$) and zinc oxide (ZnO) with an unknown dopant were supplied to NBS by Gerald Roberts of USPS.

2.5. Varnishes.

Varnish compositions used by BEP for various stamp applications were supplied to NBS by BEP via USPS. High solids versions of gravure vehicle IPI-4047 and varnish SVD-4057 were procured directly by Gerald Roberts of USPS from the manufacturers and supplied to NBS. Varnish compositions, where known, are given in Table 2.

TABLE 2

Description of Varnishes

BEP Designation	Ingredients (BEP)		Cobalt content (NBS) µg/g	Application
	Wt. %	Compound		
TG-20-T	8.4	Acryloid Polymer	018	Cottrell press
	39.2	Butyl carbitol		
	24.0	Hexylene glycol		
	15.0	Green phosphor		
	5.0	Santocel C		
	8.4	Ethyl cellulose		
TG-2407-RV	24	Acrylic Polymer	0.00	Intaglio, Rotogravure press
	18	Isopropanol		
	23	Water		
	15	Denatured Alcohol		
	20	Zinc silicate		
TG-45-T	60	Varnish formula UV 8	0.00	
	30	Green phosphor		
	5	Lo-Val 27		
	5	Hexylene glycol		

2.6. Microencapsulation of $Na_3Tb(DPA)_3 \cdot 6H_2O$.

Professor Curtis Thies of the Chemical Engineering Department, Washington University, St. Louis, MO., has carried out a microencapsulation procedure on small (1 - 10 m diameter) crystallites of $Na_3Tb(DPA)_3 \cdot 6H_2O$. The crystallites were prepared by rapidly introducing a supersaturated aqueous solution of the terbium salt (60 g in 50 mL of boiling H_2O) into a vigorously stirred 400 mL bath of either ethanol or THF at room temperature. The solids were collected by filtration or centrifugation, redispersed in toluene, and encapsulated with the chlorinated rubber Parlon S-20.

3.0 RESULTS

3.1 Molecular Structure of the Terbium-DPA Complex.

3.1.1 Overview.

Crystals of compound I were precipitated from neutral aqueous solution at 0° - 4°, and their elemental analysis corresponded to the empirical formula $Na_3Tb(DPA)_3 \cdot 6H_2O$ [Section 2.4.1.8]. Acidification and removal of sodium ions yielded Compound II, analyzing as $Tb(HDPA)_3 \cdot 2H_2O$. Compound III, obtained in colloidal form on mixing H_2DPA in wet THF with aqueous terbium nitrate (Section 2.4.1.10), yields percent composition values suggestive of $Tb(DPA)_2 \cdot H_2O$ stoichiometry, but charge balance dictates the presence of nitrate ions as well. The best empirical formula is $C_{60}H_{81}N_8O_{48}Tb_6$ which probably requires inclusion of water and THF molecules to account for the high hydrogen content. The x-ray spectrum failed to indicate a definite crystal structure for (III) [19].

The structural formula of 2,6-dipicolinic acid (H_2DPA) is shown in Figure 8. This compound slowly dissolves in aqueous sodium hydroxide. Addition of terbium nitrate results instantly in a phosphorescent complex, soluble at room temperature in concentrations below about 0.15 mole per liter. Any precipitate of (I) appearing at this or lower concentrations can be dissolved by warming the solution to 60°C for a few minutes. Pure crystals in nearly 100% yield are precipitated by cooling the solution to 4°C overnight.

3.1.2 X-Ray Analysis of $Na_3Tb(DPA)_3$

The solid state structure of $Na_3Tb(DPA)_3 \cdot 6H_2O$, as determined by single crystal x-ray diffraction is illustrated in Figures 9 and 10. A summation of

intramolecular bond lengths and angles is presented in Tables 3 and 4. Of special interest are several characteristic bond lengths. The nitrogen-to-terbium bonds average 2.501 Angstrom, and are equal within experimental error. The bonds between terbium and carboxylate oxygens show greater variation (2.399 to 2.462 Angstrom) than the experimental error of measurement (0.006 Angstrom) but the steric requirements (crowding) that might explain such differences are not apparent in a spatial model. The carbon-to-oxygen bonds of the carboxyl groups all are about 1.25 Angstroms in length and correspond more nearly to the carbonyl double bond (1.20 to 1.23 Angstroms) than to a C-O single bond (1.36 to 1.45 Angstroms), indicating the importance of the dative bond between nitrogen lone-pair electrons and terbium. If terbium-oxygen bonds were supplying the bulk of electron density to terbium, one would expect considerable single bond character in the carboxylate C-O-terbium assembly:

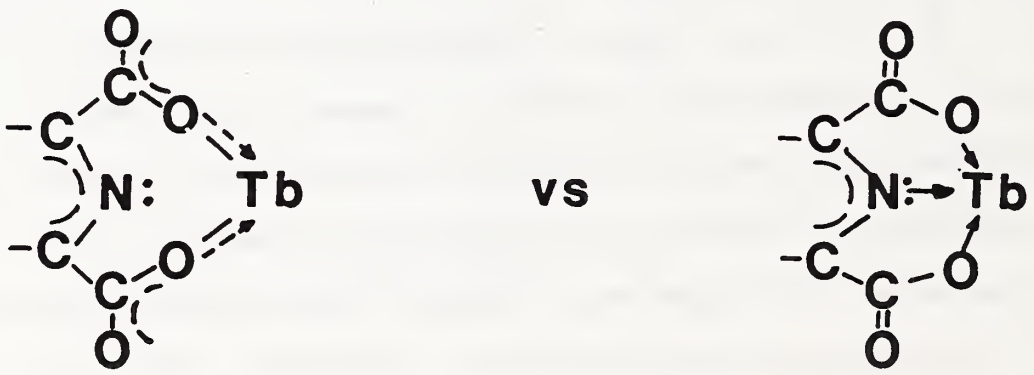

This direct inductive effect through nitrogen is also indicated by shortening of pyridine ring -C-N and -C-C bonds. For example, the C-N bond length in the DPA units is shorter at 1.34 Angstrom than expected for an aromatic nitrogen (1.429 Angstrom). Similarly the ring carbon-to-carbon double bonds are slightly shorter than those of typical aromatic bonds. The C_9-C_6 bond and the C_{11}-C_{12} bonds both are 1.37 Angstroms in length; the C_9-C_{10} bond 1.38

Table 3

Intramolecular Distances

atom	atom	distance	atom	atom	distance
TB1	O9	2.399(6)	NA3	O17	2.511(8)
TB1	O1	2.401(6)	NA3	O17	2.511(8)
TB1	O5	2.405(6)	NA4	O20	2.20(1)
TB1	O7	2.415(6)	NA4	O19	2.26(1)
TB1	O11	2.443(6)	NA4	O12	2.44(1)
TB1	O3	2.462(6)	NA4	O15	2.48(1)
TB1	N1	2.498(7)	NA4	O4	2.57(1)
TB1	N2	2.500(7)	O1	C6	1.25(1)
TB1	N3	2.506(7)	O2	C6	1.25(1)
NA1	O13	2.434(8)	O3	C7	1.26(1)
NA1	O13	2.434(8)	O4	C7	1.24(1)
NA1	O14	2.450(7)	O5	C13	1.29(1)
NA1	O14	2.450(7)	O6	C13	1.23(1)
NA1	O2	2.493(8)	O7	C14	1.30(1)
NA1	O2	2.493(8)	O8	C14	1.24(1)
NA2	O15	2.278(8)	O9	C20	1.29(1)
NA2	O16	2.351(8)	O10	C20	1.24(1)
NA2	O10	2.416(9)	O11	C21	1.28(1)
NA2	O8	2.459(8)	O12	C21	1.24(1)
NA2	O14	2.474(9)	N1	C5	1.33(1)
NA2	O17	2.53(1)	N1	C1	1.35(1)
NA2	NA4	3.67(1)	N2	C8	1.34(1)
NA3	O18	2.417(9)	N2	C12	1.34(1)
NA3	O18	2.417(9)	N3	C15	1.33(1)
NA3	O6	2.453(7)	N3	C19	1.34(1)
NA3	O6	2.453(7)	C1	C2	1.35(1)

Distances are in angstroms. Estimated standard deviations in the least significant figure are given in parentheses.

Intramolecular Distances (cont)

atom	atom	distance	atom	atom	distance
C1	C6	1.54(1)			
C2	H1	0.952			
C2	C3	1.41(2)			
C3	H2	0.950			
C3	C4	1.37(2)			
C4	H3	0.949			
C4	C5	1.36(1)			
C5	C7	1.54(1)			
C8	C9	1.37(1)			
C8	C13	1.52(1)			
C9	H4	0.951			
C9	C10	1.38(1)			
C10	H5	0.950			
C10	C11	1.39(2)			
C11	H6	0.946			
C11	C12	1.37(1)			
C12	C14	1.51(1)			
C15	C16	1.36(1)			
C15	C20	1.51(1)			
C16	H7	0.947			
C16	C17	1.39(2)			
C17	H8	0.953			
C17	C18	1.38(2)			
C18	H9	0.948			
C18	C19	1.36(1)			
C19	C21	1.52(1)			

Distances are in angstroms. Estimated standard deviations in the least significant figure are given in parentheses.

Table 4

Intramolecular Bond Angles

atom	atom	atom	angle	atom	atom	atom	angle
O9	TB1	O1	90.5(2)	O11	TB1	O3	150.9(2)
O9	TB1	O5	76.6(2)	O11	TB1	N1	134.2(2)
O9	TB1	O7	148.4(2)	O11	TB1	N2	76.3(2)
O9	TB1	O11	127.2(2)	O11	TB1	N3	63.6(2)
O9	TB1	O3	75.6(2)	O3	TB1	N1	63.0(2)
O9	TB1	N1	75.4(2)	O3	TB1	N2	74.6(2)
O9	TB1	N2	135.3(2)	O3	TB1	N3	133.6(2)
O9	TB1	N3	63.7(2)	N1	TB1	N2	117.7(2)
O1	TB1	O5	150.1(2)	N1	TB1	N3	122.0(2)
O1	TB1	O7	74.4(2)	N2	TB1	N3	120.3(2)
O1	TB1	O11	74.9(2)	O13	NA1	O13	180.00
O1	TB1	O3	127.7(2)	O13	NA1	O14	80.0(2)
O1	TB1	N1	64.7(2)	O13	NA1	O14	100.0(2)
O1	TB1	N2	134.2(2)	O13	NA1	O2	92.0(3)
O1	TB1	N3	75.9(2)	O13	NA1	O2	88.0(3)
O5	TB1	O7	128.7(2)	O13	NA1	O14	100.0(2)
O5	TB1	O11	91.5(2)	O13	NA1	O14	80.0(2)
O5	TB1	O3	75.5(2)	O13	NA1	O2	88.0(3)
O5	TB1	N1	134.3(2)	O13	NA1	O2	92.0(3)
O5	TB1	N2	64.2(2)	O14	NA1	O14	180(2)
O5	TB1	N3	74.2(2)	O14	NA1	O2	86.3(2)
O7	TB1	O11	76.2(2)	O14	NA1	O2	93.7(2)
O7	TB1	O3	91.6(2)	O14	NA1	O2	93.7(2)
O7	TB1	N1	73.0(2)	O14	NA1	O2	86.3(2)
O7	TB1	N2	64.5(2)	O2	NA1	O2	180(2)
O7	TB1	N3	134.8(2)	O15	NA2	O16	175.5(4)

Angles are in degrees. Estimated standard deviations in the least significant figure are given in parentheses.

Intramolecular Bond Angles (cont)

atom	atom	atom	angle	atom	atom	atom	angle
O15	NA2	O10	86.8(3)	O18	NA3	O6	81.2(3)
O15	NA2	O8	91.9(3)	O18	NA3	O17	93.5(3)
O15	NA2	O14	87.0(3)	O18	NA3	O17	86.5(3)
O15	NA2	O17	88.5(3)	O6	NA3	O6	180.00
O15	NA2	NA4	41.6(2)	O6	NA3	O17	88.0(2)
O16	NA2	O10	89.9(3)	O6	NA3	O17	92.0(2)
O16	NA2	O8	91.6(3)	O6	NA3	O17	92.0(2)
O16	NA2	O14	96.0(3)	O6	NA3	O17	88.0(2)
O16	NA2	O17	88.4(3)	O17	NA3	O17	180.00
O16	NA2	NA4	136.2(3)	O20	NA4	O19	173.3(5)
O10	NA2	O8	175.3(3)	O20	NA4	O12	81.5(4)
O10	NA2	O14	87.7(3)	O20	NA4	O15	103.1(4)
O10	NA2	O17	89.4(3)	O20	NA4	O4	97.1(4)
O10	NA2	NA4	48.3(2)	O20	NA4	NA2	79.3(3)
O8	NA2	O14	87.8(3)	O19	NA4	O12	103.9(5)
O8	NA2	O17	95.1(3)	O19	NA4	O15	81.7(4)
O8	NA2	NA4	129.0(2)	O19	NA4	O4	78.3(4)
O14	NA2	O17	174.7(3)	O19	NA4	NA2	102.6(4)
O14	NA2	NA4	73.4(2)	O12	NA4	O15	82.1(3)
O17	NA2	NA4	101.4(3)	O12	NA4	O4	99.0(4)
O18	NA3	O18	180(2)	O12	NA4	NA2	106.9(3)
O18	NA3	O6	81.2(3)	O15	NA4	O4	159.7(4)
O18	NA3	O6	98.8(3)	O15	NA4	NA2	37.6(2)
O18	NA3	O17	86.5(3)	O4	NA4	NA2	152.9(3)
O18	NA3	O17	93.5(3)	C6	O1	TB1	123.7(6)
O18	NA3	O6	98.8(3)	C6	O2	NA1	115.3(7)

Angles are in degrees. Estimated standard deviations in the least significant figure are given in parentheses.

Intramolecular Bond Angles (cont)

atom	atom	atom	angle	atom	atom	atom	angle
C7	O3	TB1	126.2(6)	H1	C2	C3	120.98
C7	O4	NA4	161.4(8)	C1	C2	C3	118(1)
C13	O5	TB1	125.3(6)	H2	C3	C4	120.15
C13	O6	NA3	121.9(7)	H2	C3	C2	120.55
C14	O7	TB1	124.2(6)	C4	C3	C2	119(1)
C14	O8	NA2	108.9(6)	H3	C4	C5	121.02
C20	O9	TB1	125.5(6)	H3	C4	C3	121.11
C20	O10	NA2	115.2(7)	C5	C4	C3	118(1)
C21	O11	TB1	125.2(6)	N1	C5	C4	124(1)
C21	O12	NA4	129.9(7)	N1	C5	C7	113.3(8)
NA1	O14	NA2	125.5(3)	C4	C5	C7	122(1)
NA2	O15	NA4	100.8(3)	O1	C6	O2	126(1)
NA3	O17	NA2	128.4(3)	O1	C6	C1	117(1)
C5	N1	C1	117.2(8)	O2	C6	C1	117(1)
C5	N1	TB1	122.7(6)	O4	C7	O3	127(1)
C1	N1	TB1	120.2(6)	O4	C7	C5	118(1)
C8	N2	C12	119.2(8)	O3	C7	C5	114.6(9)
C8	N2	TB1	120.3(6)	N2	C8	C9	122.0(9)
C12	N2	TB1	120.5(6)	N2	C8	C13	114.8(8)
C15	N3	C19	117.6(7)	C9	C8	C13	123(1)
C15	N3	TB1	120.8(6)	H4	C9	C8	120.78
C19	N3	TB1	121.6(6)	H4	C9	C10	120.51
N1	C1	C2	124(1)	C8	C9	C10	119(1)
N1	C1	C6	112.1(8)	H5	C10	C9	120.25
C2	C1	C6	124(1)	H5	C10	C11	120.43
H1	C2	C1	121.20	C9	C10	C11	119(1)

Angles are in degrees. Estimated standard deviations in the least significant figure are given in parentheses.

Intramolecular Bond Angles (cont)

atom	atom	atom	angle	atom	atom	atom	angle
H6	C11	C12	120.97	C18	C19	C21	123(1)
H6	C11	C10	120.83	O10	C20	O9	126(1)
C12	C11	C10	118(1)	O10	C20	C15	120(1)
N2	C12	C11	122.5(9)	O9	C20	C15	114.6(9)
N2	C12	C14	114.5(8)	O12	C21	O11	126(1)
C11	C12	C14	123.0(9)	O12	C21	C19	118.9(9)
O6	C13	O5	125(1)	O11	C21	C19	114.9(9)
O6	C13	C8	121(1)				
O5	C13	C8	114.1(9)				
O8	C14	O7	125(1)				
O8	C14	C12	120(1)				
O7	C14	C12	115.2(8)				
N3	C15	C16	124.0(9)				
N3	C15	C20	113.8(8)				
C16	C15	C20	122.3(9)				
H7	C16	C15	120.90				
H7	C16	C17	121.41				
C15	C16	C17	118(1)				
H8	C17	C18	120.47				
H8	C17	C16	120.51				
C18	C17	C16	119(1)				
H9	C18	C19	120.51				
H9	C18	C17	120.59				
C19	C18	C17	119(1)				
N3	C19	C18	122.9(9)				
N3	C19	C21	113.8(8)				

Angles are in degrees. Estimated standard deviations in the least significant figure are given in parentheses.

Angstrom and the C_{10}-C_{11} bond 1.39 Angstroms compared to the aromatic 1.395 Angstrom bond length. The x-ray results show some disorder among the waters of hydration in the unit cell. This is probably due to dehydration of the crystal during handling and data acquisition. Earlier structural work by Albertson [20] on similar systems included submerging the crystal in water during the x-ray scan to prevent effluorescence.

3.1.3. FTIR spectra.

Figures 11 through 14 represent FTIR spectra of H_2DPA, $Na_2(2,6\text{-DPA})$, $Na_3Tb(2,6\text{-DPA})_3$, and $Tb(2,6\text{-HDPA})_3$. The band assignments refer to earlier studies of picolinic acid [21,22], dipicolinic acid and calcium salts of the latter [23].

3.1.3.1 H_2DPA.

In the spectral region depicted (between 1800 and 600 cm^{-1}) are the following bands: 6 -CH bending bands between 1260 and 760 cm^{-1}; 2 -C=O bands at 1710 and 1700 cm^{-1}; 2 -C-O bending bands (1340 - 1320 cm^{-1}); 2 narrow -OH bands at 1430 and 1387 cm^{-1}; a broad -OH band between 1000 and 900 cm^{-1}; a -C-COOH band at 890 cm^{-1}; 2 -OCO bands between 715 and 680 cm^{-1}; and six ring bands at 1580, 1478, 1470, 1280, 1100, and 1020 cm^{-1}.

Intramolecular hydrogen bonding may occur between the aromatic nitrogen and one carboxylic acid group on 2,6-DPA (Figure 9), while one or possibly both carboxyl groups also participate in intermolecular bonding to give di- or oligomers; the pure acid is not readily soluble in water. Thus, we assign the two peaks at 1710 and 1700 cm^{-1} to two carboxyl carbonyls having different molecular environments.

3.1.3.2. Na_2DPA.

Neutralization of H_2DPA converts the dicarboxylic acid to its sodium salt. The strong peaks in the region of 1710 and 1700 cm^{-1} are shifted to lower frequencies; one peak of lower intensity at 1680 cm^{-1} may be attributed to the undissociated salt, while a strong new peak at 1630 cm^{-1} may be attributed to dissociated O-C=O stretching vibrations. A strong peak observed at 1580 cm^{-1} for both H_2DPA and the sodium salt, may be attributed to a ring vibration [21]. Out-of-plane ring vibrations at 478-1470 cm^{-1}, in the spectrum of the acid, experience a red shift to 1461- 1450 cm^{-1} in the salt. The spectrum of the salt differs most markedly from that of acid in the region between 1400 and 1280 cm^{-1}. With neutralization of the acid, a shoulder at 1380 cm^{-1} disappears. Two narrow, poorly resolved peaks at 1390 and 1365 cm^{-1}, and a third narrow peak of medium intensity at 1295 cm^{-1} take the place of strong, broad peaks in the spectrum of 2,6-DPA in the region of 1380 cm^{-1} (shoulder), 1345, 1325, and 1305 cm^{-1}. Near 1290 cm^{-1} is a strong peak, common to both spectra, assigned to a ring vibration [22]. The essential disappearance of a strong peak at 1310 cm^{-1} must be attributed to effects of substituting sodium for proton on the hydroxyl moiety of the carboxylic acids, owing to loss of in-plane -OH vibrations.

The major difference between the two spectra in frequencies below 1200 cm^{-1} lies in a broad band in the former between 1000 and 900 cm^{-1}, which is entirely absent from the latter, presumably due to the loss of out-of-plane bending vibrations [23].

3.1.3.3. $Na_3Tb(DPA)_3 \cdot 6H_2O$.

As expected, there is little difference between the spectrum of this complex and that of the sodium salt (Na_2DPA) in the region between 1500 and 600 cm^{-1}, and both materials manifest strong absorbance between 1600 and 1500 cm^{-1}, owing to ring vibrations. The second strong peak near 1631 cm^{-1} in both spectra implies no change in structure of the group, but there is a third peak at 1675 cm^{-1} in the spectrum of the salt which is absent from that of the complex, strongly implying that the carboxylic acid groups of the complex are equivalent to each other but exist in a different bonding situation from that of the two carboxyls of the sodium salt. These inferences are entirely consistent with the X-ray data cited above. The nature of the bond between sodium and the complex is not yet precisely defined, suggesting the structural formula presented in Figure 10.

Thus the X-ray and FTIR spectra are complementary in supporting the chemical structural formula of the complex that is indicated in Figure 10, although the precise location of the sodium is not defined by either technique, due, in part, to disordering of H_2O in the solid state X-ray sample.

3.1.3.4. $Tb(HDPA)_3 \cdot 2H_2O$.

Washing the sodium salt of the complex with dilute nitric acid (10% w/v) followed by deionized water gave a sodium-free complex having the empirical formula indicated above. Interesting changes in the spectrum result, apart from those expected in the frequencies below 1500 cm^{-1} which are attributable to the reappearance of hydroxyl groups in the complex. Comparing

this spectrum to that of $Na_3Tb(DPA)_3 \cdot 6H_2O$, a weak shoulder appears between 1780 and about 1720 cm^{-1}. Lautie et al. [21] have observed a weak absorbance in the spectrum of pyridine carboxylic acid which they assign to -C=O stretch in undissociated carboxylic acid groups which can and do form intramolecular hydrogen bonds with the aromatic nitrogen. The slight increase in the frequency that we observe in the sodium-free complex may be explained by the absence of a stabilizing intramolecular hydrogen bond. The two intense peaks at lower frequencies (1690 and 1660 cm^{-1}) we attribute respectively to out-of-plane bending of two resonating but non-equivalent bonds between terbium and the carboxylic acids; i.e., O=C-O--Tb, and HO-C=O--Tb.

3.1.4 Ultraviolet, Emission, and Excitation Spectroscopy.

Ultraviolet spectra of protonated 2,6-DPA and of $Na_3Tb(DPA)_3$ in aqueous solution are depicted in Figure 15. The peak at 268 nm for the acid may be shifted in the complex to 270 nm, but the absorption is too broad for the shift to be diagnostic of changes in the molecular environment of the chromophore. Molar absorptivities for the protonated ligand and complex are similar (ca. 4200 L $mole^{-1}$ cm^{-1}), and in good agreement with the literature [33].

Emission spectra of solid $Na_3Tb(DPA)_3 \cdot 6H_2O$ and the complex in aqueous solution are illustrated in Figure 16 for λ_{exc} = 254 nm. The excitation spectrum for $Na_3Tb(DPA)_{3(aq)}$ is shown in Figure 17 for λ_{em} = 543 nm. The emission spectra are identical in both phases, indicating that no changes in coordination number or geometry around the terbium center occur on dissolution. An energy level diagram for Tb^{+3} in a silicate glass is included in Figure 16 for band correlation. The excitation spectrum, which is

uncorrected for lamp response, suggests that irradiation at longer wavelengths than 254 nm may enhance phosphorescence output. It is possible that the optics of the Zeiss microscope system greatly attenuate the photon flux at 254 nm, giving rise to the comparatively weak emission stimulated at this wavelength. Other evidence, however, is supportive of the non-optimal nature of 254 nm excitation: (1) an excitation spectrum of aqueous $Na_3Tb(DPA)_3$ obtained on a Farrand Optical Company, Inc. fluorimeter, equipped with a xenon lamp source, was essentially identical to the results in Figure 17; i.e., very little intensity at 254 nm, and λ_{max} in the vicinity of 300 nm. (2) Literature reports on emission/excitation spectra of similar terbium complexes invariably rely on excitation wavelengths longer than 254 nm. For example, the emission at 545 nm in Tb^{+3} complexes with 5'-guanosine monophosphate [34], porcine pancreatic elastase [35], porcine trypsin [36], and uridine [37] results from excitation at 290 nm, 280 nm, 265 nm, and 298 nm respectively. A definitive answer to the question of optimal excitation wavelength must necessarily await data from Zeiss on the photon flux reaching the sample at specific wavelengths between 254 and 400 nm.

Emission from terbium complexes exhibits sufficiently long lifetime (in the ms rather than ns range) to implicate triplet state involvement [24]. It is well-documented that the energetics of terbium chelate complexes also support emission from a metal triplet state [25]. Since virtually no detectable emission results from $Tb(NO_3)_3$ or $TbCl_3$ under our experimental conditions, it is likely that the DPA ligand absorbs near UV radiation and effectively transfers energy to a terbium triplet state via rapid intersystem crossing (ligand to metal charge transfer). Another component of triplet state population may be due to direct ground state singlet → triplet

excitation in the complex. Forbidden transitions of this type are commonly observed in compounds of the heavier elements; for example, the photoinertness of (arene)$W(CO)_3$ complexes compared to their Cr analogues has been attributed to a non-labilizing singlet triplet absorption that is weakly allowed in the former group [26].

3.2. Resistance of Crystals to Quenching in Humid Air.

3.2.1 $Na_3Tb(DPA)_3 \cdot 6H_2O$.

Molecules of water coordinated to terbium induce radiationless quenching of the excited metal; anhydrous terbium chloride, for example, is strongly luminescent, whereas the hydrated complex is essentially non-luminescent [6]. Accordingly, it was necessary to determine whether (1) the bulky aromatic ligands of DPA would exclude water from the coordination sphere of the metal or (2) suffer hydrolytic dissociation under ambient conditions, and/or high humidity, since stamp phosphors may be exposed to environmental high humidities for long periods of time.

Crystals of $Na_3Tb(DPA)_3 \cdot 6H_2O$ were placed in the depression of a glass microscope slide and stored in a chamber at 95 to 100% relative humidity. Measurements of total luminescence were taken for a period of one week and the sample was then retained undisturbed in this environment for eight months, subjectively noting from time to time any apparent diminution of luminescence under a handheld ultraviolet lamp. No decrease in luminescence occurred during the initial seven-day period (Table 5), indicating that coordination of water with terbium did not occur. A final measurement of total luminescence after eight months confirmed the 100% retention of the

initial brightness. While these data are not surprising for a phosphor that is prepared in water, the verification of environmental stability is of major importance for application of the phosphor and diagnosis of mechanisms accounting for losses of phosphorescence on stamp surfaces (Section 3.19.1).

TABLE 5

Aging of $Na_3Tb(DPA)_3 \cdot 6H_2O$ crystals at 95-100 % R.H. and 27 °C

Time (days)	EMU (mV)*
0	3460
1	3797
2	3867
3	3574
7	4047

* Average of 4 measurements

3.2.2. Other terbium chelates.

Complexes of terbium with beta-diketonates are far more susceptible to luminescence loss under humid conditions than the tris-DPA complex. Table 6 shows the effect of high atmospheric humidity on crystals of tris(acetylacetonato)-terbium(III) [$Tb(AcAc)_3$], and acetatobis(anthranilato)-terbium(III) ($TbAn_2Ac$). $Tb(AcAc)_3$ loses 40% of its initial luminescence in six days and 56% in 37 days; $Tb(An_2Ac)$ loses 48% in 6 days. Anhydrous $TbCl_3$ is a much brighter luminophor (2810 EMI Units) than hydrated $TbCl_3 \cdot H_2O$. The instrument was calibrated against a standard material (microbeads coated with Tb_2O_3, or a ceramic plate coated with Mn-doped zinc orthosilicate) to maintain comparability during a given series of measurements over any period of time.

TABLE 6

Changes in luminescence with time at high relative humidity and 31 °C

TIME	LUMINOPHOR	
(Hours)	$Tb(AcAc)_3$	$Tb(An_2Ac)$
0	3300	1860
2.5	2407	1180
19	2987	977
43	2000	957
263	1480	637

3.3. Solubility of $Na_3Tb(DPA)_3 \cdot 6H_2O$.

3.3.1 In Water.

The preparation of the complex in water is described above (Section 2.4.1.8). With a molar excess of Na_2DPA (greater than 3:1) at pH of 7.3, this complex remains in aqueous solution at room temperature until the approximate saturation point is reached: 1.9% terbium (w/v), or about 0.12 mole per liter. If the complex is prepared with 1.12% terbium (0.07 mole per liter) and a stoichiometric excess of DPA, precipitation usually is not observed on standing for months at room temperature. Cooling at 4 °C overnight effects precipitation of the complex as pure crystals which can be redissolved by warming the solution to 50 or 60 °C for a few minutes. In one instance, nucleation did occur at room temperature in a solution of this concentration. Again, however, the crystals redissolved on warming and did not reprecipitate at room temperature.

3.3.2. In Organic Solvents.

The complex is insoluble in common organic solvents at room temperature. Studies performed by an outside laboratory for USPS [19] indicated crystal insolubility in: pyridine, carbon tetrachloride, chloroform, acetone, methanol, toluene, tetrahydrofuran, dimethylformamide, n-butanol, and formamide.

With the exception of formamide, these conclusions are consistent with our reported results [6]. However, the crystals dissolve (10%, weight to volume (w/v)) in formamide warmed to 60°C and remain dissolved when the solution is cooled to room temperature. Diluting one part of the formamide solution with one part of methanol or ethanol does not precipitate the crystals, although neither 50:50 mixture is capable of dissolving the crystals even on warming. Such research with mixed solvents was designed to improve the miscibility with varnishes but not pursued at length inasmuch as current NBS/USPS interest lies primarily in properties of the aqueous solution and the pure crystals. The organic solutions are highly luminescent, but again were not studied as extensively as aqueous solutions.

3.4 Properties of $Na_3Tb(DPA)_3$ in aqueous solution

3.4.1 Effects of pH.

The preparation of the phosphor uses a strong base (e.g. sodium hydroxide) to solubilize H_2DPA. Since a slight excess of NaOH would strongly affect the solution pH, we determined the effects of pH on the phosphorescence of stamp papers coated by means of the aqueous drawdown procedure (Section 2.2), and measured with a USPS phosphormeter (Section 2.1.1). The phosphorescence of aqueous mixtures of Na_2(2,6-DPA) and $Tb(NO_3)_3$ in the molar ratios of 2:1, and 3:1, and 4:1 is unaffected by pH in the range between 6.0 and 10.0 (Table 7). Acidification to a pH below 5.0 abruptly cuts back the intensity of the measured phosphorescence in all three cases. Acid hydrolysis causing partial decomposition of the complex is the presumed mechanism. In the manufacture and utilization of the complex, the pH must therefore be maintained between 6.0 and 10.0 to optimize phosphorescence. A pH of 7.0 to 7.5 is recommended to avoid corrosion problems that might be induced by a more strongly alkaline medium.

TABLE 7

Effects of pH on the phosphorescence of paper coated with aqueous mixtures of DPA and Tb.

Molar Ratio					
2:1		3:1		4:1	
pH	PMU	pH	PMU	pH	PMU
4.5	28	4.6	23	4.6	61
5.8	43	5.1	54	6.0	71
6.8	41	7.3	54	6.9	70
8.05	39	8.0	52	7.8	65
9.05	41	9.3	54	9.2	71

3.4.2. Effects of [DPA]:[Tb] Molar Ratios.

The correlation of increasing phosphorescence with an increasing molecular ratio of Na_2DPA to terbium is economically important since terbium is much more expensive (at a cost of $150 to $250 per mole [27,28]) than 2,6-DPA [at a cost of $37 per mole [29] for laboratory scale (500 g) quantities]. NMR spectra [30] indicate that complexes of different structure and lower luminescence are formed in aqueous media at the lower DPA:Tb molar ratios. We have extended the previous range of study to develop correlations of luminescence and ratios in several media to select conditions of optimal cost effectiveness in the actual processing medium; i.e., added directly to paper by drawdown, mixed into varnish (in the original aqueous medium) or isolated by high performance liquid chromatography (HPLC).

With increasing ratios of DPA to Tb, the relative luminescence of aqueous mixtures measured in a static mode (in the cavity of a microscope slide) manifests a sharp maximum at the molar ratio of 3:1 with terbiuum concentrations of 8.33×10^{-5} mole l^{-1} or greater (Figure 18). If the respective concentrations are increased by one or two orders of magnitude, the luminescence of the solution drops precipitously as soon as the molar ratio exceeds 3:1.

We observe a dense, flocculent luminescent precipitate when the molar ratio is lower than 2.75 to 1; the supernatant fluid also is strongly luminescent. The precipitate is solublized, or none is formed, when the ratio is increased to 3:1 or higher. Its formation at low ratios is strong evidence of extended intermolecular bonding, not compatible with the structure of the aqueous 3:1 complex. The decrease in luminescence with increasing ratios of

DPA:Tb (above 3:1) suggests the formation of clusters comprised of excess ligand, loosely bonded to the complex (but outside the coordination sphere of the metal) and blocking UV light from the metal-coordinated ligands.

Solutions of Na_2DPA and Tb(III) in molar ratios less than 2.75:1 experience rapid and continuous luminescence loss (within seconds) under UV light (254 nm). As illustrated in Figure 19, for molar ratios of 3:1 or greater, the loss is less rapid and much less extensive. Decline in luminescence is not characteristic of the current USPS inorganic phosphor (Zinc orthosilicate doped with manganese, Figure 20), although when left in direct sunlight for long periods of time on paper, the zincate does degrade significantly (Section 3.19.2). Published NMR spectra [30] indicate that Tb:DPA complexes of different structure are formed in solutions having a stoichiometric deficiency or excess of ligand (less or more than 3:1); i.e., that terbium in excess reacts with all of the DPA to form ligand-deficient complexes. Luminescence loss induced by UV light is reversed by turning off the light and must therefore be due to the dissociation of metal-to-ligand bonds. Empirically, a molar ratio higher than 3:1 is indicated to promote optical stability.

In actual use the phosphor may be applied either directly (in the aqueous medium) or dissolved in varnish (Section 2.2). In both matrices, the dilution of phosphor is such that a 6:1 ratio of DPA to Tb(III) shows no evidence of UV blocking, and does provide enhancement of luminescence together with UV stability. We have therefore employed the 6:1 ratio in most of the experimental matrices for calibrating systems and evaluating their environmental stability.

3.4.3. Stability of Aqueous Solutions.

Samples of $Na_3Tb(DPA)_3$ in aqueous solution retain the initial phosphorescence indefinitely. An aqueous solution of Na_2DPA and $Tb(NO_3)_3$ was prepared in June, 1985, and delivered to the testing laboratory of the Bureau of Engraving and Printing in Washington, D.C. in a 32-liter capped polyethylene vessel. After approximately six months, an aliquot was taken and returned to NBS, and a second sample was identically prepared. The old and the new samples were mixed respectively in equal concentrations into specimens of a varnish (SVD-4057), applied to stamp paper (LP-46) at a depth of 0.0254 mm (1.0 mil), heat cured identically, and tested for phosphorescence, with similar results (Table 8).

TABLE 8

Stability of aqueous solutions of $Na_3Tb(DPA)_3$

Sample	Concentration (Percent, w/w)	Phosphorescence (PMU)
BEP*	0.112	82
NBS**	0.115	83
NBS***	0.112	81

* Prepared 6/85
** Prepared 6/85
*** Prepared 12/85

3.5. Solid $Na_3Tb(DPA)_3$ as varnish taggant.

In commercial preparations, water is not added to varnishes TG-20-T or UV-8 during the introduction of phosphor taggants. Although we have obtained well-mixed systems of water and these two varnishes, we have explored

sonication as a means to introduce the solid crystal into these or any other non-miscible carrier. The key objective is to disperse the material through the varnish as evenly as possible in particles as small as possible. Sonications were performed using a Heat Systems-Ultrasonics Inc. Model W-220F instrument equipped with a standard microtip.

3.5.1 Varnish TG-20-T.

To varnish TG-20-T as received (0.5949 g in a glass mortar) was added 0.5977 g of the solid phosphor [(I), molecular weight 831.30, 19.1% terbium], giving an effective concentration of 9.57% terbium in the mixture. After manual grinding into a homogeneous mixture, 0.488 g of the mixture was diluted with 4.7609 g of varnish TG-20-T, to give a terbium concentration of 0.89% in the second mixture, in which EMI showed relatively large chunks of phosphor (about 30 micrometer on a side) dispersed among smaller chunks (1 to 3 micrometer on a side). A further dilution [adding 0.4467 g of the mixture to 4.4481 g of the varnish to give 0.081% terbium (w/w)] was sonicated for five minutes, resulting in a large number of small particles (1 to 2 micrometer on a side) dispersed homogeneously in the varnish, but no large chunks.*

A drawdown (1.0 mil) on each of three papers was given a one-minute cure at 100°C and tested for phosphorescence with relatively poor results (Table 9).

* Since sonication generates a great deal of heat, the process must be performed with cooling, e.g., immersing the container in an ice bath.

TABLE 9

Luminescence of stamp papers coated with Varnish TG-20-T tagged with $Na_3Tb(DPA)_3 \cdot 6H_2O$

Paper	Terbium (percent)	Luminescence EMI	Luminescence PMU
LP-46	0.081	615	82
LP-54	0.081	540	65
LP-23	0.081	460	52

These phosphorescence intensities are considerably lower than those expected for equal concentrations of terbium applied in either an aqueous medium (vide infra, Tables 15, 16) or mixed into an organic varnish (vide infra Table 11).

3.5.2 Varnish UV-8.

Similar experiments with varnish UV-8 result in still lower phosphorescence measured. Because the varnish is opaque to light of 254 nm (Section 3.17) it blocks out the radiant energy necessary to excite the complex to its emissive state. Varnish UV-8 (0.9210 g) and $Na_3Tb(DPA)_3 \cdot 6H_2O$ (1.3387 g) were manually ground to a paste, diluted [1.2827 g with an additional 11.7005 g of varnish], again ground to homogeneity, and finally diluted [2.9542 g further diluted with 28.9033 g of varnish] and ground to a homogeneous mixture containing 0.104% of terbium (w/w). No phosphor crystals were visible to the naked eye.

Samples of the latter (10 mL in a 25-mL graduated cylinder) were cooled to 0 ^{o}C and sonicated for five or fifteen minutes, respectively, under maximum

power. Each material was drawn down (1.0 mil) on papers LP-46, LP-54, and LP-23, and UV-cured (254 nm; Pen-Ray Model SCT-4, Ultraviolet Products, Inc.) for ten minutes. The cured surfaces were tack-free amd glossy, but low in phosphorescence values (Table 10). Under the analyzing beam of the epifluorescence microscope, it was not possible to locate images of the complex in the varnish. Two more sets of drawdowns were prepared: one set was heat-cured for 1 min at 100°C (still sticky) and the other subjected to a 10-min UV cure followed by the same heat cure. The heat-cured sample showed higher phosphorescence, but heating did not enhance the phosphorescence of the UV-cured sample (Table 10). Clearly, varnish UV-8 is an unsuitable phosphor carrier, because UV blocking prevents excitation of the dissolved complex.

TABLE 10

Phosphorescence of varnish coatings tagged with $Na_3Tb(DPA)_3$ by sonication

Varnish	Paper	Sonication time	%Tb	Cure *	PMU
UV-8	LP-23	5 min	0.104	UV	4
UV-8	LP-46	5 min	0.104	UV	7
UV-8	LP-54	5 min	0.104	UV	4
UV-8	LP-23	15 min	0.104	UV	5
UV-8	LP-46	15 min	0.104	UV	7
UV-8	LP-54	15 min	0.104	UV	5
UV-8	LP-23	15 min	0.104	Heat	16
UV-8	LP-46	15 min	0.104	Heat	23
UV-8	LP-54	15 min	0.104	Heat	18
UV-8	LP-23	15 min	0.104	UV, heat	5
UV-8	LP-46	15 min	0.104	UV, heat	7
UV-8	LP-54	15 min	0.104	UV, heat	5
TG-20-T	LP-23	5 min	0.081	UV, heat	52
TG-20-T	LP-46	5 min	0.081	UV, heat	82
TG-20-T	LP-54	5 min	0.081	UV, heat	65

* UV cure = 10 min under pen-light 254 nm source; heat = 1 min at 100 °C

3.6. Formamide solutions of $Na_3Tb(DPA)_3$.

In the search for an organic solvent for crystals of $Na_3Tb(DPA)_3$, only formamide was found to dissolve as much as 10 percent by weight of the solid (Section 3.3.2). This formamide solution was mixed into five varnishes to give the terbium concentrations (w/w) indicated in Table 11. The mixtures were coated (1.0 mil) on stamp papers LP-46, LP-54, and LP-23, cured and tested for phosphorescence. The results (Columns a in Table 11) are generally lower than those obtained by tagging the respective varnishes in the same manner with aqueous solutions of phosphor (Columns b in Table 11).

Overall, formamide solutions would offer little or no advantage over aqueous solutions in miscibility with varnishes. In view of the higher cost of the chemical, the lower brightness of the coatings, and the mild toxicity of formamide compared to deionized water, formamide compares unfavorably with water as solvent for the phosphor.

TABLE 11

Phosphorescence of varnish-coated stamp papers tagged with $Na_3Tb(DPA)_3$ in formamide or water

Varnish*	Tb (%,w/w)	LP-46 PMU		LP-54 PMU		LP-23 PMU	
		a**	b***	a	b	a	b
TG-20-T	0.058	26	200	21	98	21	90
TG-2407-RV	0.058	179	200	131	200	97	126
TG-45-T	0.176	69	128	61	102	54	126
IPI-4047	0.176	133	200	105	111	101	102
SVD-4057	0.176	62	150	65	123	58	128

* BEP designations
** Formamide as phosphor solvent
*** Water as phosphor solvent

3.7. Aqueous $Na_3Tb(DPA)_3$ as varnish taggant.

We have demonstrated that the luminescence of aqueous solutions of $Tb(NO_3)_3$ and Na_2DPA depends both on the molar ratio of DPA to Tb and the matrix in which complexation occurs. A 3:1 ratio displays the highest luminescence in static, aqueous solutions (Section 3.9.1.2.1), but in a chromatographic eluent, the 8:1 ratio gives the highest luminescence (Section 3.13.1), suggesting that the luminescence is affected by chemical associations between the matrix and the complex, or components of the aqueous mixture. A varnish matrix varying from water in both density and polarity could then be expected to vary in the correlation of molar ratio and brightness.

3.7.1. Effects of Molar Ratios ([DPA]:[Tb]) on Luminescence.

The hypothesis expressed above is strengthened by the data presented in Figure 21, illustrating the effects of molar ratios, between 0:1 and 8:1 on the phosphorescence of tagged varnish coatings (SVD-4057) on stamp paper LP-46. The enhancement effect increases most rapidly up to the ratio of about 6:1, as shown in the steepness of the slope. In subsequent calibrations of varnish coated systems, we routinely employ solutions containing this 6:1 ratio to correlate measured phosphorescence with the concentration of terbium, the more expensive component.

3.7.2. Effects of Tb concentration on luminescence.

Figure 22 illustrates the correlation of luminescence (EMI) and of phosphorescence (PMU) with terbium concentration in this particular varnish, one of several samples prepared for field testing by USPS. The

reproducibility of sample preparation and calibration, as indicated by the standard deviation (Table 12), is 11% of the average.

TABLE 12

Reproducibily of phosphorescence when liquid taggant is mixed into Varnish SVD-4057

Slope (PMU/% Tb)	Intercept (PMU)	Coefficient of Linear Correlation
689	2.6	0.999
531	4.6	0.998
515	4.2	0.998
596	1.7	0.991
661	-2.2	0.998
587	0.7	0.999
Avg. 596.7		
Standard deviation.... 68.9		

3.7.3. Effects of varnish opacity on luminescence.

In Table 13 are collected similar correlations of phosphor concentrations in a series of varnishes. These include one sample of SVD-4057 that had been stored in an air conditioned laboratory for over eighteen months, usually at 23 ^{o}C and about 50% relative humidity. The 6:1 molar ratio (DPA to terbium) is constant; the measured phosphorescence varies with the terbium concentration, the type of varnish (opaque or transparent at 254 nm; see Figure 35), and the depth, determined by the drawdown bar (see Section 2.2). Not all five varnishes are currently in use: reportedly, use of TG-2407 RV

and TG-45-T has been discontinued, but data pertaining to these materials is included to illustrate the importance of varnish transparency. The type of paper [unfilled (LP-46) or filled (LP-23, LP-54)] has an influence on the measured phosphorescence when a transparent or semitransparent varnish is employed (TG-2407-RV, TG-20-T, transparent; CR-32974, semitransparent), but little or no effect in the case of partially or completely opaque varnish (SVD-4057; TG-45-T). Similarly, the measured phosphorescence is a function of depth or thickness in the case of the transparent but not opaque varnishes. In the case of TG-45-T, SVD-4057, and CR-32974, 0.5 mil coatings tagged with the terbium phosphor in the relatively small concentrations listed in Table 13, could be used to equal or better effect than 1.0 mil coatings, indicating the use of 0.5 mil or lower thicknesses as a route to materials savings. A low phosphor concentration and a low coating thickness could likewise be employed in the case of TG-2407-RV and TG-20-T, with proportional materials savings. These observations also highlight the critical importance of enforcing a specification of 90 to 95% varnish transparency, currently met by only two of the varnishes tested (cf the UV spectra Figure 35).

TABLE 13

Phosphorescence of stamp papers coated with several $Na_3Tb(DPA)_3$-tagged varnishes using different thicknesses

Paper	Varnish	Thickness (mil)	Slope (PMU/%Tb)	Intercept (PMU)	Coefficient of Correlation
LP-46	TG-2407-RV	0.5	2640	14	0.982
"	"	1.0	3440	11	0.991
LP-23	"	0.5	1710	-0.2	0.999
"	"	1.0	2170	5	0.991
LP-54	"	0.5	1620	0.7	0.998
	"	1.0	3500	11	0.989
LP-46	TG-20-T	0.5	1670	0.4	0.986
"	"	1.0	3550	3.5	0.999
LP-23	"	0.5	1090	14	0.987
"	"	1.0	1680	18	0.963
LP-54	"	0.5	760	40	0.897
"	"	1.0	1690	6	0.999
LP-46	CR-32974	0.5	780	7	0.998
"	"	1.0	830	-1	0.997
LP-23	"	0.5	290	1.5	0.981
"	"	1.0	280	1	0.996
LP-54	CR-32974	0.5	330	0.6	0.998
"	"	1.0	330	1.8	0.998
LP-46	SVD-4057	0.3	410	4	0.999
"	"	0.5	360	3	0.993
"	"	1.0	315	1	0.993
LP-23	"	0.5	180	3	0.999
"	"	1.0	160	4	0.993
LP-54	"	0.5	200	3	0.999
"	"	1.0	170	5	0.984
LP-46	TG-45-T	0.5	290	2.8	0.991
"	"	1.0	290	-1.8	0.965
LP-23	"	0.5	370	-2.4	0.992
"	"	1.0	370	-8.2	0.954
LP-54	"	0.5	350	-2.1	0.973
"	"	1.0	370	-9	0.928

3.8. Varnishes blocking luminescence of Pre-tagged Paper.

Table 14 further illustrates the disastrous effects of light absorption by varnish coatings on the luminescence of an underlying phosphor-tagged surface. Papers were treated either with aqueous $Na_3Tb(DPA)_3$ (see Section 2.2 for the drawdown procedure) or else with inorganic phosphor (zinc orthosilicate doped with manganese; samples provided by Harrison & Sons, Ltd). The samples were checked individually for phosphorescence, coated with a given varnish, and rechecked for phosphorescence. The difference is a measure of the extent to which varnish blocks UV radiation from a phosphorescent surface.

TABLE 14

Blocking of phosphorescence by opaque varnish

Varnish	Paper	Phosphor	Plain (PMU)	Coated (PMU)
IPI-4057	LP-46	Terbium*	182	21
"	Harrison**	Zincate***	>200	22
UV-8	LP-46	Terbium	199	62
"	Harrison**	Zincate	>200	10
TG-20-T	LP-46	Terbium	146	106
"	Harrison**	Zincate	>200	>200
CR-32974	LP-46	Terbium	162	65
"	Harrison**	Zincate	>200	54

* $Na_3Tb(DPA)_3$
** Coating method of Harrison & Sons, Ltd
*** Zinc orthosilicate doped with manganese

The data in Table 14 thus prove that varnish used as a phosphor carrier must be transparent. An opaque varnish defeats the system by preventing light of excitation to reach the phosphor.

3.9. Direct Tagging With a Soluble Phosphor, Omitting Varnish.

This procedure requires a phosphor that is soluble or miscible with solvents other than varnish, a requirement met by aqueous $Na_3Tb(DPA)_3$. The general procedure for hand drawdowns with aqueous solutions is described above (Section 2.2); in principle, it is similar to varnish drawdowns. A 1.0-mil or 0.5-mil drawdown bar is used with aqueous solutions containing the phosphor in a given concentration. We usually employ the same 6:1 ratio of DPA to Tb that is used in varnishes, as explained below.

3.9.1. Effects of [DPA]:[Tb] molar ratios.

3.9.1.1. Na_2DPA added to Tb.

As in the case of varnish solutions, a series of molar ratios in aqueous solutions was applied to stamp paper, limiting the study to only one paper (LP-46), and including a range of ratios between 0:1 and 10:1 ([DPA] to [Tb]), with a terbium concentration of 1.12 percent (w/v) in water. As indicated in Figure 23, the measured phosphorescence increases with the molar ratio to a maximum in the region of 6:1 to 7:1, and remains constant up to about the 11:1 ratio. An apparent jump in phosphorescence in the range of 12:1 to 14:1 appears to be an artifact, although it may be the result of excess DPA "fixing" phosphor at the surface; i.e., retarding inward migration (a matter of considerable importance, to be discussed later, in regard to the retention

of phosphorescence in humid environments). Whatever the reason, the maximum phosphorescence obviously is obtained only with molar ratios much higher than the stoichiometric 3:1 of pure crystals precipitated from water (Section 2.4.1.8).

3.9.1.2. Na_2DPA added to $Na_3Tb(DPA)_3$.

It was of interest to determine whether the luminescence of a solution consisting of pure crystals dissolved in water would be enhanced by the addition of Na_2DPA in the same manner as mixtures of terbium nitrate and Na_2DPA. If this were the case, a quantity of crystals, rather than the bulky aqueous solution, could be transported to the site of paper manufacture or coating. A stock solution of $Na_3Tb(DPA)_3$ (0.125 mole L^{-1}) was prepared in neutral water. Test solutions were then prepared by diluting 0.1 mL portions of the stock with varying aliquots of 0.125 M Na_2DPA and enough water to make the total volume 2.00 mL. Measurements of total luminescence (EMI) were carried out as described below.

3.9.1.2.1. Luminescence in Water.

The cavity of a concave microscope slide was filled with each test solution, topped with a quartz cover slip, and tested for total luminescence (excitation=254 nm; emission = 545 nm). Table 15 shows that the total luminescence decreases when Na_2DPA is added to a solution of $Na_3Tb(DPA)_3$ - i.e., when the ligand is present in stoichiometric excess - and that the luminescence decreases further with additional ligand up to the final molar ratio of 11:1. Since liquid taggant (L.T.) prepared with terbium nitrate and ligand in the 6:1 molar ratio gives a luminescence intensity comparable to

that of $Na_3Tb(DPA)_3$ and 3 moles of excess ligand, it is unimportant in which order these components are added to a mixture.

TABLE 15

Comparability of solutions of taggant made with crystalline phosphor or with terbium nitrate and ligand in water

	$Na_3Tb(DPA)_3$/DPA	DPA/Tb	EMI (millivolt)
0	1/0	3/1	1316
1	1/1	4/1	877
2	2/1	5/1	668
3	3/1	6/1	653
4	4/1	7/1	517
5	5/1	8/1	447
6	6/1	9/1	381
7	7/1	10/1	392
8	8/1	11/1	364
L.T*	-	(6/1 -7/1)	632

* Liquid taggant, a mixture of $Tb(NO_3)_3$ and Na_2DPA

3.9.1.2.2. Phosphorescence on Paper.

Mixtures having the 6:1 molar ratio (ligand:terbium) again were prepared in water by mixing either (a) solutions of crystals and of ligand, or (b) solutions of terbium nitrate and of ligand. The respective solutions were applied by drawdown to two stamp papers and to filter paper (100% rag) and compared to a solution of the crystals (molar ratio 3:1, ligand:terbium) similarly applied. The two stamp papers (LP-46 and LP-54) both had adhesive organic backing, some of which was transported through the wet paper from the back onto the tagged, luminescent front area. The pure filter paper was tagged with each of the three solutions to avoid effects of this contamination. The luminescence measurements are summarized in Table 16.

TABLE 16

Comparability of taggant solutions made with crystalline phosphor or solutions of metal and ligand applications to paper

Sample	EMI(LP-46)	EMI-(LP-54)	EMI(Whatman)
L.T.* ([DPA]:[Tb]=6:1)	2236	2136	2249
$Na_3Tb(DPA)_3$	2193	1821	2236
$Na_3Tb(DPA)_3 + 3Na_2DPA$	1446	1526	2221

* Liquid Taggant

Thus, solutions made either by dissolving pure crystals in water, or by adding a solution of ligand to a solution of pure crystals, deliver total luminescence equal to that of liquid taggant made by mixing solutions of one mole of terbium nitrate with 6 - 7 moles of ligand.

3.9.2. Effects of Tb concentration on phosphorescence.

Figure 24 represents the phosphorescence of specimens of paper LP-46 and paper LP-54 coated with aqueous solutions of $Na_3Tb(DPA)_3$; phosphorescence is plotted against the terbium concentrations indicated for each solution. The individual solutions were prepared by diluting a stock solution containing 1.12% by weight of terbium and a 6:1 molar ratio of ligand to metal. Typically a few drops of solution are applied across the top of a sheet and drawn down under a standard bar. Some absorption is evident where the solution is first applied, resulting in local areas of high phosphor concentration and high phosphorescence, and were avoided when taking phosphorescence measurements.

For LP-46, the slope is about five times greater than that for paper LP-54, when both are defined by phosphorescence as a function of the concentration of phosphor (or terbium) in solution. For subsequent comparisons of the two papers, we selected concentrations of 0.0675% terbium (for LP-46) and 0.225% terbium (for LP-54), and used differential weighing to estimate the amount of terbium actually retained by each paper. To estimate the mass of terbium distributed over a given measured area, the paper was weighed dry, subjected to a drawdown, and quickly reweighed while wet. Each sample then was dried for one min at 100 ^{o}C prior to measuring the phosphorescence to obtain the difference in weight attributed to the retained phosphor solution. The results are summarized in Table 17:

TABLE 17

Phosphorescence as a function of terbium absorption

Paper	Weight of Solution	Weight of Terbium	PMU
LP-46	2.03×10^{-5}	13.7×10^{-9}	120
LP-54	1.98×10^{-5}	44.55×10^{-9}	74

Thus, the amount of solution taken up in this experiment was nearly the same per unit area for each paper. Projecting these data gives the estimated terbium consumption required to tag 40 billion commemorative stamps (1.0 by 1.5 inch) per year. Assuming for simplicity that a single type of paper was used to prepare all 40 billion stamps, paper LP-46 would consume 5.3 kilograms per year of terbium, and LP-54 about 17.2 Kg. These data are necessarily very

rough estimates. Repeating the experiments with nine replicate tests on paper LP-46 and again extrapolating to a 40-billion annual stamp production, the calculated average consumption was 70 $\pm$ 30 kg. Similar numbers were obtained with paper LP-54. These results indicate that engineering problems remain to be solved in production runs so that taggant retention is controlled within reasonably narrow limits. Nevertheless, the quantity of terbium required for acceptable stamp phosphorescence would be remarkably low, even in the worst case representing only about five percent of the estimated current domestic production of terbium [28].

3.10. Commercial tagging process: Harrison and Sons, Ltd, United Kingdon.

In collaboration with USPS, Harrison and Sons, Ltd (U.K.) prepared pilot scale samples of paper coated with either $Na_3Tb(DPA)_3$, or zinc orthosilicate doped with manganese ("doped zincate") to give very bright phosphorescent surfaces. Harrison mixed the NBS terbium complex in aqueous solution (1.12% terbium w/v) into a proprietary finishing formula which they found suitable as well for the zincate phosphor. The resulting surfaces presented a phosphorescence (λ_{exc} = 254 nm; λ_{em} = 545 nm) of 195 PMU (Tb complex) or 390 PMU (zincate). To treat 12000 square yards of paper required 9.4 kg of the terbium phosphor solution. Furthermore, the Bureau of Engraving and Printing (BEP) reportedly uses 52.5 million square yards of paper per year in stamp manufacture. From these data the annual consumption of terbium phosphor in stamp production by the Harrison method can be projected. Thus, 12000 yards requires 105.3 g of terbium and 658.28 g of DPA. The annual consumption of terbium in manufacturing stamps by the Harrison method would be 461 kg, and that of DPA 2880 kg for one year of production in the U.S.

Both inked and non-inked (plain) papers were prepared by Harrison. A variety of colored dyes were employed to prepare the inked stamps (labelled "Showboat"): red; red and blue; blue and yellow; and blue and green. We received supplies of these stamps coated only with the terbium phosphor, not zinc orthosilicate. The effect of dyes is to reduce the phosphorescence as indicated in Table 18, but not below an acceptable level of brightness (>40 PMU).

TABLE 18

Phosphorescence of dye-treated stamps coated with terbium phosphor

Color	Number of Stamps	Phosphorescence (PMU) Average	Standard Deviation
White	2	162	31
Red	8	57	5
Blue-red	3	64	5
Blue-yellow	2	90	9
Blue-green	4	66	4

The decrease in phosphorescence may be due to the absorption of exciting ultraviolet light or absorbance of the emitted light by chromophoric components of the proprietary dyes. An alternative possibility cannot be ruled out, pending elemental analysis of the dyes: that metallic components in trace amounts promote radiationless quenching of excited terbium. Cobalt,

for example, has been found to quench terbium complexed with 2,4-beta(diketonato)terbium(III). In this frame of reference, it would be useful to test the phosphorescence of dyed stamps similarly tagged with the zinc complex. Although none of the latter were available in the present study, USPS production stamps, which do employ this complex dispersed in varnish, typically display lower luminescence in inked than uninked stamps.

3.11. Tagging by Method of Consecutive Coating.

An alternative method for coating stamp papers consists of applying separate solutions of Na_2DPA and of $Tb(NO_3)_3$ in consecutive steps. The experimental objectives were: (1) to make the most efficient use of terbium (the more expensive component) and (2) to deposit the ligand as a surface film or saturate that would complex with Tb at the immediate surface and retard its migration into the region just below the surface of the paper.

Solutions of Na_2(2,6-DPA) (0.02M, 0.3342% by weight) and terbium (0.002 M, 0.0318% by weight) were drawn down consecutively over premeasured areas of preweighed paper. Subtracting the weight of dry paper gave the liquid uptake for a given area. In turn, the amount of chemical per unit area was calculated from the weight and the concentration by weight of each solution. Calibration curves based on the terbium consumption of plain, clay-filled and unfilled papers both are indicated in Figure 25. Extrapolating to the production of 40 billion commemorative stamps per year indicates an annual terbium requirement of 45.2 kg to gain a phosphorescence of 110 PMU with either paper, a much smaller amount than that required by the Harrison method (Section 3.10, above).

3.12. Excitation of Harrison Papers at Selected Wavelengths.

As pointed out in Sections 3.1.4 (Figure 17) and 3.14.1.1 (Table 19), 254 nm excitation of pure $Na_3Tb(DPA)_3$ results in poorer emission output than that observed with 300 nm excitation. Emission spectra were recorded at various excitation wavelengths upon non-inked Harrison and Sons Tb treated paper to aid in defining optimal phosphor performance. Salient results are illustrated in Figure 26. Between 270 and 350 nm limits of excitation, the paper itself becomes increasingly more blue-luminescent. Comparison of the dotted line and the solid line in Figure 26 shows that at 350 nm the emission output is virtually all due to paper rather than $Na_3Tb(DPA)_3$ (paper spectrum run on untreated LP-46). Green emission output is fairly constant between 270 and 310 nm. We conclude that the observations discussed earlier for crystalline $Na_3Tb(DPA)_3 \cdot 6H_2O$ excitation hold for the phosphor on paper as well; i.e., that excitation at wavelengths longer than 254 nm will deliver more phosphorescence.

3.13. Chromatography of $Na_3Tb(DPA)_3$ Solutions.

Modern liquid chromatography manifests slight differences in the porperties of molecules (size, shape, polarity) through differences in their affinity for, and retention on, the surfaces of selected packing materials. With lanthanide nitrates at a given concentration and Na_2DPA concentrations varied to give a range of different molar ratios, complexation might be controlled by distinctly different mechanisms. If the ligand is deficient, all of the ligand might be consumed to generate a proportional concentration of $Na_3Tb(DPA)_3$, with an excess of Tb in solution; or all of the Tb might be

associated with all of the ligand to form complexes having fewer than three DPA ligands of the formula $Na_nTb^{(3-n)+}(DPA)_n$, where "n" = 1 to 3.

3.13.1. SCX microbore HPLC.

We used a strong cation exchange column (SCX, Section 2.1.2) to retain cations selectively and to differentiate between complexes of different ionic charge; and an octadecanoate substituted (C_{18}) to differentiate complexes of different organic ligation, i.e. different numbers of DPA per complex.

The results of SCX chromatography are summarized in Figures 27 and 28. The retention volume is constant throughout the series, indicating that the same compound is eluted, regardless of the starting molar ratio. This is consistent with formation of a single complex, and not a set of complexes depending on the ratio. However, the intensity of the measured fluorescence does not reach a maximum at the 3:1 ratio, but rather at a ratio of almost 8:1 (Figure 28), and that maximum is followed by a precipitous decrease in luminescence when the ratio is increased to 9:1 or higher. The luminescence is essentially constant on increasing the ratio above 9:1. These data might be interpreted as evidence that: (a) complexes in solution favor a different orientation and stoichiometry than the 3:1 stoichiometry of pure crystals; or (b) formation of the complex is favored by an excess of DPA. Neither explanation is consistent with the measurements on static solutions that we report above (Section 3.9.1.2.1).

A more plausible explanation is that Tb(III) is adsorbed onto the surface of the packing whenever the injected sample has a deficiency of DPA, and the adsorbed ions are scavenged competitively by DPA^{2-} when the latter is in excess. The location of the peak, then, is accidental; the 8:1 ratio happens

to coincide with maximum mobilization of adsorbed ions. The same peak is found when Eu(III) is deposited instead of Tb. When injections are made from the same solutions in the absence of a column, there is no sharp peak at the 8:1 or any other ratio ("FIA", Figure 29), but a maximum is reached near the 4:1 ratio. This suggests some retention and scavenging of ions on the packing surface.

3.13.2. Reverse Bonded Phase (C_{18}) HPLC.

Bonded phase chromatography (C_{18}, Figure 30) manifests similar increase in luminescence up to a ratio far exceeding 3:1, again suggesting cation retention and progressive scavenging, most likely owing to uncovered -SiOH groups.

3.13.3. Thin Layer Chromatography (TLC).

Thin layer chromatography of similar [DPA]:[Tb] mixtures shows a similar pattern in retention and release (Figure 31). In this experiment, a spot was deposited on a plate and then eluted with water. Mobilization is progressive with an increasing molar ratio.

3.13.4. Stamp paper as a chromatographic substitute.

The correlation between thin layer and column chromatography is highly relevant to the stabilization of luminescence at stamp surfaces coated with aqueous solutions of $Na_3Tb(DPA)_3$. We have pointed out that the crystals are highly resistant to humidity, but coatings on stamp paper tend to migrate inward (Section 3.19.1) in environments of high humidity. While the phosphorescence of the tagged side diminishes over a period of several days,

that of the reverse side steadily increases up to a point of equilibrium. Full utilization of the phosphor will depend on its immobilization at the surface; that is, to set up a surface chemistry such that the substrate (paper) has a stronger affinity than the mobile phase (water) for the phosphor. This might be done by making the phosphor more aliphatic (condensing an aliphatic chain onto the DPA molecule); modifying the stamp surface physically or chemically; or encapsulating the phosphor in a transparent material with a low affinity for water ("microencapsulation" Section 3.21). Microencapsulation is a promising but unperfected technique for immobilizing phosphor. Inasmuch as the phosphor does work very well when immobilized in a transparent varnish such as Varnish TG-2407-RV (Sections 3.16.1.4, 3.16.1.5.1), we anticipate obtaining the same excitation and emission phenomena with phosphors encapsulated within sufficiently thin transparent walls.

3.14. Performance of Inorganic Phosphors.

3.14.1. Zincate phosphors.

To complement the data in hand on $Na_3Tb(DPA)_3 \cdot 6H_2O$ and to provide comparisons in environmental tests on papers treated with the terbium phosphor, we studied three traditional inorganic heterogeneous phosphors supplied by USPS: the currently used manganese-doped zinc orthosilicate ($ZnSiO_4 \cdot Mn$), zinc sulfide doped with copper ($ZnS \cdot Cu$) and zinc oxide with an unknown dopant ($ZnO \cdot X$).

3.14.1.1. Emission and Excitation Spectra.

Figure 32 illustrates a superposition of normalized emission spectra of the three phosphors. All show appreciable emission in the green region of the

visible spectrum (500 - 560 nm), although ZnO·X has a maximum just below 500 nm and emits blue-green rather than pure green. Table 19 lists non-corrected, non-normalized emission intensities for the solid zincates along with data for $Na_3Tb(DPA)_3 \cdot 6H_2O$, using the wavelengths of maximum emission. Two points of significance obtain: $Na_3Tb(DPA)_3 \cdot 6H_2O$ is intrinsically the brightest of the phosphors, and radiation at 254 nm does not give optimal excitation for any of the phosphors. As discussed in Section 3.1.4, however, photon flux at each wavelength of excitation will ultimately have to be considered as a normalizing factor to make this data quantitative.

TABLE 19

Emission intensities for green phosphors

Phosphor	λ_{em} (nm)	λ_{exc} (nm)	Intensity* (Relative Units)
$Na_3Tb(DPA)_3 \cdot 6H_2O$	543	254	98.5
		270	148
		280	298
		290	581
		300	918
$ZnSiO_4 \cdot Mn$	530	254	39.0
		270	39.9
		280	45.8
		290	47.0
		300	36.0
ZnS·Cu	537	254	29.2
		270	40.6
		290	152
		310	275
		366	473
ZnO·X	500	254	20.9
		270	25.0
		290	79.2
		310	134
		366	215

* Emission = 548 nm

3.14.1.2. UV Stability.

As stated earlier (Section 3.4.2), $ZnSiO_4 \cdot Mn$ undergoes no photobleaching over 15 minutes when exposed to radiation of 254 nm. Degradation does obtain after long exposures to direct sunlight either out of doors or through glass, indoors, however.

3.14.2 Terbium Polypyrazolyl- and Polyimidazolylborate Complexes.

These complexes were synthesized and briefly evaluated as alternatives to the terbium-DPA system. It was apparent in their synthesis that the compounds were almost totally insoluble in water and all other common solvents. Elemental analysis of the product formed between the terbium nitrate and sodium-tris(pyrazol-1-yl)borate suggests a cluster structure that is also shared by the analogous europium complex. The emission spectrum of "$Tb_x(HBPz_3)_y$", Figure 33, is virtually identical in band position to that of $Na_3Tb(DPA)_3 \cdot 6H_2O$, Figure 16, but its absolute intensity of emission at 543 nm is 60% of that observed for the latter.

Interestingly, the complexes formed from terbium nitrate and the sodium salts of polyimidazol-1-yl borates do not emit sharply in the green spectral region. A broad band of blue-green emission is found instead. The sodium salts themselves have very similar emission spectra, and we conclude that in the $Tb_x(H_{4-y}BIm_y)_z$ family, the emissive excited state is of π- π^* ligand-centered origin rather than the expected ligand - metal charge transfer type seen in $Na_3Tb(DPA)_3 \cdot 6H_2O$ and the terbium-polypyrazol-1-yl family (cf. Figures 33 and 34).

3.15. I.R. Study of Solution Species Arising from $Na_3Tb(DPA)_3$ and Excess Na_2DPA.

A degree of uncertainty has arisen both in published literature [31] and in some of our own chromatographic data as to the structure and stoichiometry of aqueous complexes of terbium and sodium dipicolinate as compared to that of pure crystals. We have obtained infrared spectra of a solution of the pure crystals and of solutions containing both the pure crystals and added molar increments of Na_2DPA.

All of the spectral data were obtained on aqueous solutions using a cylindrical Circle Cell (Spectra Tech, Stamford, CT), equipped with an ATR crystal of zinc selenide. A band due to (O - C = O) stretching at 1390 cm^{-1} was common to $Na_3Tb(DPA)_3$ and Na_2DPA in water, and the extinction coefficients for 1390 cm^{-1} were determined to be 1.41 b^{-1} and 1.34 b^{-1} for the species, respectively, where b is the spectral pathlength, assumed to be constant. Aqueous samples containing $Na_3Tb(DPA)_3$ and 0, 1, 2, 3, 4, and 5 extra moles of Na_2DPA were prepared and examined in the Circle Cell. The observed absorbance at 1390 cm^{-1} was compared to that calculated for both components being present in a non-interacting fashion, with additive absorbance. For example, when $[Na_3Tb(DPA)_3] = 0.0356$ and $[Na_2DPA] = 0.107$, the calculated absorbances are $(0.0356) \times (1.41\ b^{-1}) \times (b) = 0.0502$, and $(0.107) \times (1.34\ b^{-1}) \times (b) = 0.143$. The total calculated absorbance at 1390 cm^{-1} is 0.193. Comparison of the calculated and measured absorbances of all samples yields a linear correlation coefficient of 0.9996, strongly indicating that no complexes different from $Na_3Tb(DPA)_3$ are formed. Furthermore, the spectrum in the carbonyl region fails to manifest any new bands (possibly ascribable to new complexes) when

the [DPA]:[Tb] ratios exceed 3:1. We conclude from these data that the 3:1 complex is the only one present, even in the presence of a large stoichiometric excess of ligand in aqueous solution.

3.16. Aging Studies.

3.16.1. Long term stability of phosphors in varnish.

3.16.1.1. Overview of aging in sunlight and darkness.

Prior to issuance of the previous, comprehensive Annual Report in April, 1985 [6], considerable data had been acquired on the environmental behaviour of the terbium phosphor in BEP varnishes. Many illustrations were provided in that report, detailing the stability of the phosphor in varnish under long-term outdoor and indoor exposure. Further studies are reported here on the comparison of stabilities in varnish among $Na_3Tb(DPA)_3$, $ZnSiO_4 \cdot Mn$, and $ZnS \cdot Cu$.

3.16.1.2. $Na_3Tb(DPA)_3$ in varnish CR 32974.

A dispersion of $Na_3Tb(DPA)_3 \cdot 6H_2O$ was prepared in varnish CR 32974. This was drawn down (0.5 mil) on multi-colored experimental stamp paper sheets (Paper #3, Table 1). Drawdowns of comparable PMU readings were performed using appropriate concentrations of the inorganic phosphors. Samples were aged outdoors during July-September, 1986, in Rockville, MD, and under light and dark laboratory conditions at NBS. The data in Table 20 summarize our findings in this series.

TABLE 20

Phosphor aging studies in Varnish CR-32974
applied (0.5 mil) to 6-color experimental stamps

$Na_3Tb(DPA)_3 \cdot 6H_2O$*

Time (Days)	Outdoors (PMU)	Indoor Window (PMU)	Indoor Lab (PMU)	Indoor Dark (PMU)
0	164**	148**	145**	156**
2	152	120	120	128
4	144	115	122	126
6	152	119	122	132
11	148	112	122	132
15	148	110	128	134
19	152	112	130	134
27	138	106	124	132
43	146	106	130	136
50	140	108	128	142
64	136	100	124	132
$ZnS \cdot Cu$***				
0	154	152	136	130
2	162	136	138	128
4	134	99	136	126
6	126	90	136	135
11	120	79	128	132
15	112	68	132	136
19	116	47	128	132
27	122	48	122	134
43	116	41	128	128
50	124	33	120	132
64	114	35	120	132
$ZnSiO_4 \cdot Mn$****				
0	136	140	140	132
2	134	140	132	126
4	136	144	132	126
6	136	143	138	122
11	140	138	136	126
15	146	148	140	128
19	144	148	148	128
27	144	150	140	128
43	152	144	144	130
50	152	146	146	132
64	148	150	137	124

* Terbium content 0.468 percent (w/w)
** Green phosphorescence; λ_{exc} = 254 nm
*** Phosphor content 16.6 percent (w/w)
**** Phosphor content 8.41 percent (w/w)

3.16.1.3. Zincate phosphors in varnish CR-32974.

In a manner observed on earlier terbium samples in varnish, there is an initial decrease in phosphorescence in each environment, but no real decline in signal thereafter. The zincate phosphors are apparently quite stable in varnish except for the single scenario of ZnS·Cu exposed to outdoor light filtered through a sorth-facing office window. The abrupt loss of phosphorescence in this case is not understood, especially since the luminescence from the corresponding sample exposed to unfiltered sunlight outdoors decreases in a slower fashion. The indoor sample was directly in the output path of the office air conditioning unit, and it is possible that trace impurites in the recirculated air of the Chemistry Building catalyzed a degradation process.

Finally, it should be noted that 18 times more $ZnSiO_4$·Mn or 35 times more ZnS·Cu was required than the amount of terbium phosphor used to obtain the same intensity of phosphorescence on all samples, again showing that a small quantity of a well designed phosphor can go a long way, provided the varnish is not exceedingly opaque. In this respect, again, CR-32974 itself is not very well designed, lacking good transparency at 254 nm. (see Figure 35 for the UV spectra of varnishes).

3.16.1.4. $Na_3Tb(DPA)_3$ and $Tb(acac)_3$ in varnishes TG-20-T and TG-2407-RV.

During the course of this entire project, many experimentally tagged samples were prepared, tested and stored for as long as two years, usually in closed envelopes in a closed desk drawer in an air-conditioned office. We also performed long term exposure of stamps to sunlight filtered through a south-facing office window. Tables 21-27, 29 represent a broad range of specimens including Harrison "Showboat" stamps tagged with $Na_3Tb(DPA)_3$ and

the stamp papers listed in Table 1, varnish coated and tagged with either $Na_3Tb(DPA)_3$ (about 0.067% terbium, by weight in varnish) or $Tb(AcAc)_3$ (about 0.44% terbium by weight).

3.16.1.4.1. $Tb(AcAc)_3$

The earlier NBS inter-laboratory report to USPS [6] showed that both phosphors resisted the harsh sunlight exposure in a south-facing window for at least 68 days. The total aging period we report now extends to 780 days. In this period of time, the gummed samples lost all of their backing. The multicolored samples (Paper No. 3, Table 1) faded to the extent that the original colors could barely be discerned. The papers curled and cracked to the extent that deterioration in physical properties would end their usefulness. Tables 21 and 22 summarize the retention of phosphorescence.

Every sample tagged with $Tb(AcAc)_3$ shows a large increase in phosphorescence, some of them as much as 600% over the original value. Apparently the system attained a maximum after one year. Little change occurred between days 360 and 780.

TABLE 21

Protracted sunlight exposure in south-facing window of $Tb(AcAc)_3$-doped Varnish TG-20-T

Time (days)	Paper* 1*	2*	3*	4*	5*	6*
	PMU					
0	11	12	12	10	16	14
15	15	19	16	14	21	20
46	23	28	28	20	31	28
68	26	32	33	23	34	32
138	37	38	42	23	44	38
360	56	56	50	23	50	35
780	60	62	55	22	52	32

* See Table 1 to identify papers

As shown in Table 22, the taggant system using varnish TG-2407-RV behaved somewhat differently, with higher initial phosphorescence and a lower rate of increase. However, the increases follow an initial period of decreasing phosphorescence that continued for about 15 days before a long period of increasing brightness that continued for at least one year. The initial decrease presumably represents migration into the paper, which is halted after a period of time by chemical and physical changes in the system analogous to encapsulation. At day 780, the percentage of increase in phosphorescence is less than that for varnish TG-20-T only because the initial brightness in TG-2407-RV was much higher. The final intensities are comparable.

TABLE 22

Protracted sunlight exposure in south-facing window of $Tb(AcAc)_3$-doped Varnish TG-2407-RV

Time (days)	Paper*						
	1**	2**	3**	4**	5**	6**	5***
0	29	48	29	41	71	70	164
15	21	36	31	25	41	44	163
45	24	43	39	27	44	43	123
70	24	44	39	30	47	44	108
140	26	45	47	34	62	55	80
360	33	60	52	46	86	78	55
780	34	67	60	55	92	85	40

*See Table 1
** $Tb(AcAc)_3$ in varnish, 0.44 % Tb
*** $Na_3Tb(DPA)_3$ in varnish, 0.066 % Tb

3.16.1.4.2. $Na_3Tb(DPA)_3$

The last column to the right in Table 22 shows the response of the system consisting of varnish TG-2407-RV tagged with phosphor $Na_3Tb(DPA)_3$.

Considering the differences in phosphor concentration, the initial phosphorescence is higher by about two orders of magnitude than that of the $Tb(AcAc)_3$-tagged varnish. The brightness decreases about 50% in 140 days, and another 12% in 360 days, with little change thereafter. The $Na_3Tb(DPA)_3$-tagged specimen still displays much stronger performance after 780 days of exposure. Extrapolating to the higher concentration, the phosphorescence of 0.44% Tb, as the dipicolinate, would be 270 PMU, three times higher than that observed for 0.44% of terbium as $Tb(AcAc)_3$ on paper No. 5 (see Table 22). More important is the retention of a phosphorescence intensity of 55 PMU after one year of exposure and 40 after two years. The minimum required for USPS instrument specifications is about 17 PMU.

The Martin-Marietta Corporation recommended to USPS [2], that terbium chelates be deleted from the list of candidate stamp taggants, on the basis of their instability, unavailability, and cost. The current data do not support this recommendation owing to the stability and ease of synthesis of $Na_3Tb(DPA)_3$. The brightness and stability of this lanthanide chelate suggest that its implementation in varnish based technology should be strongly considered. Indeed, the terbium phosphor could still be useful in varnish-free systems if the problem of water-induced migration is overcome (vide infra).

3.16.1.5. Ambient Aging of Varnish Coatings Tagged with $Na_3Tb(DPA)_3$

3.16.1.5.1 Varnishes TG-20-T and TG-2407-RV

Tables 23 and 24 further demonstrate the long-term stability of $Na_3Tb(DPA)_3$ under ambient conditions. In varnish TG-20-T the

phosphorescence is shown to increase with time, whereas with TG-2407-RV, there occurs a decrease of about 7% in two years. While a loss of that magnitude is of no practical importance, it does exemplify that physico-chemical differences in varnish affect both the initial phosphorescence and its retention; since varnish TG-2407-RV is less viscous, its migration into the paper occurs more rapidly than with TG-20-T. In the present examples, the retention of high initial phosphorescence is notable because the substrate consisted of inked (black and white, or multi-colored) papers. We have shown that inks depress phosphorescence compared to plain paper (Section 3.10).

TABLE 23

Protracted exposure to ambient conditions of $Na_3Tb(DPA)_3$-tagged varnish TG-20-T on inked or pigmented stamp paper.

Tb (%)	Paper			
	Inked (days)		Pigmented (days)	
	0	720	0	720
	PMU		PMU	
0.0	1.0	1.5	1.0	1.0
0.023	42	44	27	23
0.047	48	61	42	53
0.070	80	95	72	80
0.094	85	116	117	134
0.117	123	140	120	134
Slope	938	1147	1090	1249
Intercept	8.3	9.1	-0.6	-2.3
Linear correlation	0.976	0.993	0.984	0.983

TABLE 24

Protracted exposure to ambient conditions of $Na_3Tb(DPA)_3$-tagged varnish TG-2407-RV on pigmented paper

Tb (%)	Time (days) 0 PMU	720 PMU
0.0	1.0	1.5
0.0129	39.5	26
0.0258	63	49
0.0368	114	104
0.0515	146	128
0.0614	168	152
Slope	2675	2471
Intercept	2.4	-2.8
Linear correlation	0.9945	0.9907

3.16.1.5.2 Varnish SVD-4057

The data in Table 25 show that $Na_3Tb(DPA)_3$ in varnish SVD-4057 under ambient conditions is similarly stable, compared to TG-2407-RV, at least for well over one year. The relatively low initial brightness is due to the partial opacity of this varnish to UV light at the wavelength of 254 nm (Section 3.17).

TABLE 25

Protracted exposure to ambient contions of $Na_3Tb(DPA)_3$-tagged varnish SVD-4057 on pigmented paper

Tb (%)	Time (days) 0 PMU	720 PMU
0.0	1.5	2.5
0.044	26.5	25
0.088	52	44
0.132	88	68
0.176	102	87
0.220	132	118
Slope	594	511
Intercept	1.6	1.2
Linear Correlateion	0.996	0.997

3.16.2. Comparison of Five Varnishes on Three Papers.

Table 26 is a summary comparison of five tagged coatings on three plain stamp papers currently used by BEP. In 470 days, there are changes ranging from 0% (TG-2407-RV) to a 45% decrease (TG-45-T on LP-54), with an average loss of 13.3% over the 1.3-year period. A stamp in current circulation ("Joseph Priestley") lost 33% of its initial phosphorescence under the same conditions and time period, from an initial 50 PMU to a final 32 PMU.

TABLE 26
Protracted ambient exposure of 5 varnish-tagged coatings on 3 stamp papers

Varnish	Tb (%)	Paper					
		LP-23-G		LP-46		LP-54	
		Time (days)					
		0	488	0	488	0	488
TG-45	0.22	158	118	160	110	128	75
SVD-4057	0.11	77	69	95	84	80	65
TG-2407-RV	0.11	200	200	200	200	200	200
IPI-4047	0.11	69	57	164	136	64	58
TG-20-T	0.11	200	183	200	172	200	180

3.17. Absorption Spectra of Varnishes.

Since the varnishes currently used by BEP are multicomponent proprietary mixtures of organic compounds, it is important to know their absorbance characteristics at 254 nm, the radiation line used by USPS phosphor meters to excite tagged stamp surfaces. Varnishes were applied with the 0.5 mil drawdown bar directly to the face of a quartz cuvette, and after appropriate curing (by heating at 100°C or irradiating with a medium pressure Hg lamp), their spectra were measured. A composite picture of the results is given in Figure 35. The four varnishes of immediate interest to BEP and USPS all absorb to varying degrees at 254 nm. Not surprisingly, varnish UV-8

(which must absorb in the near UV to be cured to a tack-free condition) completely absorbs the incident energy at 254 nm (A > 3.0; the absorbance is 99.9%). The most transparent of the four varnishes is TG-20-T, which absorbs 4% of the incoming radiation. The use of any varnish will attenuate to some extent the emission intensity of suitable phosphors and ultimately require a higher phosphor loading than a varnish-free system. Hence, if a varnish is employed, its transparency is vital to the efficient functioning of the USPS facer-canceller systems. That is why varnish TG-2407-RV, with little absorption at 254 nm, is an efficient carrier of phosphor $Na_3Tb(DPA)_3$, although this varnish has been discarded by BEP because of reported chalking during production runs. We cannot emphasize too strongly the importance of enforcing a specification for the transparency of varnish carriers.

3.18. Long Term stability of surfaces coated with aqueous taggant [$Na_3Tb(DPA)_3$].

Table 27 includes data on aqueous applications of $Na_3Tb(DPA)_3$ to paper placed in the south-facing window and exposed to sunlight, or else stored in an office desk. The difference in loss of brightness after 660 days is comparatively small, indicating that the migration mechanism is the primary cause - i.e., that phosphor diffuses into the paper substrate, diminishing the quantity at the surface. The total average loss (about 35%) is equal to that experienced by the USPS "Joseph Priestley" stamp (33%) over the same period of time.

TABLE 27

Protracted ambient stability of liquid taggant containing $Na_3Tb(DPA)_3/DPA^{-2}$ coated on three stamp papers.

Paper	Time (days)			
	Darkness		Sunlight	
	0	660	0	660
1*	100	66	110	58
2*	48	38	52	24
3*	23	18	31	23

* See Table 1 for identification of papers.

3.19. Environmental Testing of Phosphors on Paper Substrates.

3.19.1 Harrison and Sons Showboat Stamps.

These multicolored, non-varnished stamps were tagged with 0.02 percent terbium, using aqueous $Na_3Tb(DPA)_3$ in a proprietary process. As reflected in Table 18 data, the stamps initially exhibited phosphorescence (PMU) values between 57 and 90, depending on the color of the ink. A strip of the stamps was hung in a ventilated cardboard box that was continually held in ambient Montgomery County temperature and humidity during June-August, 1986. Temperature, humidity, and PMU readings were recorded throughout the study. The box also contained samples of a non-inked terbium-treated paper, a paper treated with 3% $ZnSiO_4$·Mn (both prepared by Harrison and Sons) and a U.S. commemorative stamp ($ZnSiO_4$·Mn phosphor; appropriate BEP varnish). Figure 36 illustrates changes in PMU vs. time for representative samples, and Figure 37 correlates fluctuations in PMU readings with relative humidity during a the initial stages of the study. It is clear that a humid environment drastically diminishes the phosphorescence of terbium-treated papers; Figure 37 suggests that the phosphorescence is partially recovered when the relative

humidity drops and the atmosphere is correspondingly drier. The effective use of low surface loadings of terbium phosphor in a varnish-free system ultimately will require a strategem for preventing the physical or chemical changes due to humidity. The stability of the phosphor itself in a humid environment (Table 5, Section 3.2.1) indicates that surface immobilization could be an efficient strategem for the tagged system.

Among the most likely scenarios for phosphor degradation are: (1) simple migration of intact $Tb(DPA)_3^{-3}$ phosphorescent center from the surface into the subsurface body of the stamp; (2) loss of DPA^{-2} by similar chromatographic elution into the subsurface; (3) chemical interactions between the phosphor and components of the coating formulation (e.g., trace transition metals that quench excited terbium); or (4) quenching of terbium by inner sphere coordination with excess molecules of water, a phenomemon previously observed for terbium complexes with sterically smaller ligands than DPA [6].

Experiments wherein pure $Na_3Tb(DPA)_3 \cdot 6H_2O$ was dissolved in water and treated with $CaCO_3$, TiO_2, $Al_2SiO_7 \cdot 2H_2O$, and corn starch (all common paper whiteners or fillers) showed no loss of total solution luminescence as measured by EMI. Experiments in which water-soluble sugars (models for cellulose, the principal component of paper) were stirred with the phosphor, also failed to result either in a diminution of luminescence or a significant change in the FTIR spectrum of the complex. Together these experiments virtually rule out quenching of the phosphor by cellulose or common paper additives.

The possibility of quenching by water <u>in the cellulosic environment</u> was probed by another experimental protocol: a Showboat stamp was enclosed within a quartz flow cell through which was directed a stream of argon saturated with

either H_2O or D_2O. The latter is incapable of causing radiationless deexcitation of terbium [18]. The results of this experiment are set out in Table 28.

TABLE 28

Effects of atmospheric moisture (H_2O or D_2O) on the luminescence of stamp paper coated with $Na_3Tb(DPA)_3$: Harrison method

Time (hrs)	EMI (H_2O)*	EMI (D_2O)*	PMU (H_2O)	PMU (D_2O)
0	1120	1050	176	184
3	750	1098	-	-
6	-	1085	-	-
16	546	-	86	-
22	-	1080	-	176

* Total luminescence as measured in mV on EMI photomultiplier tubes

It is interesting that in the case of D_2O, loss of luminescence is negligible compared to that of H_2O. Since $Na_3Tb(DPA)_3 \cdot 6H_2O$ is completely stable in its luminescence output in air at 100 percent RH and in aqueous solutions, another explanation must be invoked for these results. It is conceivable that the terbium center on paper is less hydrated than in the pure crystals (i.e, water of hydration may be displaced by cellulose units); and that further hydration under H_2O does result in partial quenching. This is not necessarily inconsistent with the stability of crystals in a humid environment, since the crystals undoubtedly are at equilibrium with that environment. As noted above, D_2O would not cause similar quenching.

It is also reasonable to expect that phosphor migration would be promoted by water, acting as a quasi chromatographic eluent, much more efficiently than by the heavier and chemically less labile D_2O. One

consequence might be that the complexed metal suffers exposure to glycosidic linking oxygens that might promote displacement of ligand-to-metal bonds, but this is essentially ruled out by the stability of luminescence in aqueous solutions of the phosphor with cellulose model compounds. Thermodynamic arguments are supportive. The loss of DPA^{2-} would require a more powerful ligating group unless extraordinary entropic factors come into play. The DPA^{2-} ligand is tridentate (as proven by bonding interactions between two oxygens and nitrogen per ligand group in the pure crystals), and simple glycosidic or other cellulose oxygens do not provide more advantageous sites.

There remains to a fair certainty the conclusion that simple phosphor migration is the main reason for phosphorescence decline in a humid environment.

In verification, we have showed that the intact phosphor appears on the reverse side of papers following migration. Aqueous drawdowns of $Na_3Tb(DPA)_3$ were applied to paper LP-46, and it was ascertained by luminescence measurements that the reverse side contained no phosphor (through soaking or adventitious spotting). Emission spectroscopy showed characteristic bands for the complex on one side but not the reverse side. During prolonged exposure to an atmosphere of high humidity, the luminescence of the coated side diminished steadily while that of the reverse side increased until the two sides were equally luminescent. Emission spectra of both sides were identical at this point, indicating that the phosphor traversed the thickness of the paper without structural modification

To complement the results described above with a higher concentration of phosphor on both sides, we placed samples of dry paper flat on the surface of an aqueous solution of phosphor. On standing overnight, the aqueous solute

migrated upward through the paper so that by morning the upper side was heavily coated with phosphor. Attenuated total reflectance IR spectra showed that the phosphor structure remained intact after traversing the thickness of the paper. Figures 38 and 39 illustrate the results of this experiment.

Taken together, all of our evidence supports the idea that if migration of phosphor is prevented or drastically retarded, it should be feasible to produce bright, humidity-stable, varnish-free stamps with minimal quantities of terbium. It remains to be seen whether or not microencapsulation of phosphor, or modification of the DPA^{-2} ligand to ensure its anchorage to cellulose, are reasonable means to accomplish this goal.

Showboat stamps were also evaluated for phosphorescence stability in relatively constant NBS ambient temperture (23°C) and humidity (50%) in a south-facing window, and in a sealed, screw-top jar held at 0° - 4°C in a dark refrigerator. Results are summarized in Table 29. Since the moisture content of the atmosphere is relatively low at this temperature, migration is not an available pathway and cold treatment retards phosphorescence decline.

TABLE 29

Environmental aging of Showboat stamps
coated with aqueous $Na_3Tb(DPA)_3$: Harrison process

South-facing Window.

Time	Principal Color			
(Days)	Red (PMU)	Yellow (PMU)	Blue (PMU)	White (PMU)
0	60	66	90	75
6	54	65	74	68
26	34	39	48	41
30	36	40	55	44
37	42	43	53	45
68	37	38	48	36
124	34	39	46	34
149	34	35	43	37
Refrigerator Storage*				
0	43	48	71	56
3	42	48	68	53
10	41	48	72	54
17	42	48	68	54
22	42	46	68	53
59	42	50	67	52
80	44	46	62	46

* 0° - 4 °C

3.19.2 Harrison and Sons Non-inked Papers.

Plain stamp papers were prepared by the Harrison method described above to yield surfaces treated with phosphor but without the effects of inks, with 0.02% solutions of terbium phosphor, or 3.0% solutions of the manganese-doped zincate. Samples of these were subjected to outdoor aging to combine effects of ambient humidity and sunlight. Other samples were exposed to sunlight filtered through a south-facing office window, overhead laboratory fluorescent lighting, and dark laboratory conditions (in a closed drawer to give protection from overhead light). Figures 40 and 41 illustrate changes in PMU during the time of outdoor exposure (in either sunlight or a closed box) for

the terbium phosphor or zincate treated papers, respectively. Table 30 summarizes changes that occurred in the laboratory and office environments.

TABLE 30

Indoor aging of plain stamp papers coated with aqueous $Na_3Tb(DPA)_3$: Harrison process

Time (days)	South-facing window	Fluorescent light	Darkness
0	188	192	192
10	182	180	187
30	142	164	182
50	100	152	164
80	82	120	132
190	62	90	118

The plain zincate coated paper had an exceedingly high initial phosphorescence (estimated to be higher than 380 PMU) and remained above the measureable 200 PMU in all cases up to day 80. In the office window after 190 days, however, its phosphorescence had diminished to 128, or about 33% of the original, nearly the same percentage loss experienced by the terbium phosphor coated paper.

These data indicate a slow migration of phosphor from the surface of the terbium papers into the body under each environmental condition. In terms of the percent of loss on exposure to outdoor sunlight, both phosphors are about the same after 250 hours, although different mechanisms must be assigned to account for the respective losses. That is, the terbium phosphor migrates inward, whereas the manganese-doped zincate probably experiences dissociation of the components of the complex. Thus one can predict that encapsulation of the terbium phosphor would retard or eliminate the loss of phosphorescence on exposure to sunlight, but should confer little or no protection to the zincate

complex. Again, however, it must be stressed that we have employed accelerated aging conditions which are unrealistically harsh. One does not normally store an uncancelled stamp in direct sunlight for months at a time and the effects of sunlight on either of the phosphors are not particularly alarming.

3.20. Time Constants in Phosphorescence Decay.

Decay curves are shown in Figures 42 to 51. Phosphorescence was measured during 10 ms following illumination for 20 ms, with radiation of 254 nm. Both green (500 to 560 nm) and green-red [red = (600 - 630) nm] phosphorescence measurements are obtained by cancellation detectors in the field [32], and consequently both measurements are of interest here. Europium compounds characteristically luminesce in the red region. Though not directly related to the development of a green phosphor, the subject of this report, europium phosphors represent another rare earth complex of current and future impact in USPS research.

Zinc orthosilicate doped with manganese (Figure 42) displays much longer green and green-red time constants (3.4 and 3.2 ms) than "Tb(DPA)", Section 2.4.1.10, prepared as the complex in THF and coated directly on paper (Figure 43). The terbium phosphor $Na_3Tb(DPA)_3$ in varnish TG-2407-RV, shows relatively long decay times (Figure 44) of 2.0 ms (green) and 1.47 ms (green-red), compared to either "Tb(DPA)" or $Na_3Tb(DPA)_3$ in varnish SVD-4057. Figure 45 is a comparison of the effects of the two varnishes on decay time.

TABLE 31

Figure	Materials	Emission Region	Time Constant (ms), k*
42	Zinc orthosilicate	Green	3.36
	(no varnish)	Green-red	3.19
43	"Tb(DPA)"	Green	1.41
	(no varnish)	Green-red	1.18
44	$Na_3Tb(DPA)_3$	Green	2.00
	(in TG-2407-RV)	Green-red	1.47
45	$Na_3Tb(DPA)_3$	Green	1.42
	(in SVD-4057)	Green-red	1.30
46	$Na_3Tb(DPA)_3$		
	(in TG-2407-RV)	Green-red	1.59
	(in SVD-4057)	Green-red	1.32
47	$Tb(AcAc)_3$**	Green	1.58
	(TG-2407-RV)	Green-red	1.45
48	$Tb(AcAc)_3$**	Green	1.45
	(TB-2407-RV)	Green-red	1.24
49	$Na_3Tb(DPA)_3$***	Green	1.60
	(no varnish)	Green-red	1.48
50	$Na_3Tb(DPA)_3$****	Green	1.65
	(no varnish)	Green-red	1.45
51	Eu_2O_3	Red	1.01
	(ceramic)	Red-green	1.01

* Decay curves; $y=e^{-kx}$, where y = emission intensities, x = time, k = time constant (column 4)

** Following six months' exposure to sunlight in a south-facing office window.

*** Following three months' exposure to sunlight in a south-facing office window.

**** Following three months' storage in a desk drawer.

Figures 46 and 47 are decay curves for $Tb(AcAc)_3$ in varnishes TG-2407-RV and TG-20-T (0.44% Tb) on a clay-filled paper after exposure for about six months to sunlight through a south-facing office window. Figure 48 is the curve obtained for $Na_3Tb(DPA)_3$ in varnish TG-2407-RV (terbium = 0.66%) similarly exposed to sunlight for six months. Figures 49 and 50 are curves obained with $Na_3Tb(DPA)_3$ directly applied to unfilled paper from aqueous solution and aged in sunlight or in the dark for at least three months. The time constants are given in Table 31. Sunlight exposure does not shorten the decay time constant of the phosphor directly applied to the unfilled paper, but it is somewhat shortened in varnish, possibly owing to different coordination geometries in the latter. The time constant stability of the aqueous phosphor on paper is further encouragement for its direct application in the absence of varnish.

The lower decay time constant of europium oxide (red and red-green both give 1.01 ms constants; Figure 51) is probably acceptable for the anticipated use of this phosphor as a tagging ink. Luminescence will be read during the "on" period of the excitation and emission cycle. However, greater brightness and longer decay times may be characteristic of certain europium chelates that would permit using smaller amounts of europium with savings in materials costs.

3.21. Encapsulation Studies.

The first batch (6 gm) of chlorinated rubber-encapsulated $Na_3Tb(DPA)_3 \cdot 6H_2O$ was received from Curtis Thies in early December, 1986. Half of the sample consisted of particles less than 60 μm in diameter, and the remainder ranged from 60-100 μm in size. Examination of the "capsules" under the fluorescence microscope indicated that (1) total luminescence was

essentially equal to that of pure untreated phosphor, and (2) that particles had sharp edges rather than the rounded appearance expected for microcapsules. These facts suggested that most of the phosphor was outside rather than inside the Parlon S-20 coating. Extraction of the product with deionized water led to a diminution of luminescence by a factor of 100 and a strong green emission signal in the eluant, confirming the poor quality of the "capsules". Thies et al. will try their experiments again with polymethylmethacrylate and polyvinylchloride coating materials. Little has ever been attempted in the encapsulation of totally ionic solids, and new technological approaches may be necessary to successfully enclose $Na_3Tb(DPA)_3 \cdot 6H_2O$.

3.22. Terbium Complexes With Other Dicarboxylic Acids

Enhanced phosphorescence quantum yield in $Na_3Tb(DPA)_3$ *vs* $TbCl_3$ or $Tb(NO_3)_3$ is due to ligand-to-metal charge transfer occurring subsequent to excitation of the aromatic ring in 2,6-DPA^{-2}. Facile charge transfer requires a chemical link between the aromatic ligand system and terbium; hence, 2,6-DPA^{-2} with its capacity to bind terbium in a tridentate fashion should be the best of the isomeric pyridine dicarboxylic acids in terms of energy transfer to the tb(III) phosphor. To test this hypothesis, complexes were prepared from $Tb(NO_3)_3$ and the disodium salts of 2,4-DPA and 3,5-DPA, and their total luminescence in the solid state was compared to that observed from $Na_3Tb(DPA)_3 \cdot 6H_2O$. Additionally, complexes of Tb^{+3} and the anions of pyridine-2-carboxylic acid and isophthalic acid were made and examined. Relative luminescence data is summarized in Table 32.

TABLE 32

Luminescence vs ligand structure in TbL_3^{-3}

Ligand	Relative Luminescence
2,6-DPA	98
2,4-DPA	45
3,5-DPA	40
Isophthalate*	54
2-MPA**	31

* dianion of 1,5-benzenedicarboxylic acid; i.e., 2,6-DPA with no nitrogen in the aromatic ring
** pyridine-2-monocarboxylic acid

Indeed, the tridentate 2,6-DPA dianion imparts the greatest luminescent output to Tb^{+3} centers.

3.23. Summary of Ancillary Experiments.

In the course of the final year of this project, USPS personnel requested, and NBS agreed to perform various minor modifications of the original research plan in the form of specific experiments, readily addressed only by NBS and designed to answer significant research questions arising from current results in both laboratory and field applications of $Na_3Tb(DPA)_3$, and to facilitate transfer of the technology to USPS at the end of our contract.

3.23.1. Phosphorescence vs. Particle Size.

Microencapsulation of phosphor particles is a promising technique for their immobilization at stamp surfaces. As yet, few data are available to

indicate the requisite particle size or tolerance. It is probable, however, that the capsule walls will exceed particle dimensions by a factor of ten. For the most efficient use of the phosphor, laboratory experience suggests limiting particle size to less than ten μm on a side. Starting with crystalline $Na_3Tb(DPA)_3 \cdot 6H_2O$ of size range 0.1 to 0.5 mm, successive grinding in a glass mortar, an agate mortar and a Wiggle-Bug dental amalgamator equipped with a stainless steel ball mill produced a series of smaller particles of 10 - 15 μm. The particle size was estimated by epifluorescence microscopic imaging by comparison with a calibrated grid. It was determined that the total luminescence of particles did not depend on particle size over the range studied. Encapsulated particles will be tested for total luminescence by the same technique as soon as they are available.

3.23.2. UV Absorbance of Latex Rubber.

The manufacture of certain paper stocks includes a step in which latex rubber is applied to the substrate surface. Electronic spectra of two latex samples obtained at NBS showed appreciable absorbance in dilute THF solution between 200 - 300 nm, indicating that this component can act as a blocker toward phosphor excitation with radiation of 254 nm wavelength. In fact, virtually all organic additives (whether varnishes or paper additives) also are potential UV blockers, except for aliphatic hydrocarbons, which do not absorb at this wavelength. This is further evidence of the need to immobilize phosphors at the stamp surface in a matrix that does not absorb UV light.

4.0 CONCLUSIONS

Data presented in this and previous reports support the effectiveness of $Na_3Tb(DPA)_3 \cdot 6H_2O$ as a replacement phosphor for the zincate family in the production of varnished postage stamps. The terbium chelate complex imparts a degree of phosphorescence equal to that observed with 20% to 50% by weight of $ZnSiO_4 \cdot Mn$, with terbium levels of only 0.03 percent to 0.012% in BEP varnishes. Varnished stamp facsimiles tagged with terbium are sufficiently stable under all service environments examined to project a suitable product lifetime. At the loading levels indicated, the raw materials necessary to manufacture $Na_3Tb(DPA)_3 \cdot 6H_2O$ are cost effective compared to zincate phosphors, and the projected quantity of terbium to be consumed annually is only around 5% of the total U.S. production. As stated earlier (Section 3.17), and reiterated among recommmendations (Section 5.0, below), a judicious selection of varnish can effect a positive control on the amount of any phosphor used: maximum varnish transparency at the excitation wavelength translates into less phosphor usage. In any event, combinations of the terbium phosphor and BEP varnishes are either homogenous solutions or extrememly small and soft particle dispersions that will not lead to abrasion and equipment problems induced by zincate phosphors at USPS field stations.

Application of $Na_3Tb(DPA)_3 \cdot 6H_2O$ in a varnish-free fashion will require additional process control and molecular design to insure the required PMU value over long shelf storage in humid environments. The complex itself is completely stable to water, but because of its moderate solubility in water, high relative humidity will distribute the phosphor throughout a stamp paper matrix and severely diminish surface phosphorescence.

This migration effect is not observed in varnishes, due to their hydrophobic, organic nature. Zincate phosphors in varnish-free media are also not susceptible to migration because of their insolubility in water. Preliminary work reported here (Section 3.3.11) suggests that improved paper coating strategies may be of value in retarding phosphor migration. For example, a double coating process wherein Na_2DPA is first applied, followed by $Tb(NO_3)_3$, which forms the desired complex in situ, leads to a facsimile that stands up to 100% relative humidity treatment better than one coated with preformed phosphor. Two other means of thwarting migration are immediately apparent: microencapsulation of $Na_3Tb(DPA)_3 \cdot 6H_2O$ with a UV-transparent, hydrophobic shell, or chemical linkage of the terbium center to the cellulosic backbone of the paper. The former approach, which is, in effect, introducing varnish at the small particle level, has proven to be experimentally difficult in the first iteration (Section 3.21). The latter, more chemical approach, will invoke another significant research effort in order to ascertain its feasibility.

The choice of the tridentate ligand, 2,6-DPA dianion, as a partner for Tb^{+3} in phosphor preparation remains indisputably superior in terms of phosphor brightness, tractability and stability. Isomers of 2,6-DPA^{-2} and the closely related isophthalate dianion all form green-emissive complexes with Tb^{+3}, but their luminescence in the solid state and in aqueous solution all are relatively low compared to 2,6-DPA. Polypyrazolylborate complexes of terbium are intractable, insoluble polymers that, at best, are expensive substitutes for zincate phosphors. Terbium-dione complexes are susceptible to radiationless quenching by water, adding a degradation problem to the migration difficulty already discussed.

26. Geoffroy, G. L., Wrighton, M.S., Organometallic Photochemistry, Academic Press, New York, 1979.

27. Union Molycorp, Price Schedule, Lanthanide oxides. April 1, 1986. Schedule reproduced in Appendix 3.

28. Hedrick, J. B., Metals and Minerals, 1982. Minersls Yearbook, Vol. I United States Department of the Interior. U. S. Government Printing Office, Washingon, 1983. pp 705 - 714. Price quotation reproduced in Appendix 4.

29. Aldrich Chemical Company. Quotation for 2,6-pyridine-dicarboxylic acid. Catalog, 1986-87. Page 1145, reproduced in Appendix 5.

30. Alsaadi, B. M., Rossotti, F. J. C., Williams, R. J. P. Studies of lanthanide(III) pyridine 2,6-dicarboxylate complexes in aqueous solution. Structures and ^{1}H nuclear magnetic resonance spectra. J. Chem. Soc. Dalton Transactions, 597 (1980).

31. Copeland, R. A., and Brittain, H. G., Study of the possible self association between 1:1 complexes of lanthanides and pyridine-2,6-dicarboxylic acid. J. Inorg. Nucl. Chem. 43 (10), 2499 (1981).

32. Peng, J. Y. Personal communication.

33. Miller, T. L., and Senkfor, S. I., Spectrofluorometric determination of calcium and lanthanide elements in dilute solution. Anal. Chem. 54, 2022 (1982).

34. Formoso, C., Fluorescence of nucleic acid - terbium(III) complexes. Biochem. Biophys. Res. Comm. 53, 1084 (1973).

35. deJersey, J., and Martin, R. B., Lanthanide probes in biological systems: the calcium binding site of pancreatic elastase as studied by terbium luminescence. Biochemistry 19, 1127 (1980).

36. Epstein, M., Levitzki, A., and Reuben, J., Binding of lanthanides and of divalent metal ions to procine trypsin. Biochemistry 13, 1777 (1974).

37. Davis, S. A., and Richardson, F. S., Circularly polarized luminescence induced by terbium-nucleoside interactions in aqueous solution. J. Inorg. Nucl. Chem. 42, 1793 (1980).

13. Janowski, A., Sadlej, N. Complexes of aurintricarboxylic acid with rare earth metal ions - luminescence properties and energy transfer. J. Luminescence 3, 198 (1970).

14. Fisher, R. P., Winefordner, J. D. Optimization of experimental conditions for spectrofluorimetric determination of europium, samarium, and terbium as their hexafluoroacetylacetone-trioctylphosphine oxide complexes. Anal. Chem. 43 (3), 454, March (1971).

15. King, R.B., Heckley, P. R. Lanthanide nitrate complexes of some macrocylic polyethers. J. Amer. Chem. Soc. 96 (10), 3118 (1974).

16. Bagnall, D. W., Tempest, A. C., Takats, J., Masino, A. P. Lanthanoid poly(pyrazol-1-yl) borate complexes. Inorg. Nucl. Chem. Letters 12, 555 (1976).

17. Trofimenko, S. The coordination chemistry of pyrazole-derived ligands, Chem. Rev. 72 (5), 497 (1972).

18. Donato, H., Jr., Martin, R. B. Dipolar shifts and structure in aqueous solutions of 3:1 lanthanide complexes of 2,6-dipicolinate. J. Am. Chem. Soc. 94 (12), 4129 (1972).

19. Morris, R. E., Flohr, K. W. Characterization of stamp taggants. Report from Artech Corporation for USPS. Contract no. 104230-83-D-1291. January, 1985.

20. Albertson, J. On the crystal structure of hexagonal trisodium tris(pyridine-2,6-dicarboxylato)ytterbate. Acta. Chem. Scand. 26 (3) 1005 (1972).

21. Lautie, A., Limage, M. H., Novak, A. Spectes de vibration et structure de l'acide pyrrolecarboxylique-2 cristallise. Spectochimica Acta 33A, 121 (1977).

22. Paris, M., Thomas, G., and Merlin, J. C. Structure de l'acide picolique. Bull. Soc. Chim. France 707 (1961).

23. Carmona, P. Vibrational spectra and structure of crystalline dipicolinic acid and calcium dipicolinate trihydrate. Sprectrochimica Acta 36A, 705 (1980).

24. Balzani, B., Carassiti, V. Photochemistry of Coordination Compounds, Academic Press, London, 1970.

25. Whan, R. F., Crosby, G. A. Luminescence studies of rare earch complexes: benzoylacetonate and dibenzoylmethide chelates. J. Mol. spect. 8, 315 (1962).

7.0 REFERENCES

1. Haller, W. Production of enamel coated steel sheet luminescence standards for U. S. Postal Service. Contract no.104230-82-T-1612

2. Martin-Marietta Corporation. Improved tagging varnish for postage stamp contract. Prepared for United States Postal Service Research and Development Labs, Rockville, MD, March, 1982.

3. Peng, J. Y., Surface adhesion mechanisms of tagging phosphors on the surface of postage stamps. Materials Division, Office of Postal Technology Research, Rockville, MD, December, 1979.

4. Moeller, T. "The Lanthanides," Chapter 44 in Comprehensive Inorganic Dickenson, eds., Pergamon Press, London, 1973.

5. a) Stites, J. G., McCarty, C. N., Quill, L. L. VIII. The rare earth rare earth acetylacetonates. J. Am. Chem. Soc.70, 3142 (1948) and references therein. (b) Weissman, S. I. J. Chem. Phys. 10, 214 (1942)

6. Parks, E. J., Olson, G.J., Brinckman, F. E. Environmental factors and mechanisms controlling degradation of terbium(III) chelates: development of effective new terbium phosphors for postage stamsp. NBSIR 85-3132(R) for USPS. March, 1985.

7. Halverson, F., Brinen, J. S., Leto, J. R., Photoluminescence of lanthanide complexes. II. Enhancement by an insulating sheath. J. Chem. Phys. 41 (1) 157 (1957).

8 Parks, E. J., Olson, G. J., Johannesen, R. B., Brinckman, F. E. Environmental factors and mechanisms controlling degradation of terbium(III) chelates: development of effective new terbium phosphors for postage stamps. Contract No. 104320-82-T-1612 with USPS, August, 1983.

9. ibid., MO6, September, 1984.

10. ibid., MO8, December, 1985.

11. Parker, G. A., "Hydrogen Peroxide in Organic Solvents," in Colorimetric Determination of Nonmetals, D. F. Boltz and J. A. Howell, eds. John Wiley and Sons, N.Y. 1978. pp 314 - 315.

12. Taketetsu, T. Spectrofluorometric determination of terbium, europium and samarium with pivaloyltrifluoroacetone and tri-n-octylphosphine oxide in micellar solution of monoxylethylene dodecylether. Talanta 29, 397 (1982).

6.0 ACKNOWLEDGMENTS

The authors are indebted to Mr. Todd K. Trout, of NBS and the University of Maryland, for valuable technical assistance in developing new measurement techniques for excitation and emission spectra and thin layer chromatography. Dr. Wolfgang Haller of NBS directed the preparation of a green luminescent ceramic plate that served as a standard for comparing various luminiphors during the course of this project. We thank Ms. Marietta Nelson of the Information and Resources Services Division, NBS, for assistance in designing an automated literature search on relevant developments in lanthanide technology. We thank Dr. Curtis Thiess of Washington University, St. Louis, MO. for performing preliminary basic research on the encapsulation of aqueous $Na_3Tb(DPA)_3 \cdot 6H_2O$. Drs. G. J. Olson and R. B. Johannesen, both of NBS, developed automation technology for quantifying the luminescence of phosphors in real time. We acknowledge the assistance of Dr. K. L. Jewett and Mr. W. R. Blair of NBS who provided both technical advice and laboratory assistance in preparing liquid chromatograms of terbium and europium phosphors. We are indebted to Dr. Rance Velapoldi of NBS for valued discussions of lanthanide coordination phosphors and phosphorescence.

6.1 Disclaimer.

Certain suppliers of chemicals and equipment are identified by name in this report in order to specify the experimental conditions. In no case does this imply endorsement or recommendation by the National Bureau of Standards, nor does it imply that the particular brands of chemicals and equipment are necessarily the best for the purpose.

5.0 RECOMMENDATIONS

The tagging combination of $Na_3Tb(DPA)_3 \cdot 6H_2O$ and organic varnishes deserves strong consideration for implementation by USPS, provided that varnishes are sufficiently tailored to provide maximum transparency at the wavelength of excitation, currently 254 nm. The varnish TG-20-T is unique among those currently used by BEP in that it absorbs only 4% of incident 254 nm radiation in a 0.5 mil film. The remaining varnishes absorb moderately to completely at 254 nm, and their use will require inordinate amounts of any phosphor if the 254 nm status quo is maintained.

In varnish-free media, the migration of $Na_3Tb(DPA)_3 \cdot 6H_2O$ induced by atmospheric water vapor has to be minimized for completely successful application. The preliminary encapsulation experiments under way at Washington University, St. Louis, should be further pursued, even though the first attempt utilizing chlorinated rubber (Parlon S-20) failed to yield a useful product. Research into paper coating strategies and ligand-cellulose anchoring chemistry should be undertaken in a serious effort to use the terbium phosphor without varnish.

Implementation of terbium phosphor, with or without varnish, must consume a minimal amount of terbium to be cost effective. To this end, an examination of the possibility of tuning up facer - cancellers to excite the complex at around 300 nm should be undertaken, pending our ability to quantitatively show that excitation is more efficient in this wavelength regime. A shift in excitation wavelength may indeed be beneficial for the optimization of zincate phosphors as well (Section 3.14.1.1). The UV blockage inherent in varnishes is less at 300 nm than at 254 nm (except for varnish UV-8) and it may be possible to use an almost vanishingly small amount of phosphor for acceptable PMU response if the wavelength change is made.

Postal service facer-canceller machinery currently operates via exitation by the 254 nm line of a mercury lamp, and emission readings run in the 500 - 600 nm region. Data in Section 3.1.4 for $Na_3Tb(DPA)_3$ and in Section 3.14.1.1 for zincate phosphors, supported by literature examples [34-37], suggest that excitation closer to 300 nm would lead to enhanced phosphorescence intensity in all cases. Quantitation of these observations will ultimately depend on photon flux vs. wavelength data that we are soon to receive from Zeiss.

Appendix 1: Figure Captions

Figure 1. Schematic cross section of a stamp.

Figure 2. Emission spectra of $ZnSiO_4 \cdot Mn$ in the solid state, and on Harrison and Sons tagged paper (3% loading). λ_{exc} = 254 nm.

Figure 3. Time line diagram for original USPS/NBS contract.

Figure 4. Photomicrograph of a production stamp surface ("Science and Industry") showing large, luminescent particles of $ZnSiO_4 \cdot Mn$ (125x).

Figure 5. Photomicrograph of varnish TG-2407-RV containing $Na_3Tb(DPA)_3 \cdot 6H_2O$ applied to LP-46 paper (250x).

Figure 6. Schematic drawing of apparatus for epifluorescence analysis of chromatographic eluants.

Figure 7. Schematic drawing of the Zeiss epifluorescence system used in the current study.

Figure 8. Pyridine-2,6-dicarboxylic acid (dipicolinic acid, H_2DPA).

Figure 9. Pluto drawing of the dipicolinic acid dianion (DPA).

Figure 10. Pluto drawing of the asymmetric unit present in solid $Na_3Tb(DPA)_3 \cdot 6H_2O$.

Figure 11. Fourier transform infrared (FTIR) spectrum of H_2DPA via diffuse reflectance in KBr.

Figure 12. FTIR spectrum of Na_2DPA via diffuse reflectance in KBr.

Figure 13. FTIR spectrum of $Na_3Tb(DPA)_3 \cdot 6H_2O$ via diffuse reflectance in KBr.

Figure 14. FTIR spectrum of $Tb(HDPA)_3 \cdot 2H_2O$ via diffuse reflectance in KBr.

Figure 15. UV spectra of $Na_3Tb(DPA)_3 \cdot 6H_2O$ (dotted line) and H_2DPA (solid line) in water. Absorbance values are not relative.

Figure 16. Emission spectra of $Na_3Tb(DPA)_3 \cdot 6H_2O$ in the solid state and in water. λ_{exc} = 254 nm.

Figure 17. Excitation spectrum of aqueous $Na_3Tb(DPA)_3$. λ_{em} = 546 nm

Figure 18. Luminescence vs DPA:Tb ratio in aqueous solutions of Na_2DPA + $Tb(NO_3)_3$. Concentrations are of Tb (8.33×10^{-3} - 8.33×10^{-5} M). λ_{exc} = 254 nm.

Figure 19. Relative luminescence vs irradiation time (λ = 254 nm) for various aqueous ratios of DPA:Tb.

Figure 20. Relative luminescence vs irradiation time (λ = 254 nm) for solid $ZnSiO_4 \cdot Mn$.

Figure 21. Phosphorescence on LP-46 paper of various DPA:Tb ratios in varnish SVD-4057. Drawdown = 1.0 mil. λ_{exc} = 254 nm.

Figure 22. Correlation of phosphorescence (PMU) and total luminescence (mV, EMI units) for various Tb concentrations in varnish SVD-4057. Drawdown = 1.0 mil. DPA:Tb held at 6:1. λ_{exc} = 254 nm.

Figure 23. Phosphorescence vs DPA:Tb ratio on LP-46 tagged with aqueous DPA/Tb samples. Drawdown = 1.0 mil. λ_{exc} =254 nm.

Figure 24. Phosphorescence vs Tb concentration in 6:1 DPA:Tb samples applied as aqueous solutions to papers LP-46 and LP-54. Drawdown = 0.5 mil. λ_{exc} = 254 nm.

Figure 25. Phosphorescence vs Tb concentration on unfilled and clay-filled papers treated consecutively with aqueous Na_2DPA and $Tb(NO_3)_3$. DPA:Tb = 6:1. Drawdown = 0.5 mil. λ_{exc} =254 nm.

Figure 26. Total luminescence of $Na_3Tb(DPA)_3$ tagged paper (Harrison and Sons, 0.02% Tb) at two excitation wavelengths compared to total luminescence of an unfilled, untagged paper (LP-46).

Figure 27. SCX chromatograms of aqueous solutions of Na_2DPA and $Tb(NO_3)_3$ in molar ratios from 0.9:1 to 7.4:1. Luminescence vs retention time.

Figure 28. SCX chromatography of various DPA:Tb ratios in aqueous solution. Eluant analysis shows luminescence maximum at 8:1.

Figure 29. SCX (open circles) and flow injection analysis (closed circles) on aqueous solutions of varying DPA:Eu rations. Luminescence mole ratio.

Figure 30. Reverse phase chromatographic results on aqueous solutions of varying DPA:Tb ratios. Luminescence vs mole ratio.

Figure 31. Thin layer chromatograms (SiO_2) illustrating elution of DPA-Tb complexes with water. Bright areas are due to luminescence excited at 254 nm.

Figure 32. Normalized emission spectra of $ZnSiO_4 \cdot Mn$, $ZnS \cdot Cu$, and $ZnO \cdot X$ in the solid state. λ_{exc} = 254 nm.

Figure 33. Emission spectrum of solid precipitated from aqueous mixtures of terbium nitrate and sodium tris(pyrazol-1-yl)borate. λ_{exc} = 254 nm.

Figure 34. Emission spectra of sodium tetrakis(imidazol-1-yl)borate, and the complex formed between it and terbium nitrate. Solid state spectra. λ_{exc} = 254 nm.

Figure 35. UV spectra of varnishes used by the Bureau of Engraving and Printing. Samples drawn down at 0.5 mil thickness and cured on a quartz cuvette.

Figure 36. Phosphorescence vs time curves for Harrison and Sons terbium tagged "Showboat" trading stamps. Outdoor aging during June, July, 1986 in Montgomery County, MD. Principle colors: (·) = yellow, (o) = blue, (*) = green, ( ) = red.

Figure 37. Phosphorescence (lower curve) and relative humidity (upper curve) vs time relations observed during outdoor aging (June, 1986; Montgomery Country, MD) of Harrison and Sons uninked Tb-tagged paper.

Figure 38. Attenuated total reflectance (ATR) FTIR spectrum (lower curve) of the reverse side of a Tb-tagged paper sample held in high relative humidity. Upper curve illustrates diffuse reflectance FTIR of genuine $Na_3Tb(DPA)_3 \cdot 6H_2O$ in KBr.

Figure 39. Attenuated total reflectance (ATR) FTIR spectrum of the non-exposed side of an unfilled paper floated for 16 hrs on an aqueous solution of $Na_3Tb(DPA)_3 \cdot 6H_2O$. (*) = strong carbonyl stretches due to migrated $Na_3Tb(DPA)_3$.

Figure 40. Phosphorescence and % phosphorescence loss vs time for outdoor exposure of Harrison and Sons uninked Tb paper (0.02% Tb). Open circles = samples exposed to direct sunlight on NBS grounds in April-May, 1986. Closed circles = samples outdoors but in the dark for the same time period.

Figure 41. Phosphorescence and % phosphorescence loss vs time for outdoor exposure of Harrison and Sons uninked $ZnSiO_4 \cdot Mn$ paper (4%). Exposure to direct sunlight on NBS grounds in April-May, 1986.

Figure 42. Phosphorescence decay curves for solid $ZnSiO_4 \cdot Mn$.

Figure 43. Phosphorescence decay curves for "Tb(DPA)(THF)" complex on unfilled paper.

Figure 44. Phosphorescence decay curves for $Na_3Tb(DPA)_3 \cdot 6H_2O$ in varnish TG-2407-RV on unfilled paper.

Figure 45. Comparative phosphorescence decay curves for $Na_3Tb(DPA)_3 \cdot 6H_2O$ in varnishes TG-2407-RV and SVD-4057 on unfilled papers.

Figure 46. Phosphorescence decay curves for $Tb(acac)_3$ in varnish TG-2407-RV on unfilled paper after 6 months of aging in a south facing window.

Figure 47. Phosphorescence decay curves for $Tb(acac)_3$ in varnish TG-20-T on unfilled paper after 6 months of aging in a south facing window.

Figure 48. Phosphorescence decay curves for $Na_3Tb(DPA)_3 \cdot 6H_2O$ in varnish TG-2407-RV on unfilled paper after 6 months of aging in a south facing window.

Figure 49. Phosphorescence decay curves for $Na_3Tb(DPA)_3 \cdot 6H_2O$ applied in aqueous solution to unfilled paper after 3 months of aging in a south facing window.

Figure 50. Phosphorescence decay curves for $Na_3Tb(DPA)_3 \cdot 6H_2O$ applied in aqueous solution to unfilled paper after 3 months indoors in the dark.

Figure 51. Phosphorescence decay curves for Eu_2O_3 solid on a ceramic plate.

Appendix 2: Table Headings

1. Designation of papers used in accelerated aging and luminescence studies.

2. Composition of BEP varnishes.

3. Bond lengths in $[Tb(DPA)_3]^{-3}$.

4. Bond angles in $[Tb(DPA)_3]^{-3}$.

5. Aging of $Na_3Tb(DPA)_3 \cdot 6H_2O$ crystals at 95-100% R.H. and 27°C.

6. Changes in luminescence with time at high R.H. and 31°C.

7. pH effects on Tb^{+3}/DPA^{-2} emission.

8. Stability of aqueous solutions of $Na_3Tb(DPA)_3$.

9. Luminescence of stamp papers coated with varnish TG-20-T tagged with $Na_3Tb(DPA)_3 \cdot 6H_2O$.

10. Phosphorescence of varnish coatings tagged with $Na_3Tb(DPA)_3$ by sonication.

11. Phosphorescence of varnish coated stamp papers tagged with $Na_3Tb(DPA)_3$ in formamide or water.

12. Reproducibility of phosphorescence when liquid taggant is mixed into varnish SVD-4057.

13. Phosphorescence of stamp papers coated with several $Na_3Tb(DPA)_3$-tagged varnishes of differing thickness.

14. Blocking of phosphorescence by opaque varnish.

15. Comparability of solutions of taggant made with crystalline phosphor, or with terbium nitrate and ligand in water.

16. Comparability of taggant solutions made with crystalline phosphor, or solutions of metal and ligand applied to paper.

17. Phosphorescence as a function of terbium absorption.

18. Phosphorescence of dye treated stamps coated with terbium phosphor.

19. Emission intensities for green phosphors.

20. Phosphor aging studies in varnish CR-32974 applied (0.5 mil) to 6-color experimental stamps.

21. Protracted sunlight exposure in a south facing window of $Tb(acac)_3$-doped varnish TG-20-T.

22. Protracted sunlight exposure in a south facing window of $Tb(acac)_3$-doped varnish TG-2407-RV.

23. Protracted ambient stability of liquid taggant containing $Na_3Tb(DPA)_3/DPA^{-2}$, coated on three stamp papers.

24. Protracted exposure to ambient conditions of $Na_3Tb(DPA)_3$-tagged varnish TG-20-T on inked or pigmented stamp paper.

25. Protracted exposure to ambient conditions of $Na_3Tb(DPA)_3$-tagged varnish TG-2407-RV on pigmented paper.

26. Protracted exposure to ambient conditions of $Na_3Tb(DPA)_3$-tagged varnish SVD-4057 on pigmented paper.

27. Protracted ambient exposure of 5 tagged varnish coatings on 3 stamp papers.

28. Effects of atmospheric moisture (H_2O or D_2O) on the luminescence of stamp paper coated with $Na_3Tb(DPA)_3$: Harrison method.

29. Environmental aging of "Showboat" stamps coated with aqueous $Na_3Tb(DPA)_3$: Harrison process.

30. Indoor aging of plain stamp papers coated with aqueous $Na_3Tb(DPA)_3$: Harrison process.

31. Decay constants for selected phosphor/environment/aging combinations.

32. Luminescence <u>vs</u> ligand structure in TbL_3^{-3}.

Appendix 3

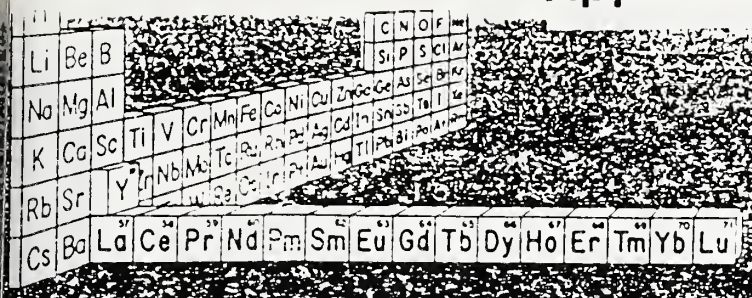

Price schedule

LANTHANIDE OXIDES

April 1, 1986

Code No.	Oxide	Purity (%)	Lb in Std Container	1 Lb to Standard	Standard Container
5000	EUROPIUM	99.99	25	$ 800.00	$ 725.00
5200	LANTHANUM	99.99	300	7.50	7.00
5310	CERIUM	95.0	200	5.25	4.50
5350	CERIUM	99.0	200	8.75	8.00
5400	NEODYMIUM	96.0	300	5.50	5.00
5410	NEODYMIUM	99.9	50	45.00	40.00
5500	PRASEODYMIUM	96.0	300	17.50	16.80
5600	YTTRIUM	99.99	50	55.00	52.50
5700	GADOLINIUM	99.9	55	60.00	55.00
5775	GADOLINIUM	99.99	55	65.00	60.00
5780	GADOLINIUM	99.99	55	70.00	65.00
5810	SAMARIUM	96.0	55	40.00	35.00
8100	TERBIUM	99.9	55	400.00	375.00
8250	DYSPROSIUM	85.0	50	45.00	40.00

$20,625 for 55 lb Tb_4O_7

FOB: Louviers, Colorado
Mtn. Pass, California
York, Pennsylvania

Terms: Net 30 days

Minimum Order: $50

Prices subject to change without notice

THE LANTHANIDE MINERAL

MOLYCORP

Appendix 3a

Product (oxide)	Percent[1] purity	Quantity (pounds)	Price per pound
Cerium	99.9	1-199	$8.75
Europium	99.99	1-24	900.00
Gadolinium	99.99	1-49	65.00
Lanthanum	99.99	1-299	7.50
Neodymium	99.99	1-49	80.00
Praseodymium	95.0	1-299	17.50
Samarium	95.0	1-109	80.00
Terbium	99.99	1-49	575.00
Yttrium	99.99	1-49	50.00

[1]Purity expressed as percent of total REO.

Nominal prices for various rare-earth products were quoted by Research Chemicals, net 30 days, f.o.b. Phoenix, Ariz., effective October 1, 1982:

Element	Oxide[2] price per kilogram	Metal[3] price per kilogram
Cerium	$20	$125
Dysprosium	110	300
Erbium	200	650
Europium	1,300	7,500
Gadolinium	140	485
Holmium	650	1,600
Lanthanum	10	125
Lutetium	5,200	14,200
Neodymium	80	250
Praseodymium	130	310
Samarium	130	330
Terbium	1,200	2,800
Thulium	2,600	5,000
Ytterbium	225	575
Yttrium	94	430

[1]Minimum 99.9% purity, 1- to 20-kilogram quantities.
[2]Lagot form, 1 to 6 kilograms, from 99.9% grade oxides.

FOREIGN TRADE

Exports of ferrocerium and other pyrophoric alloys containing rare earths totaled 24,383 kilograms in 1982, a 145% increase from the 1981 level. Major destinations were the Republic of Korea (50%), Japan (30%), and Hong Kong (7%).

Exports of rare-earth metal ores, excluding monazite, decreased 50% from the 1981 total of 9,586,505 kilograms to a total of 4,836,389 kilograms in 1982. Exports in 1982 were valued at $11,347,652. Major destinations were Japan (53%), the Federal Republic of Germany (24%), and the United Kingdom (8%).

Exports of thorium ore, including monazite, decreased 29% in 1982 from the 1981 level. France received all of the reported total of 91,508 kilograms valued at $103,356.

Australia has been the principal import source of monazite for the United States since 1977. Imports of cerium oxide increased substantially in 1982 compared with that of 1981. France remained the largest source of imported rare-earth oxides. Imports of rare-earth alloys, including mischmetal, were significantly lower in 1982 as a result of the depressed state of the domestic steel industry. Brazil continued to be the leading supplier of imported rare-earth alloys.

Table 2.—U.S. imports for consumption of monazite, by country

Country	1978		1979		1980		1981		1982	
	Quantity (metric tons)	Value (thousands)	Quantity (metric tons)	Value (thousands)	Quantity (metric tons)	Value (thousands)	Quantity (metric tons)	Value (thousands)	Quantity (metric tons)	Value (thousands)
Australia	5,018	$1,154	5,656	$1,501	4,933	$1,749	7,469	$2,158	6,600	$2,830
Liberia	53	<1	--	--	--	--	--	--	--	--
Malaysia	1,257	255	561	161	215	101	--	--	603	240
South Africa, Republic of	--	--	3	2	--	--	--	--	--	--
Thailand	767	193	37	13	--	--	--	--	--	--
Total	6,995	1,603	6,287	1,677	5,148	1,850	7,469	2,158	7,203	3,070
P.EO content[e]	3,847	XX	3,458	XX	2,831	XX	4,108	XX	3,962	XX

[e]Estimated. XX Not applicable.

Taken from Minerals Yearbook, Vol I. Metals and Minerals, 1982. United States Department of the Interior. U.S. Government Printing Office, Washington, 1983. pp 705 - 714. James B. Hedrick, author.

Appendix 3b

TO: Ed Parks 31 July 84

FROM: Marietta Nelson, Librarian
Information Resources and Development Division
National Bureau of Standards

SUBJ: World production of Terbium

I talked to James Hedrick of the U.S. Bureau of Mines, who wrote the chapter on RARE EARTHS in "Minerals Yearbook."

He claims that the figures for total production are almost impossible to obtain, because the companies don't want to make the information public. In addition, they often don't separate Terbium from other rare earths.

The best he can do is to give you the estimated figures for production at the largest producer of separated Terbium (it's the second largest for rare earth production). It's called S. A. Rhone-Poulenc, and is located in France. When the company is working at full production, it produces about 8 metric tons of Terbium Oxide (Tb_4O_7) per year. Its U.S. subsidiary is Rhone-Poulenc of Monmouth Junction, N.J. (the mining operation is in Freeport, Texas). The U.S. branch hopes to produce 6.4 metric tons of Terbium Oxide when it gets into full operation.

Mr Hedrick says that the producers hope to increase their capacity by 80%, if the demand can be sustained and increased.

He has not able to give me export/import figures--I could possibly try elsewhere, but I have a feeling that I would keep getting referred back to Mr Hedrick!

Let me know if you want me to try elsewhere, or if you have any specific questions that I could ask Mr Hedrick.

Appendix 3c

To order
Toll-free USA/ Canada
800-558-9160

Technical Inquiries/ other correspondence
Toll-free USA/ Canada
800-231-8327

Telephone 414-273-3850
TWX 910-262-3052 Aldrichem Mi
Telex 26 843 Aldrich MI
FAX 414-273-4979

Aldrich Chemical Company, Inc.
940 West Saint Paul Avenue
Milwaukee, Wisconsin 53233 USA

P6,380-8 ★ **2,6-Pyridinedicarboxylic acid, 99%** [*499-83-2*] 25g 10.00
(dipicolinic acid) 100g 28.80
500g 107.10

FW 167.12 mp 248-250° (dec.) *Bell.* 22,154
NMR 2(2),670A *FT-IR* 1(2),791D *MSD Book* 1,1561D
Disp. A *IRRITANT*

Chelating agent. Competitive inhibitor of glutamate dehydrogenase[1] and an enzymatic inhibitor.[2,3] Also induces sporulation.[4] The sodium salt rapidly removes the catalytically essential zinc ion from the metalloenzyme carbonic anhydrase.[5,6] Binds Mn^{++} without proton release to allow dye coupling.[7] 1. *Biochim. Biophys. Acta*, 258, 343 (1972). 2. *J. Biol. Chem.*, 249, 6817 (1974). 3. *J. Bacteriol.*, 117, 1017 (1974). 4. *J. Biol. Chem.*, 244, 5636 (1969). 5. *J. Biochem. Tokyo*, 79, 43 (1976). 6. *Biochemistry*, 19, 2045 (1980). 7. *Ibid.*, 20, 2226 (1981).

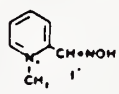
P6,020-5


P6,200-3

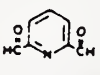
25,600-5


P6,320-4

FIGURE 1

Schematic diagram of a stamp

(not drawn to scale)

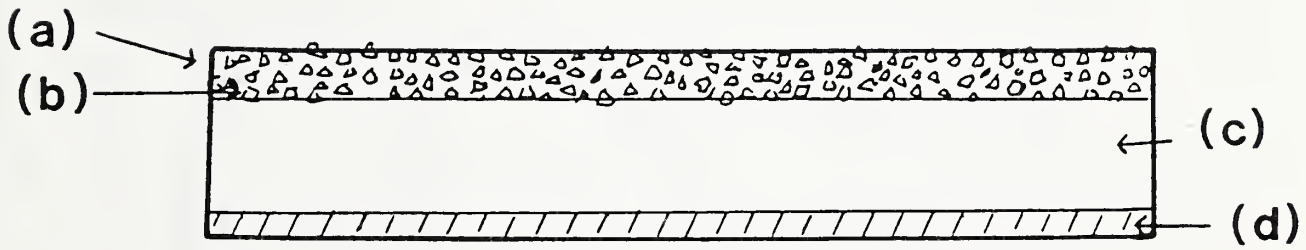

a) Varnish layer, 0.0125 mm (0.5 mil) in thickness

b) Particulate phosphor ($ZnSiO_4$:Mn) immiscible with organic varnish

c) Paper substrate, usually prepared from chemical wood pulp; may be clay filled.

d) Gum backing.

FIGURE 2

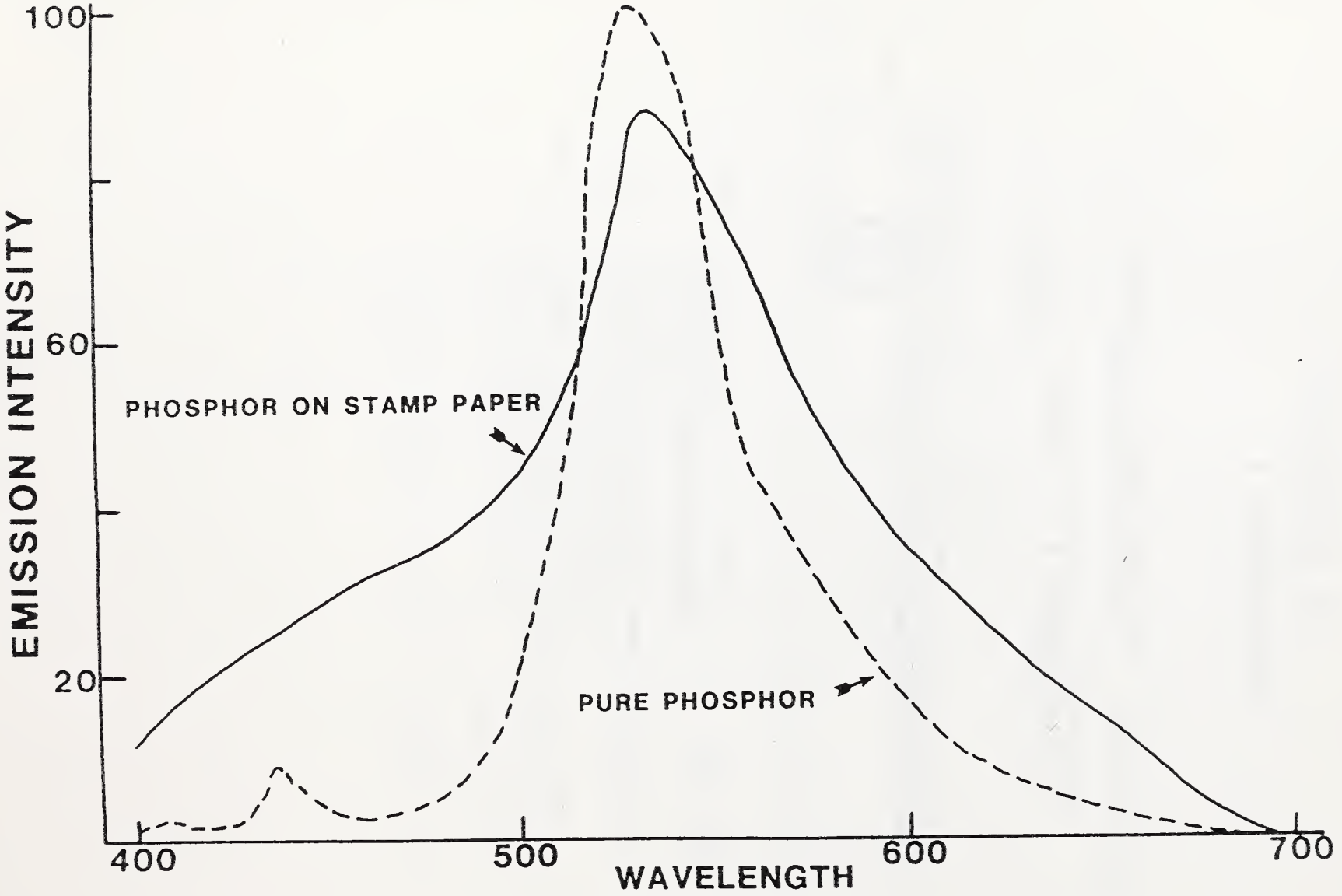

Emission spectra of $ZnSiO_4 \cdot Mn$ in the solid state, and on Harrison and Sons tagged paper (3% loading). λ_{exc} = 254 nm.

FIGURE 3

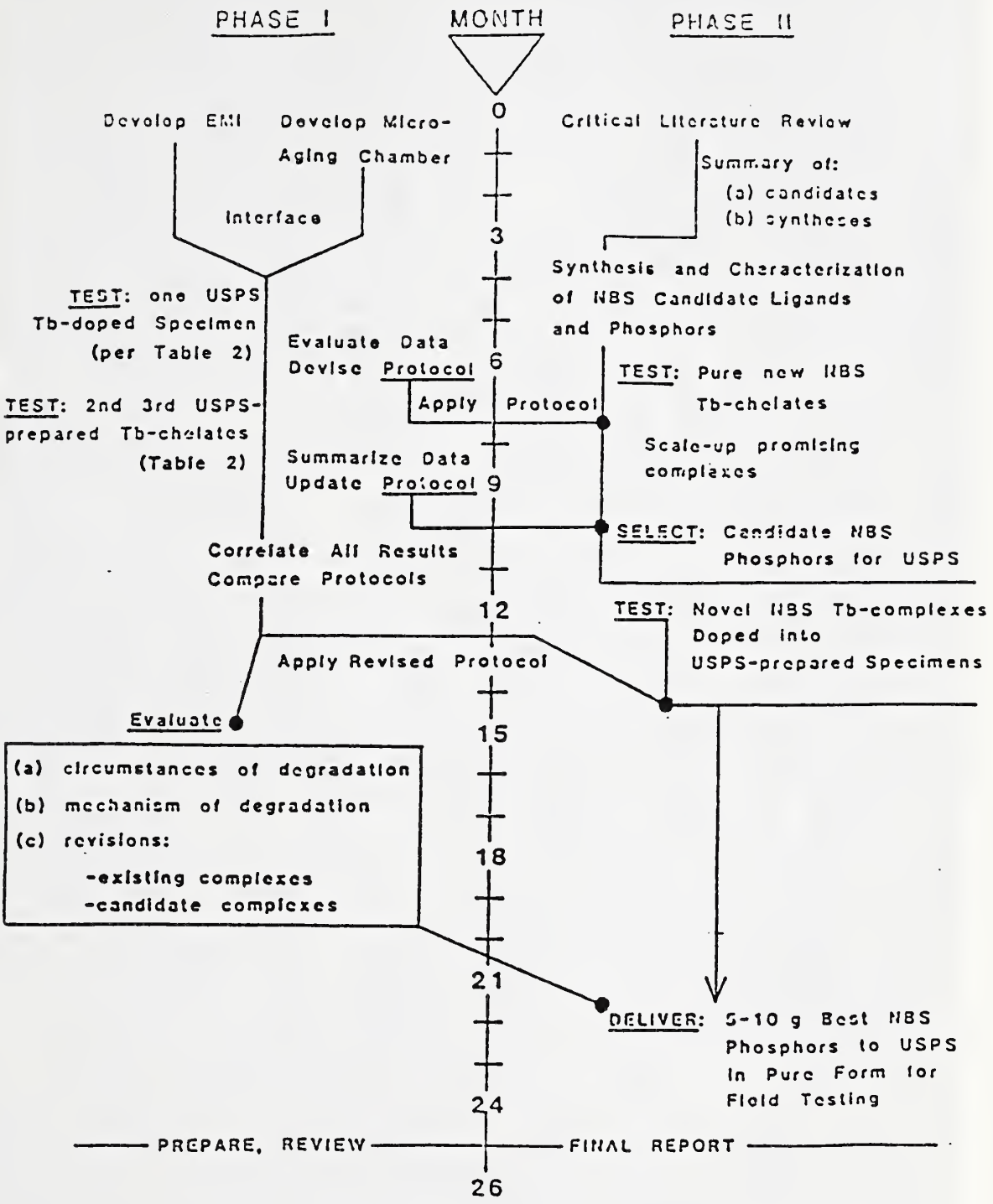

Time line diagram for original USPS/NBS contract.

FIGURE 4

Photomicrograph of the surface of a current stamp ("Science and Industry"), showing surface crystals. Expansion 125.

FIGURE 5

Photomicrograph of varnish TG-2407-RV containing $Na_3Tb(DPA)_3 \cdot 6H_2O$ applied to LP-46 paper (250x).

FIGURE 6

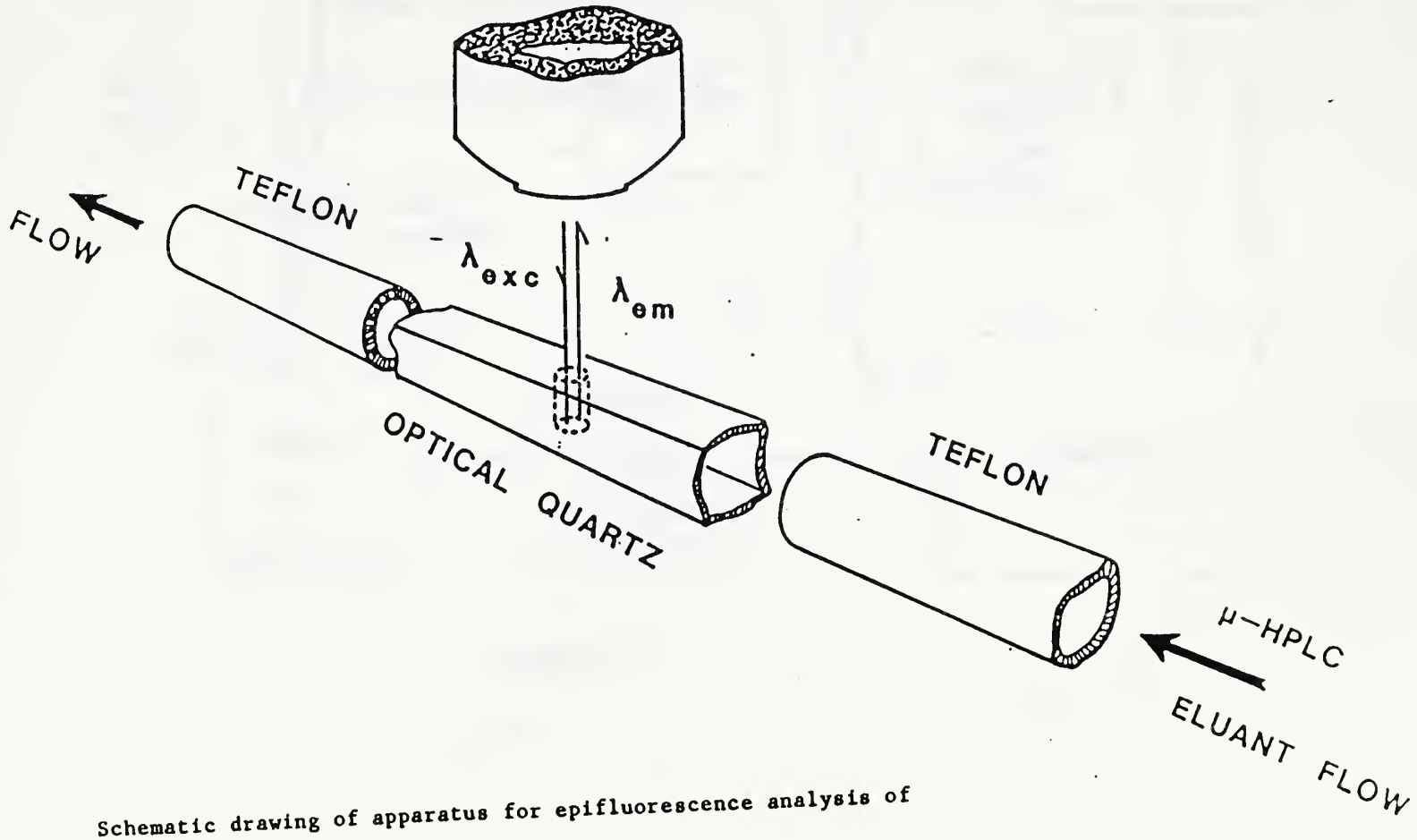

Schematic drawing of apparatus for epifluorescence analysis of chromatographic eluants.

FIGURE 7

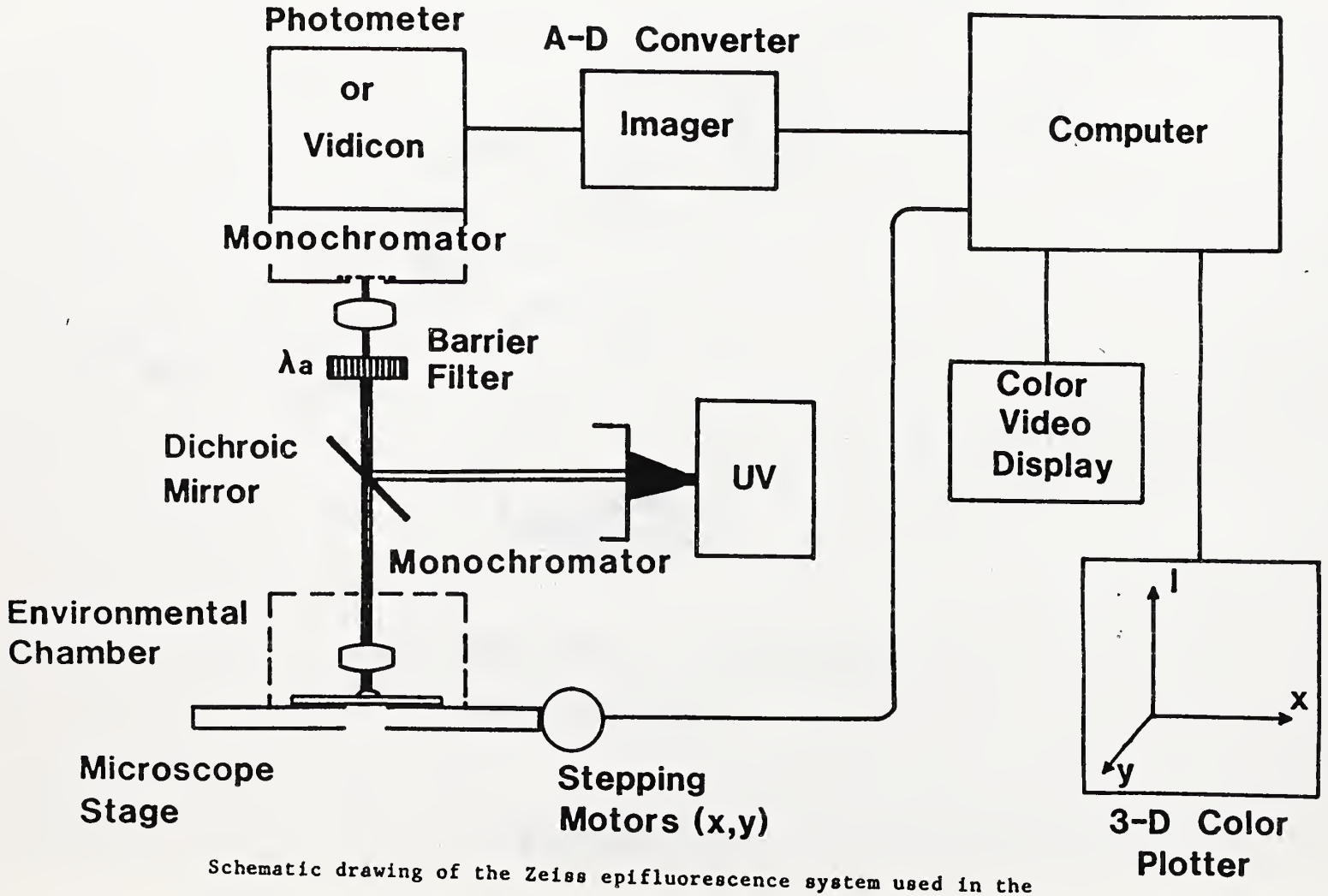

Schematic drawing of the Zeiss epifluorescence system used in the current study.

FIGURE 8

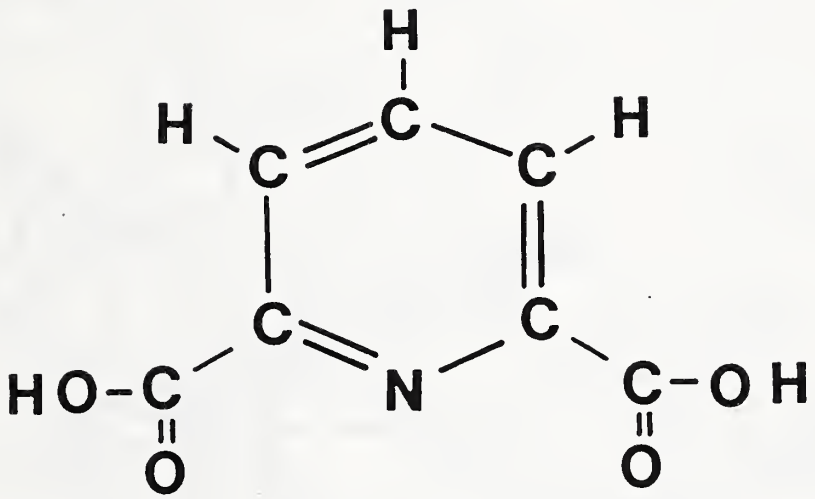

Pyridine-2,6-dicarboxylic acid (dipicolinic acid, H_2DPA).

FIGURE 9

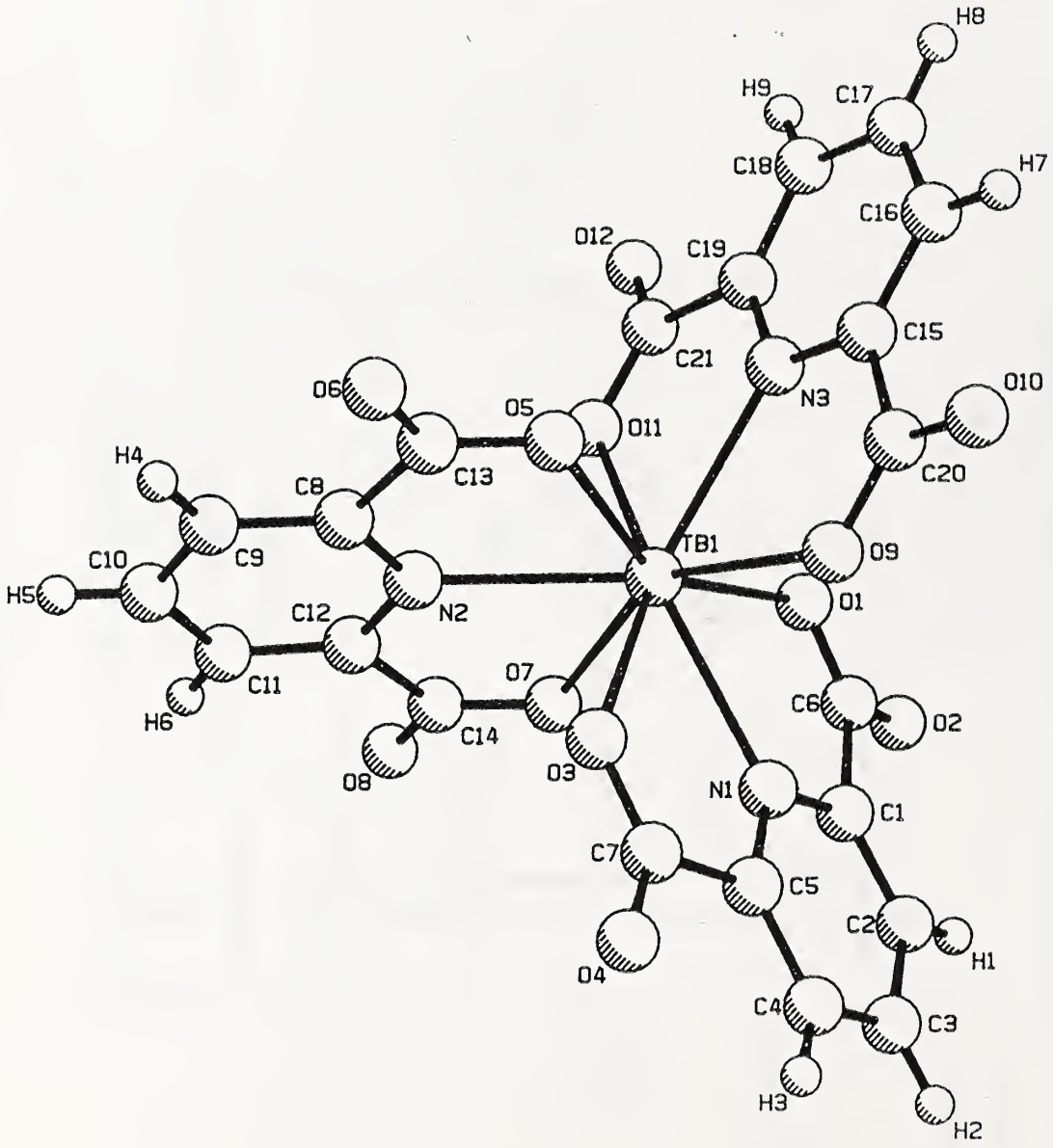

Pluto drawing of the dipicolinic acid dianion (DPA).

FIGURE 10

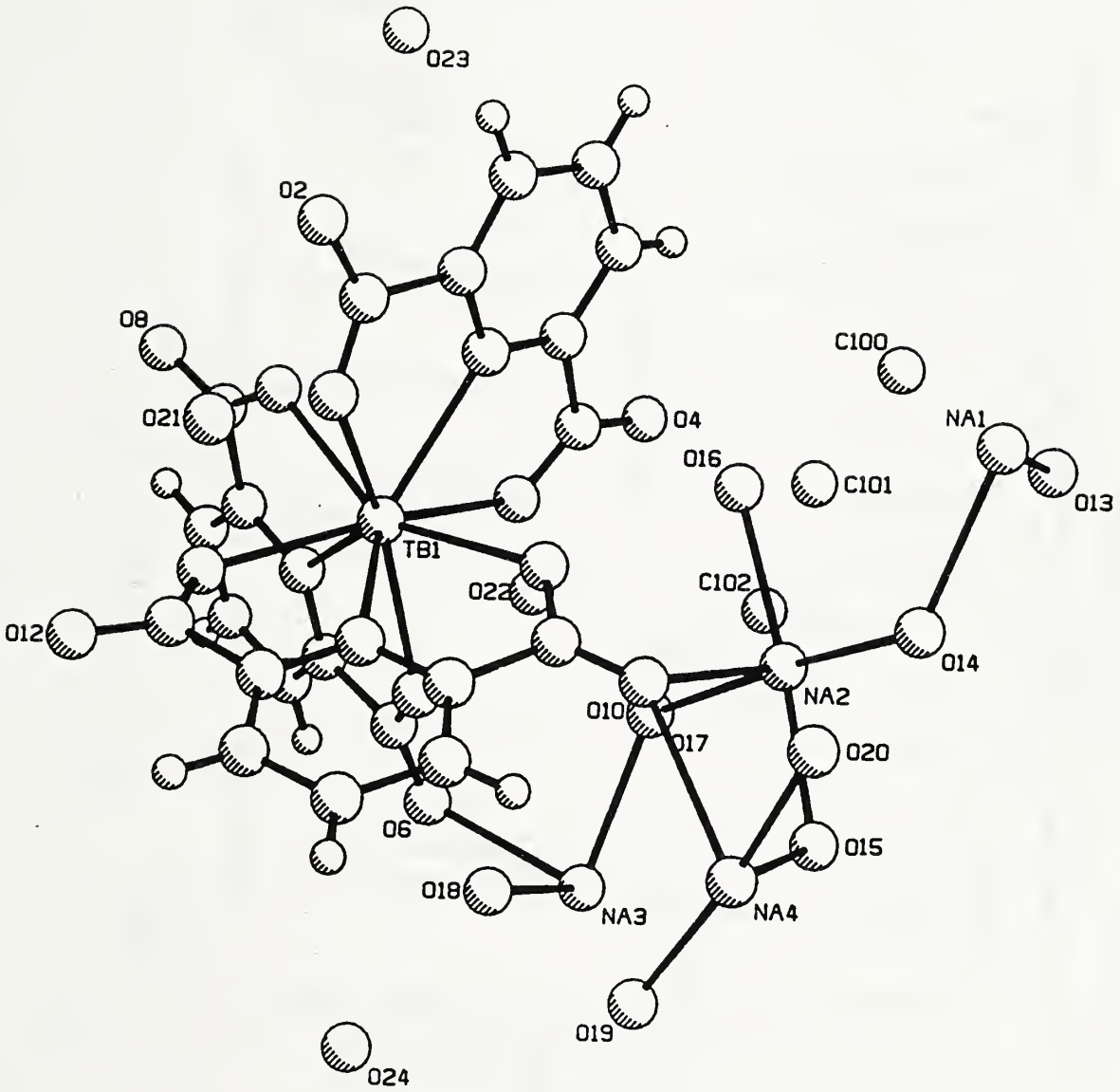

Pluto drawing of the asymmetric unit present in solid $Na_3Tb(DPA)_3 \cdot 6H_2O$.

FIGURE 11

Fourier transform infrared (FTIR) spectrum of H_2DPA via diffuse reflectance in KBr.

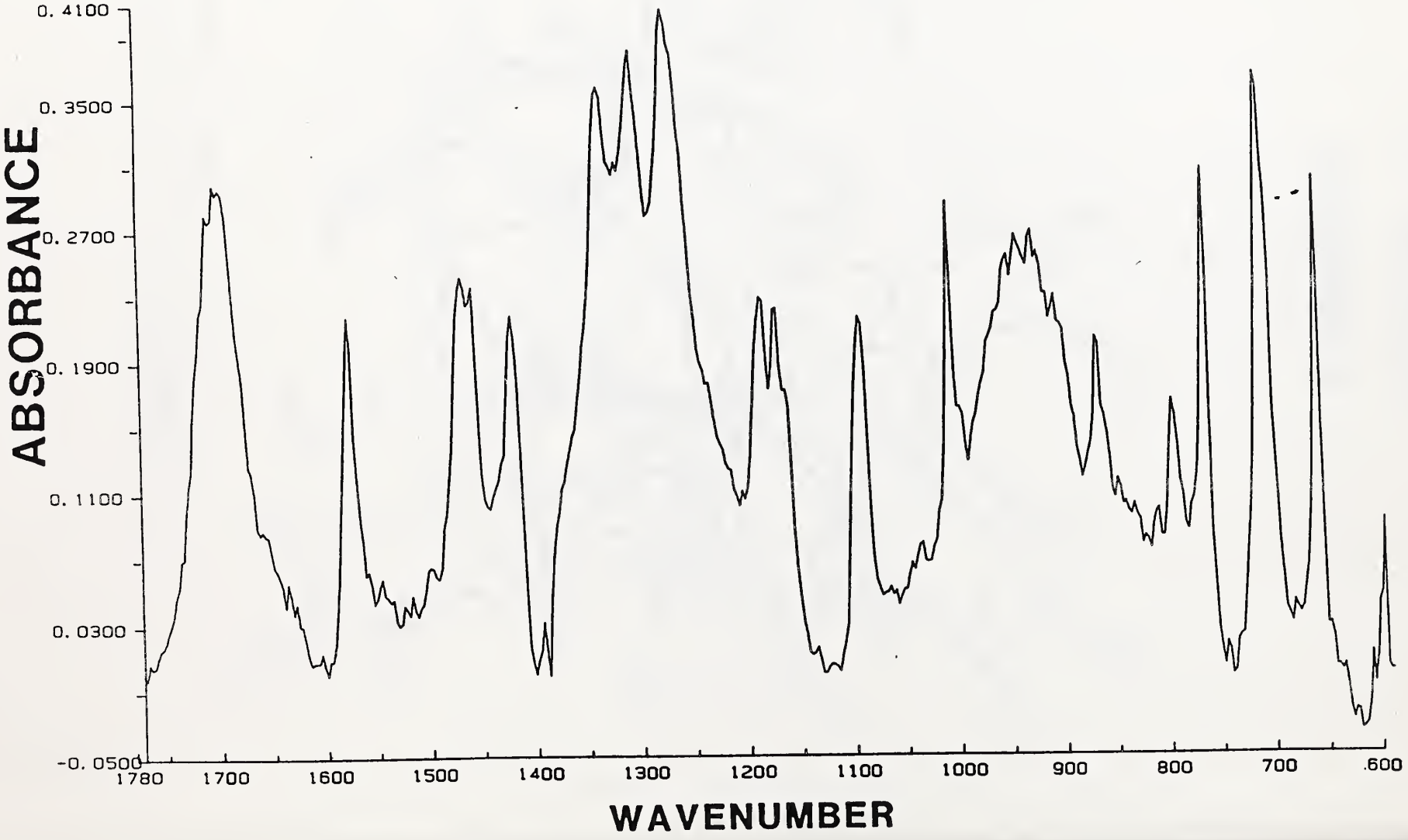

FIGURE 12

FTIR spectrum of Na_2DPA via diffuse reflectance in KBr.

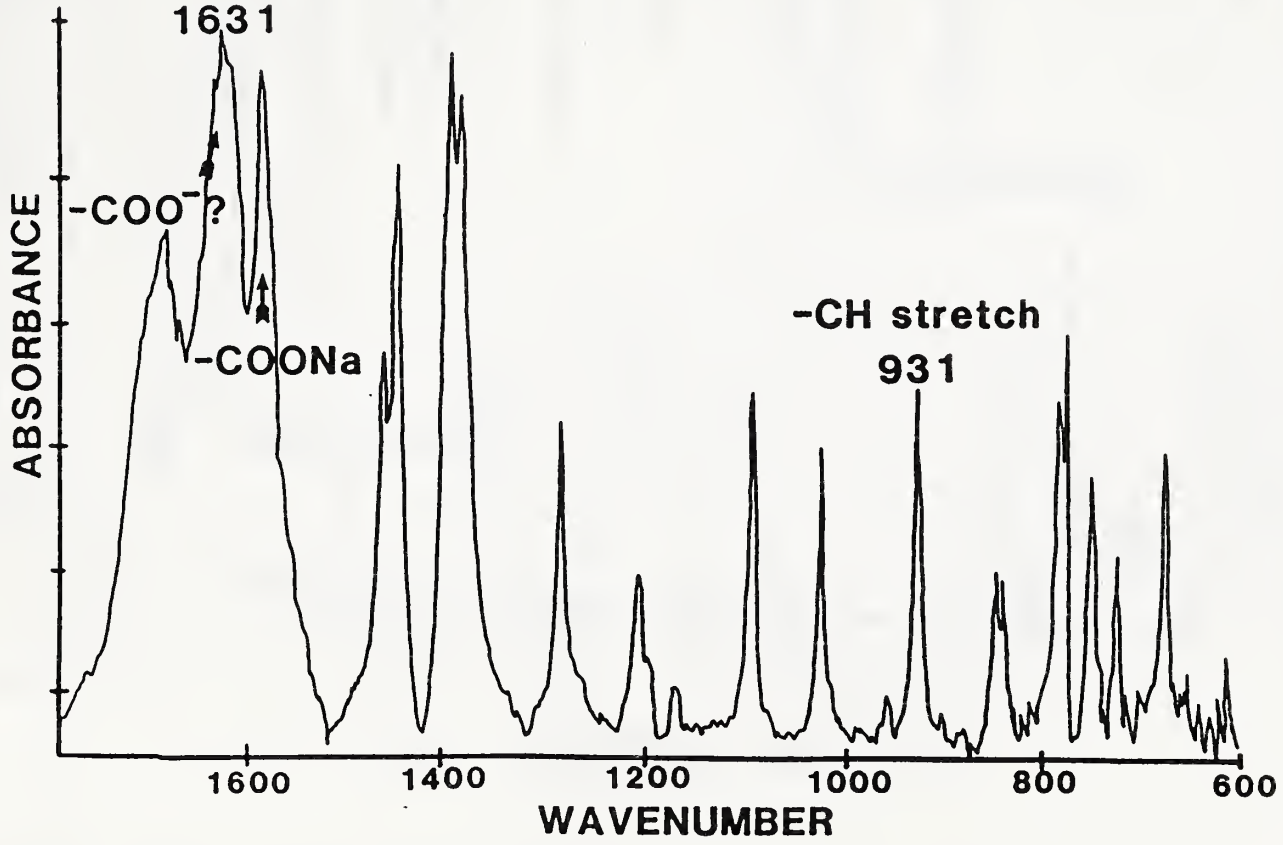

FIGURE 13

FTIR spectrum of $Na_3TB(DPA)_3 \cdot 6H_2O$ via diffuse reflectance in KBr.

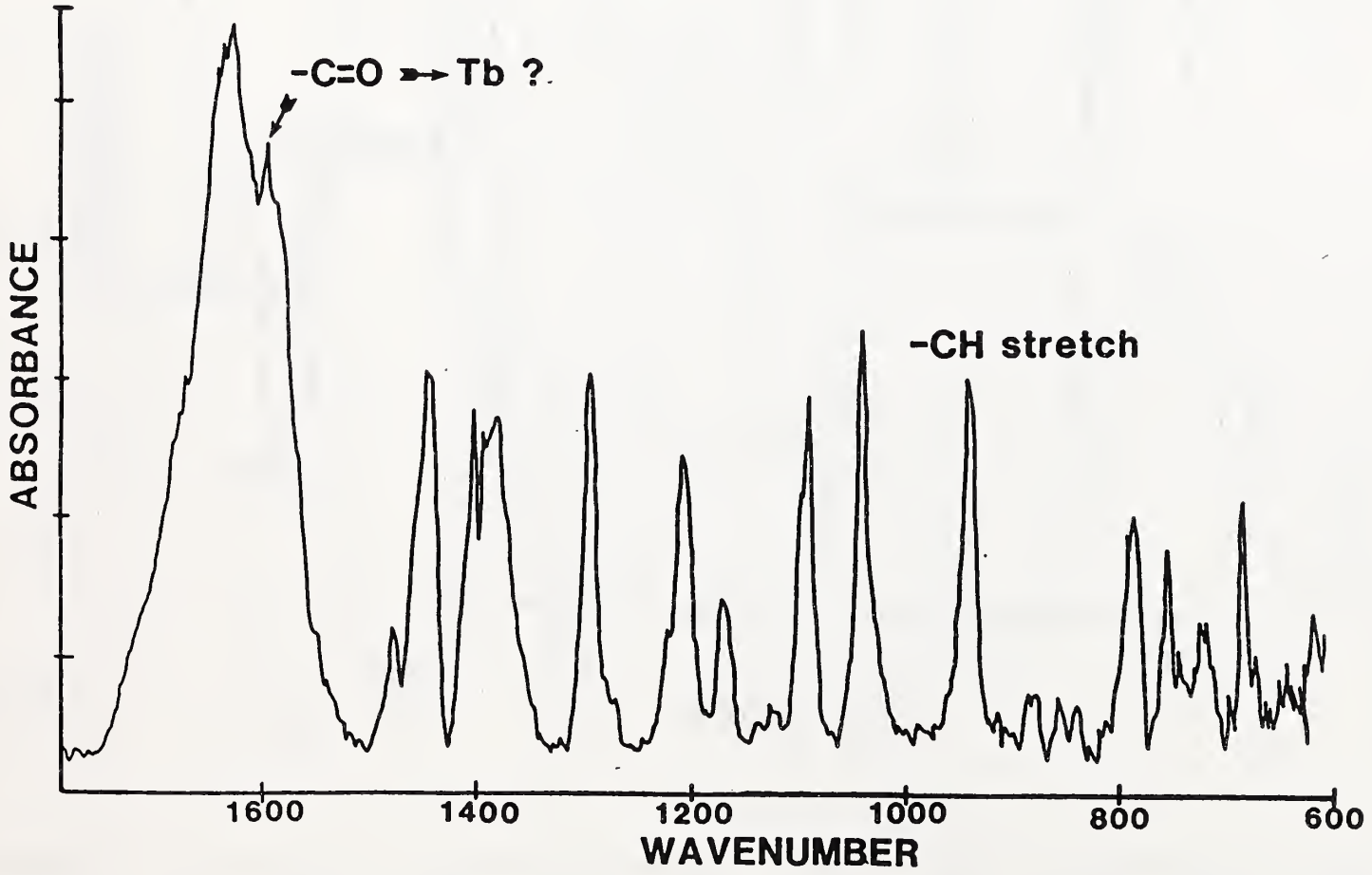

FIGURE 14

FTIR spectrum of $Tb(HDPA)_3 \cdot 2H_2O$ via diffuse reflectance in KBr.

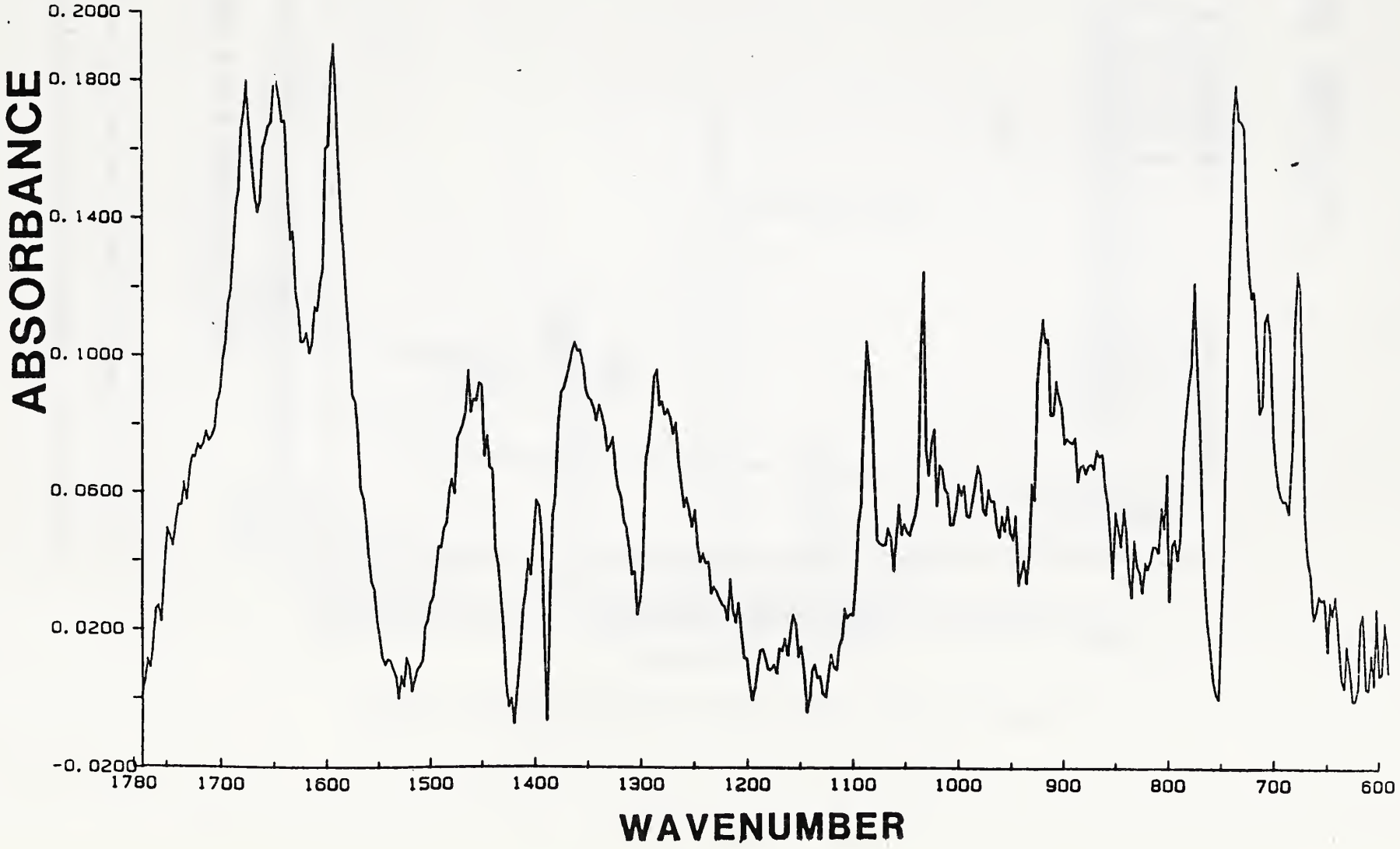

FIGURE 15

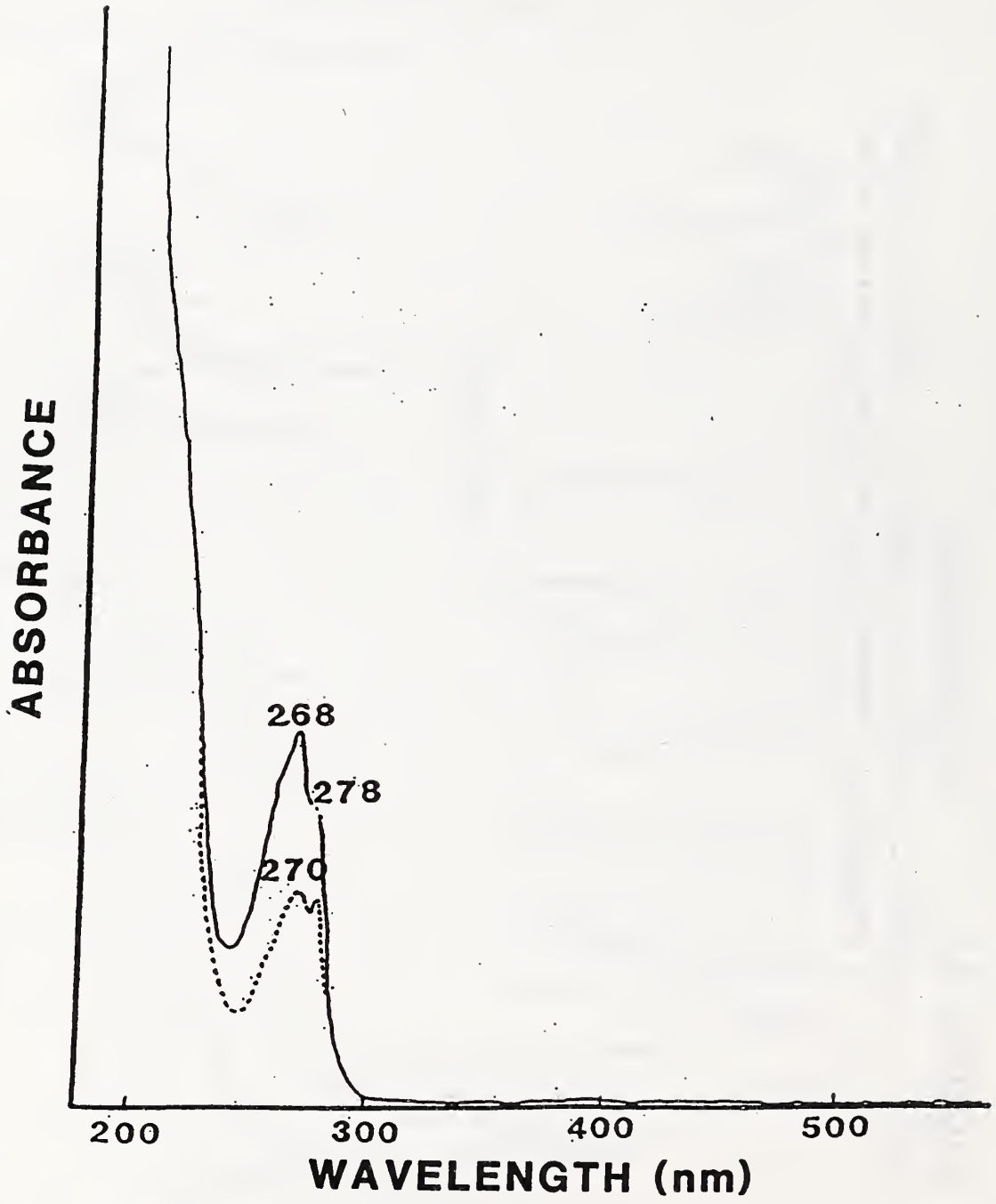

UV spectra of $Na_3Tb(DPA)_3 \cdot 6H_2O$ (dotted line) and H_2DPA (solid line) in water. Absorbance values are not relative.

FIGURE 16

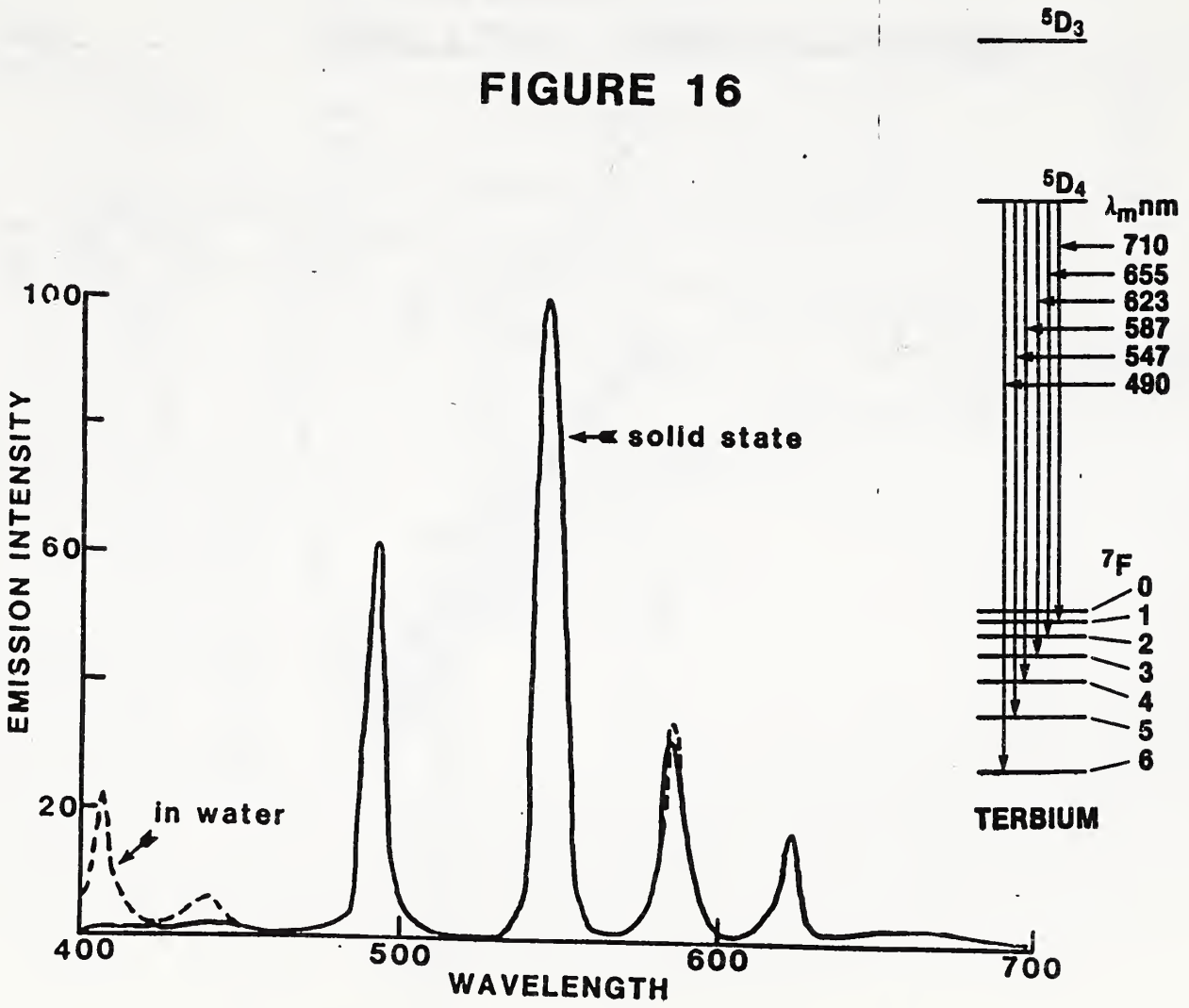

Emission spectra of $Na_3Tb(DPA)_3 \cdot 6H_2O$ in the solid state and in water. λ_{exc} = 254 nm.

FIGURE 17

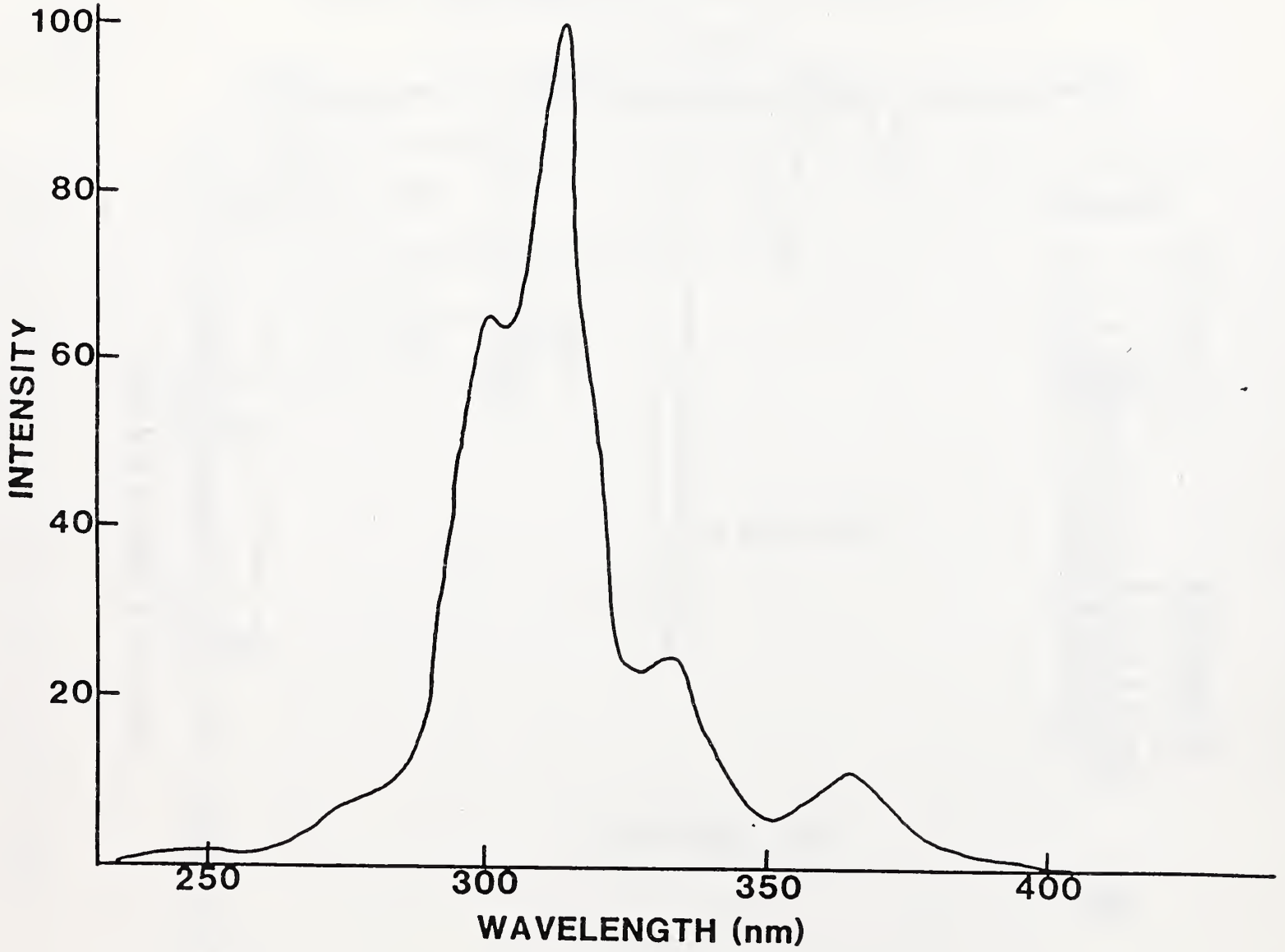

Excitation spectrum of aqueous $Na_3Tb(DPA)_3$. λ_{em} = 546 nm

FIGURE 18

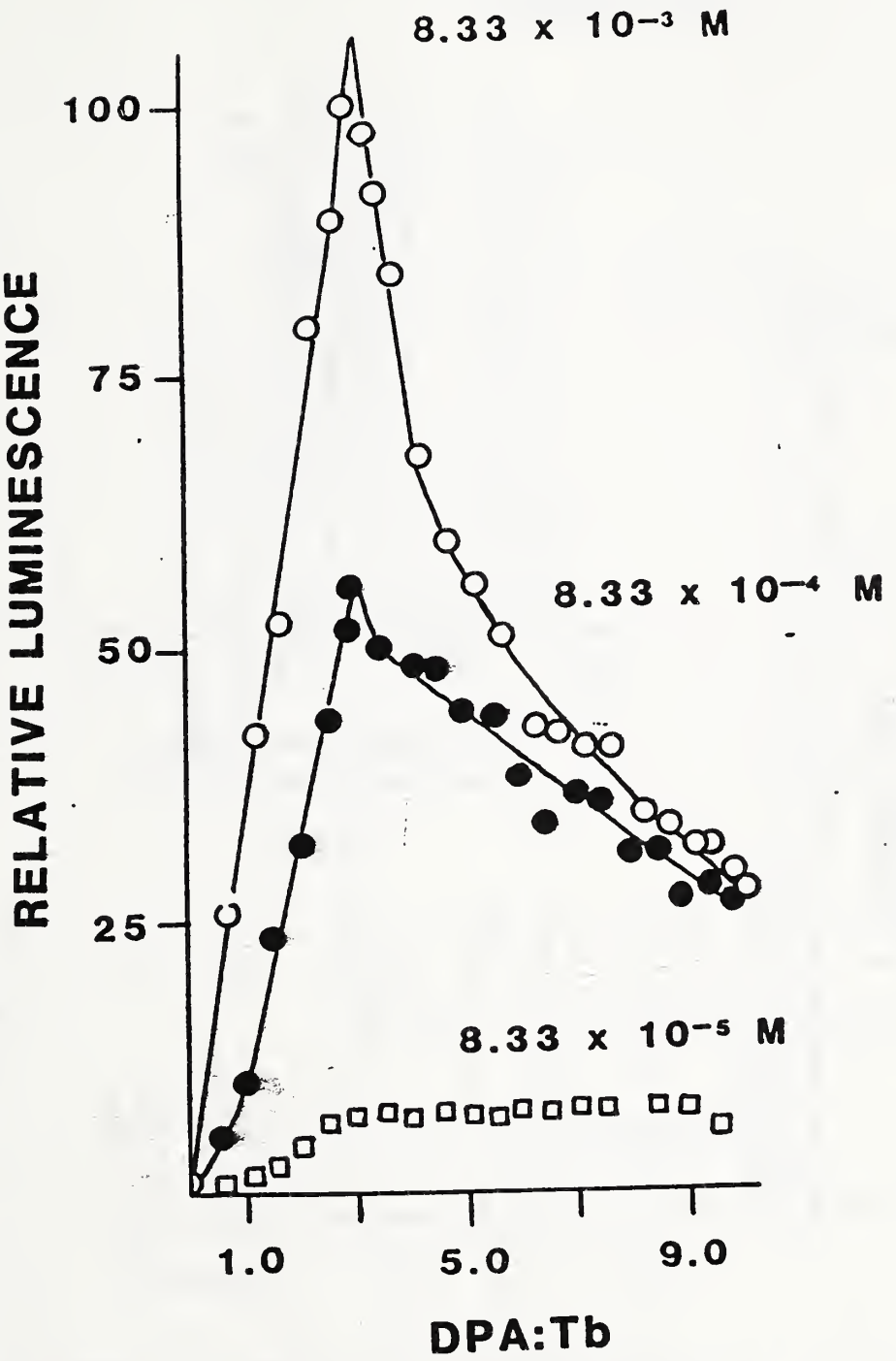

Luminescence vs DPA:Tb ratio in aqueous solutions of Na_2DPA + $Tb(NO_3)_3$. Concentrations are of Tb (8.33×10^{-3} - 8.33×10^{-5} M). λ_{exc} = 254 nm.

FIGURE 19

Relative luminescence vs irradiation time (λ = 254 nm) for various aqueous ratios of DPA:Tb.

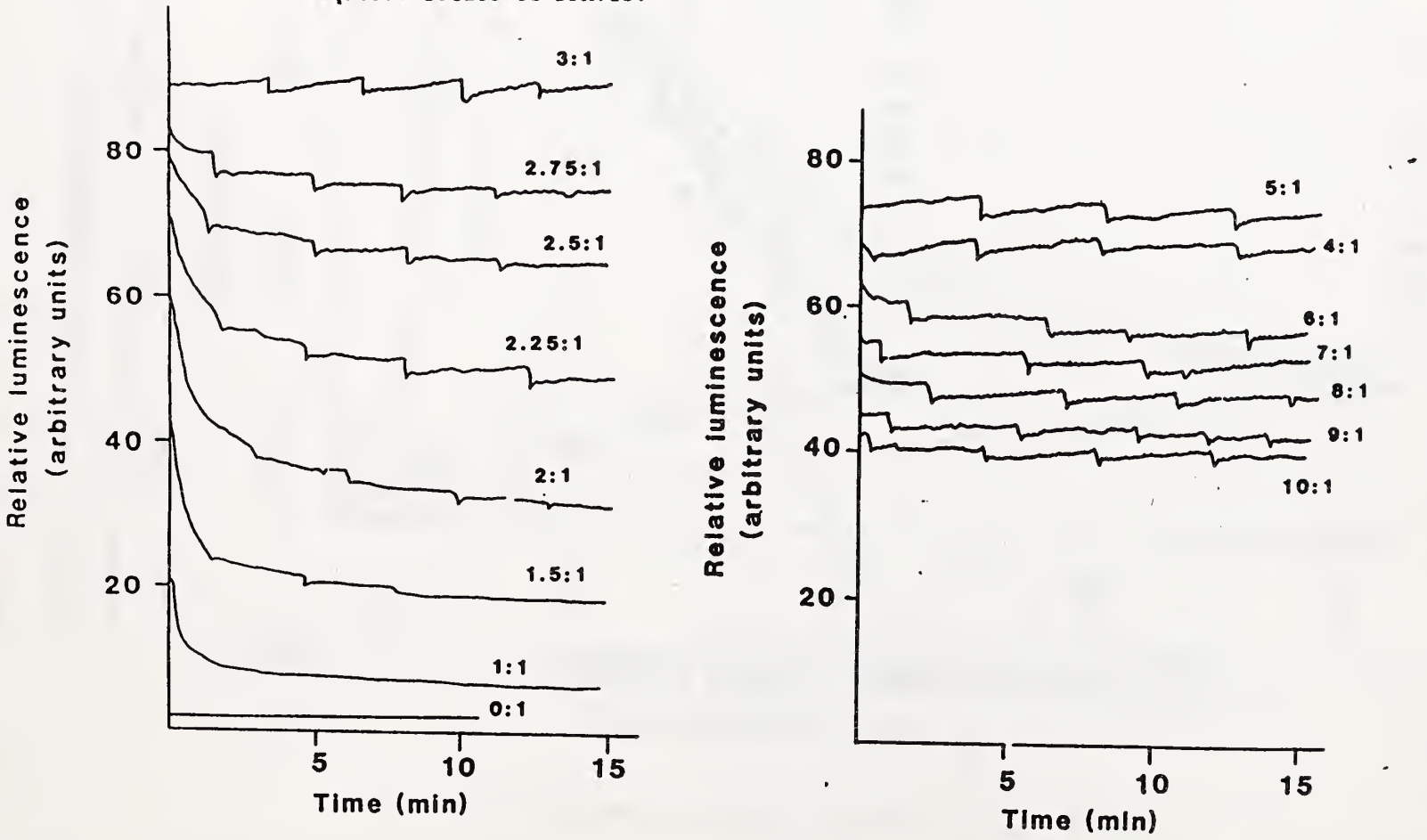

Figure 20

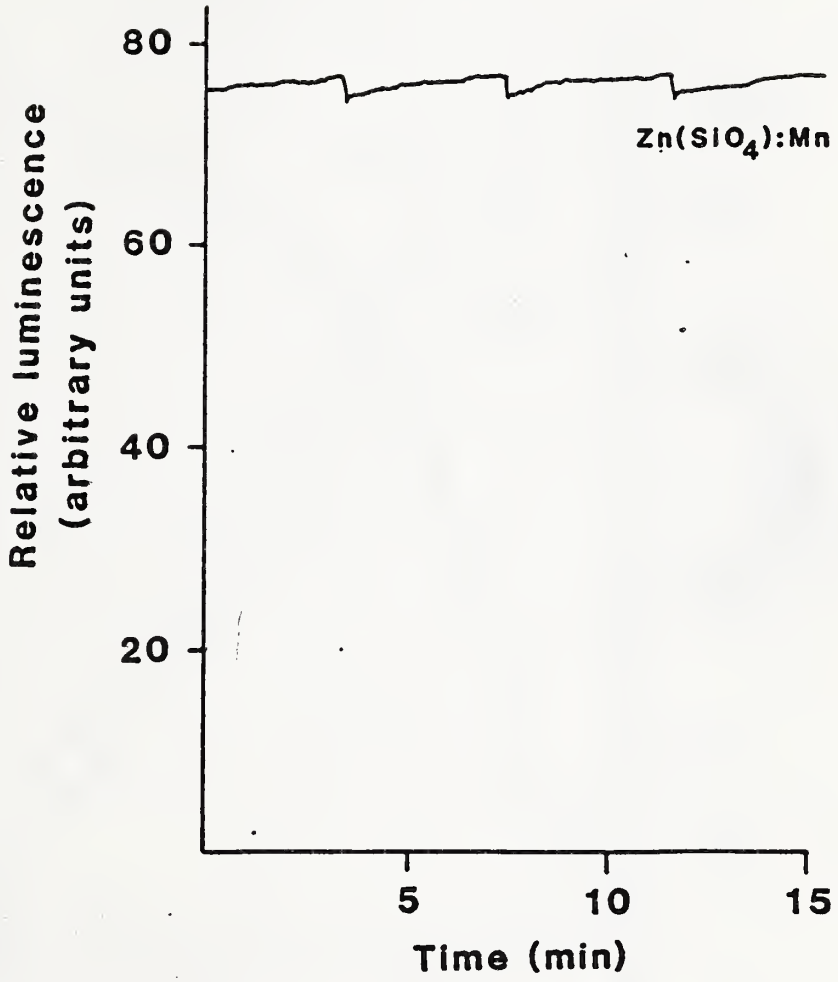

Relative luminescence vs irradiation time (λ = 254 nm) for solid $ZnSiO_4$·Mn.

FIGURE 21

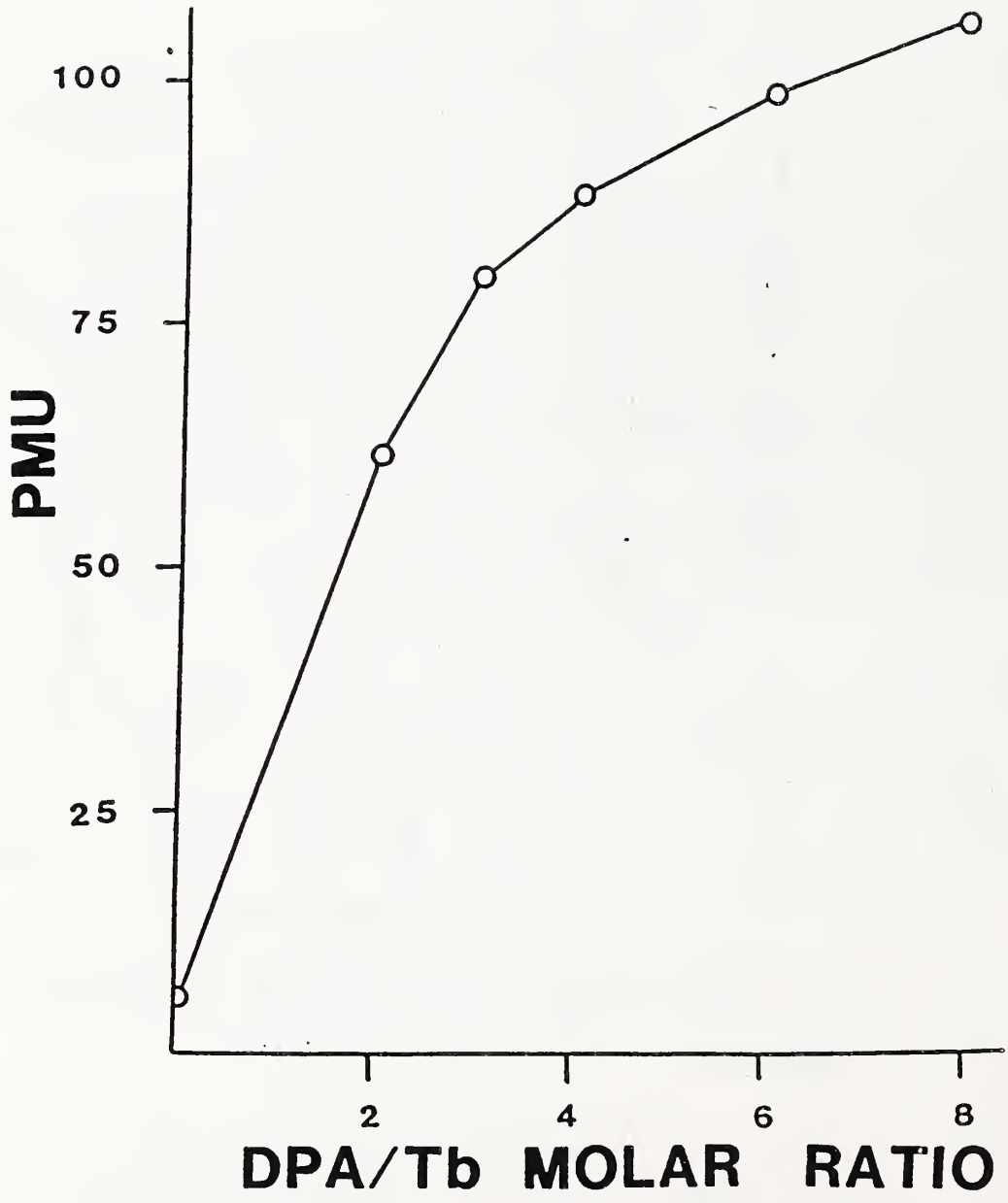

Phosphorescence on LP-46 paper of various DPA:Tb ratios in varnish SVD-4057. Drawdown = 1.0 mil. λ_{exc} = 254 nm.

FIGURE 22

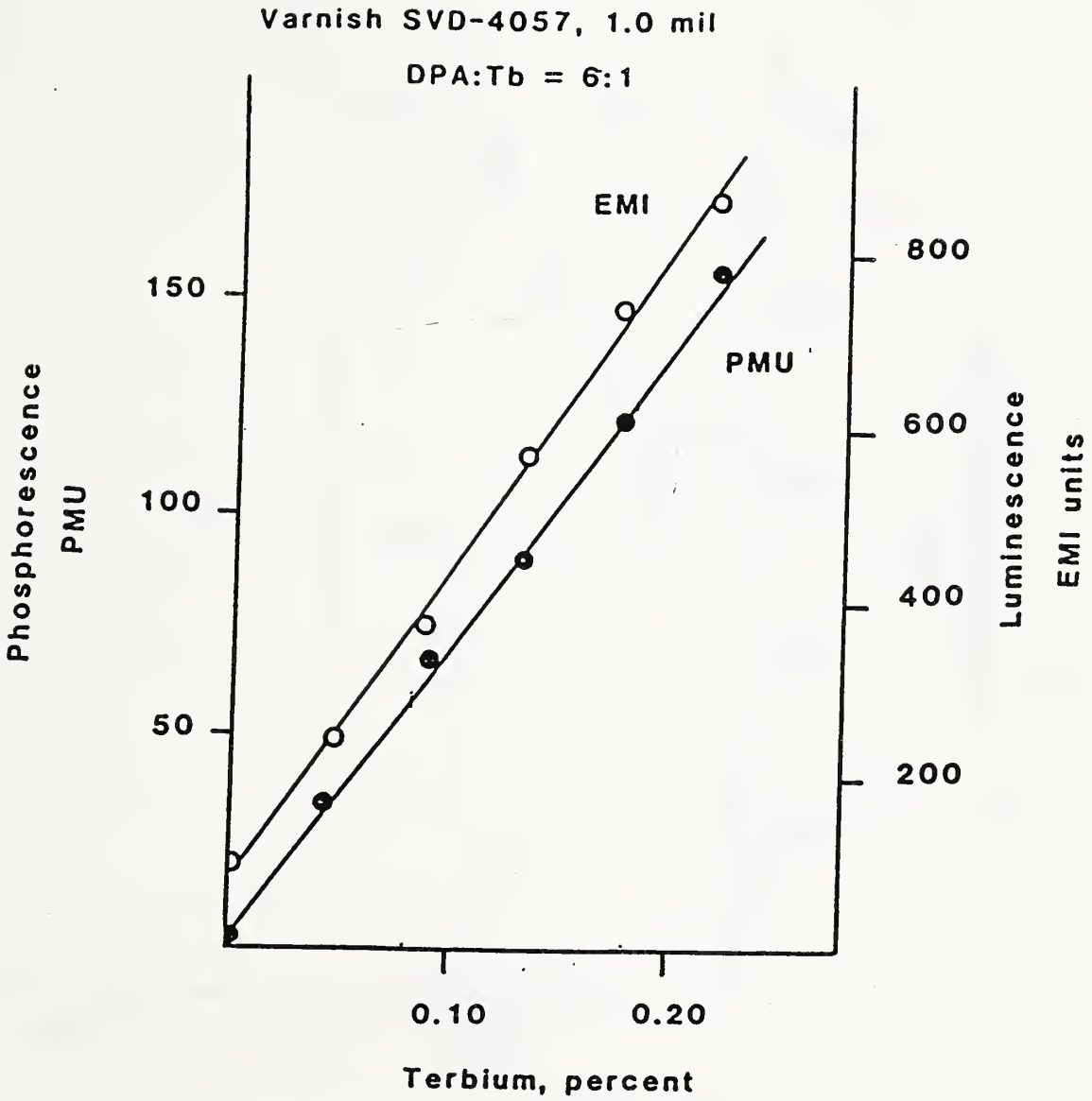

Correlation of phosphorescence (PMU) and total luminescence (mV, EMI units) for various Tb concentrations in varnish SVD-4057. Drawdown = 1.0 mil. DPA:Tb held at 6:1. λ_{exc} = 254 nm.

FIGURE 23

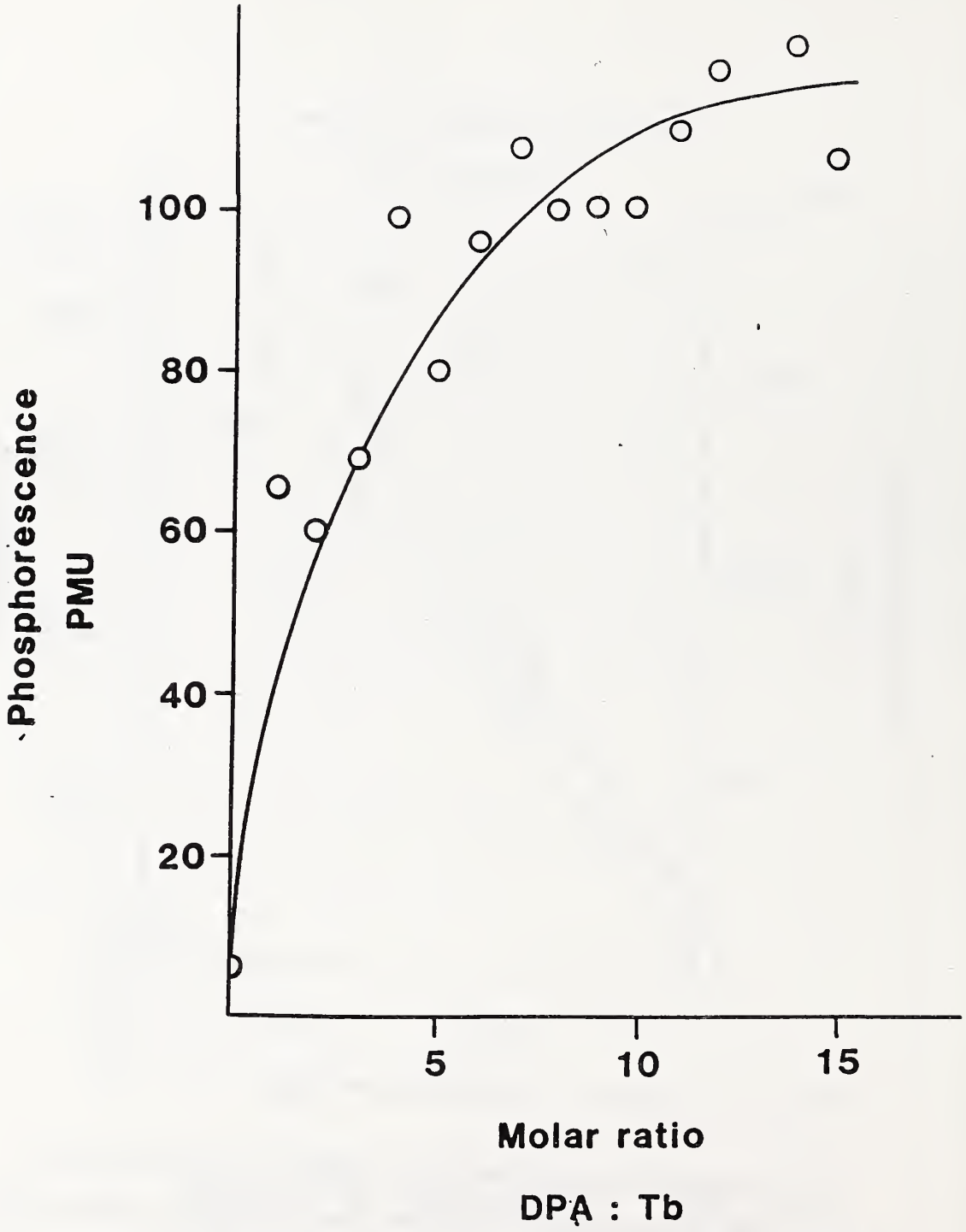

Phosphorescence vs DPA:Tb ratio on LP-46 tagged with aqueous DPA/Tb samples. Drawdown = 1.0 mil. λ_{exc} =254 nm.

FIGURE 24

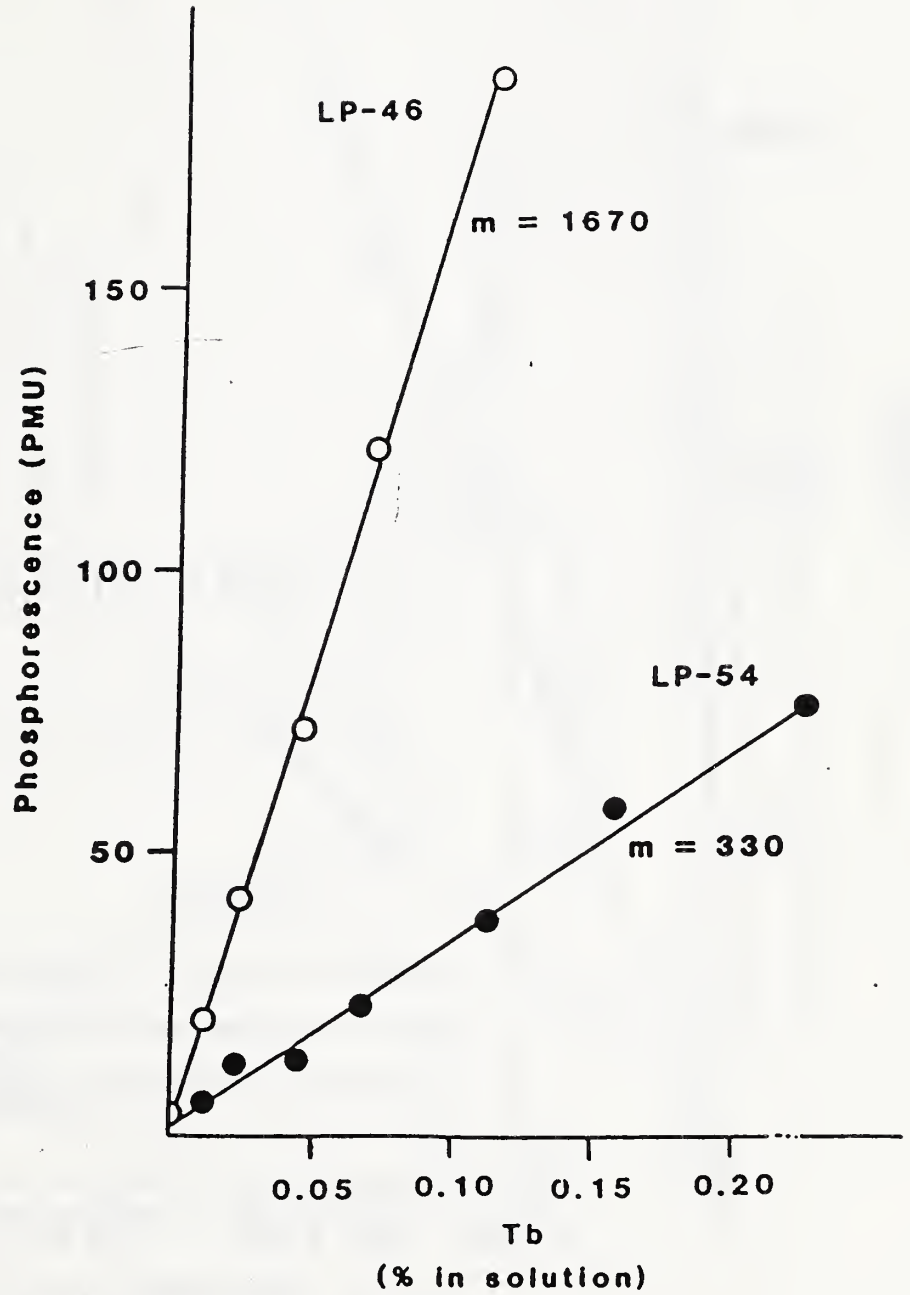

Phosphorescence vs Tb concentration in 6:1 DPA:Tb samples applied as aqueous solutions to papers LP-46 and LP-54. Drawdown = 0.5 mil. λ_{exc} = 254 nm.

FIGURE 25

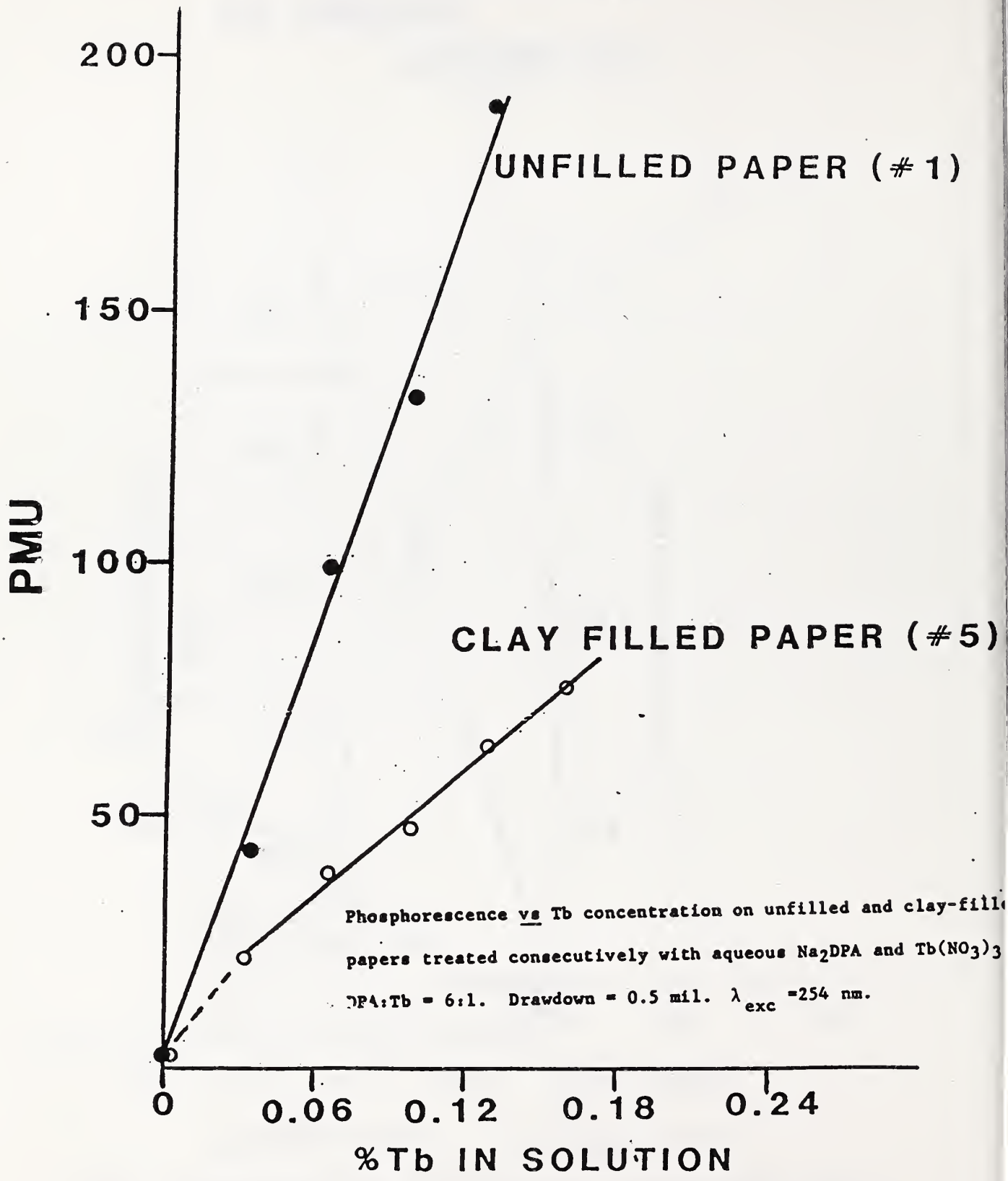

Phosphorescence vs Tb concentration on unfilled and clay-fill
papers treated consecutively with aqueous Na_2DPA and $Tb(NO_3)_3$
DPA:Tb = 6:1. Drawdown = 0.5 mil. λ_{exc} =254 nm.

FIGURE 26

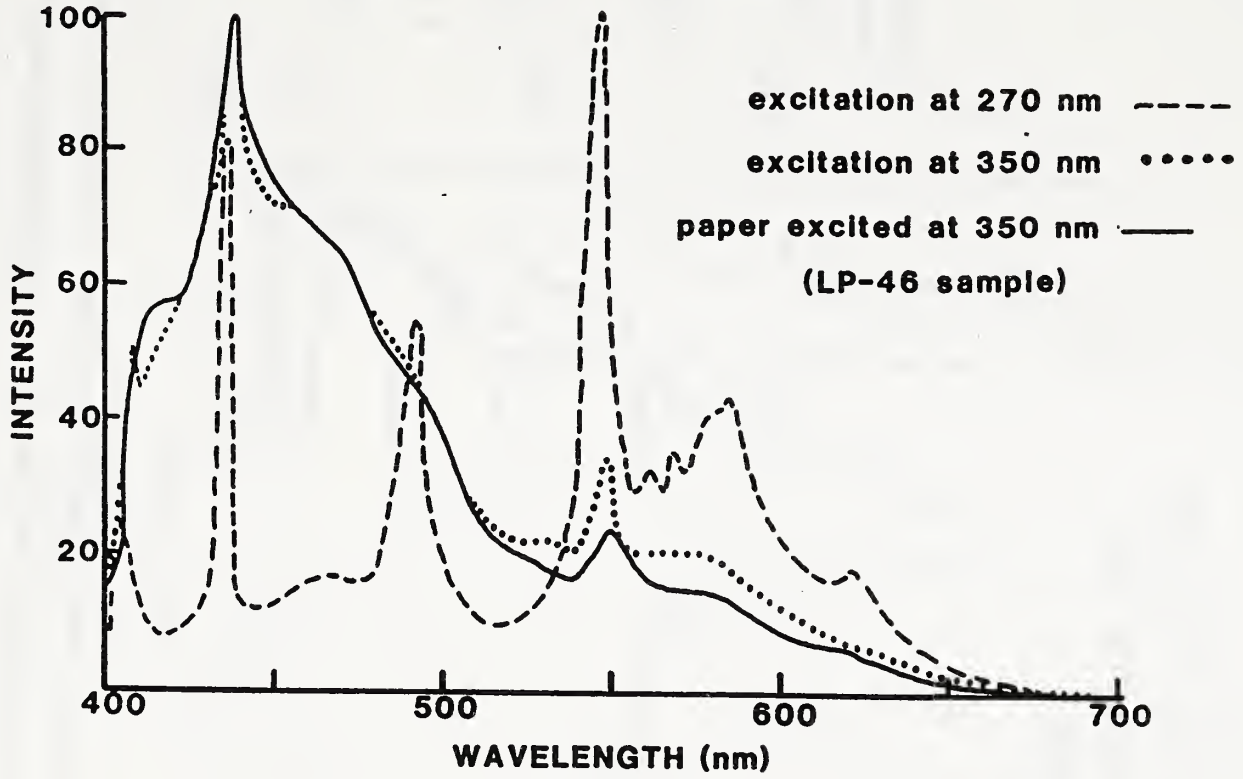

Total luminescence of $Na_3Tb(DPA)_3$ tagged paper (Harrison and Sons, 0.02% Tb) at two excitation wavelengths compared to total luminescence of an unfilled, untagged paper (LP-46).

FIGURE 27

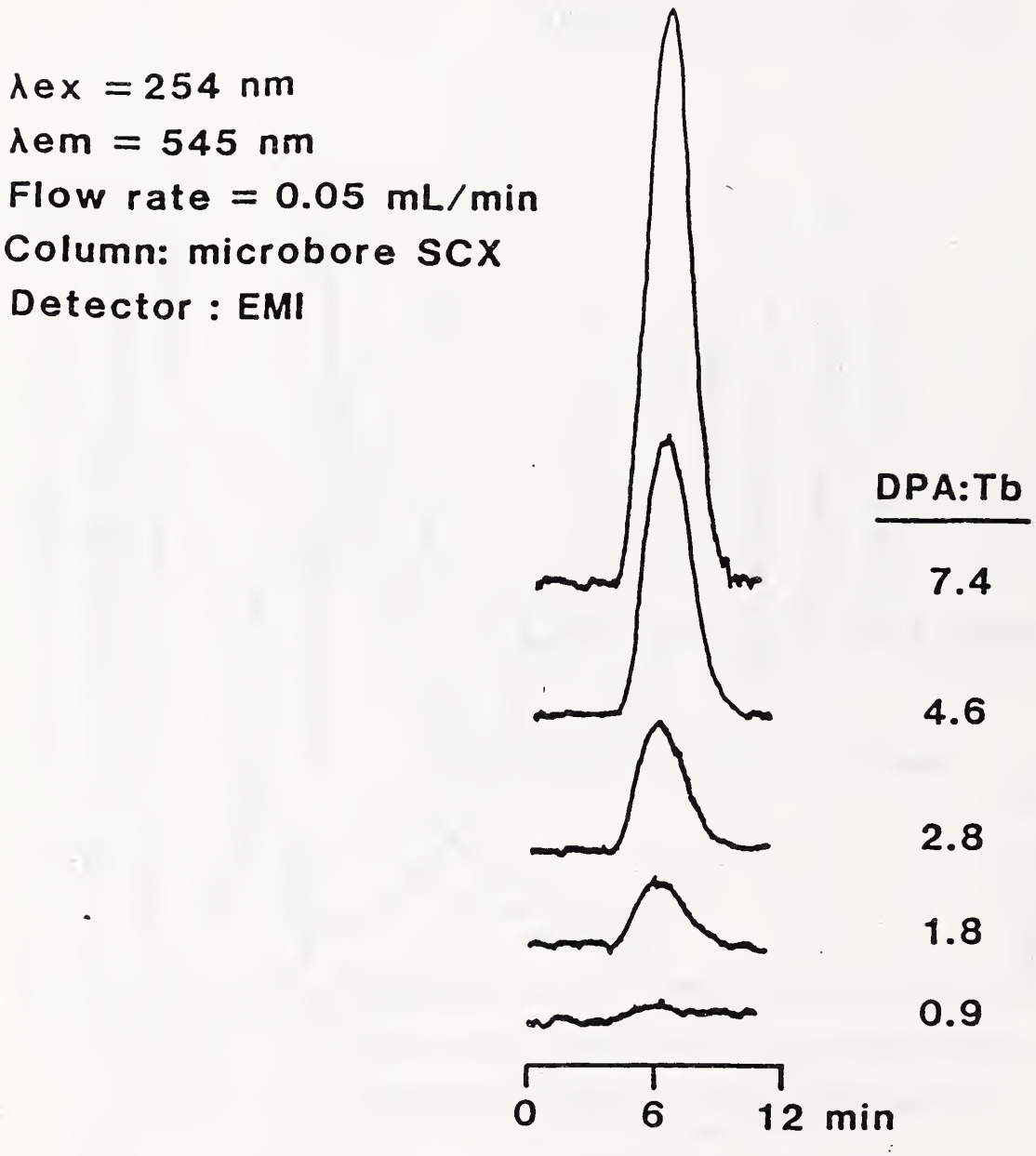

SCX chromatograms of aqueous solutions of Na_2DPA and $Tb(NO_3)_3$ in molar ratios from 0.9:1 to 7.4:1. Luminescence vs retention time.

FIGURE 28

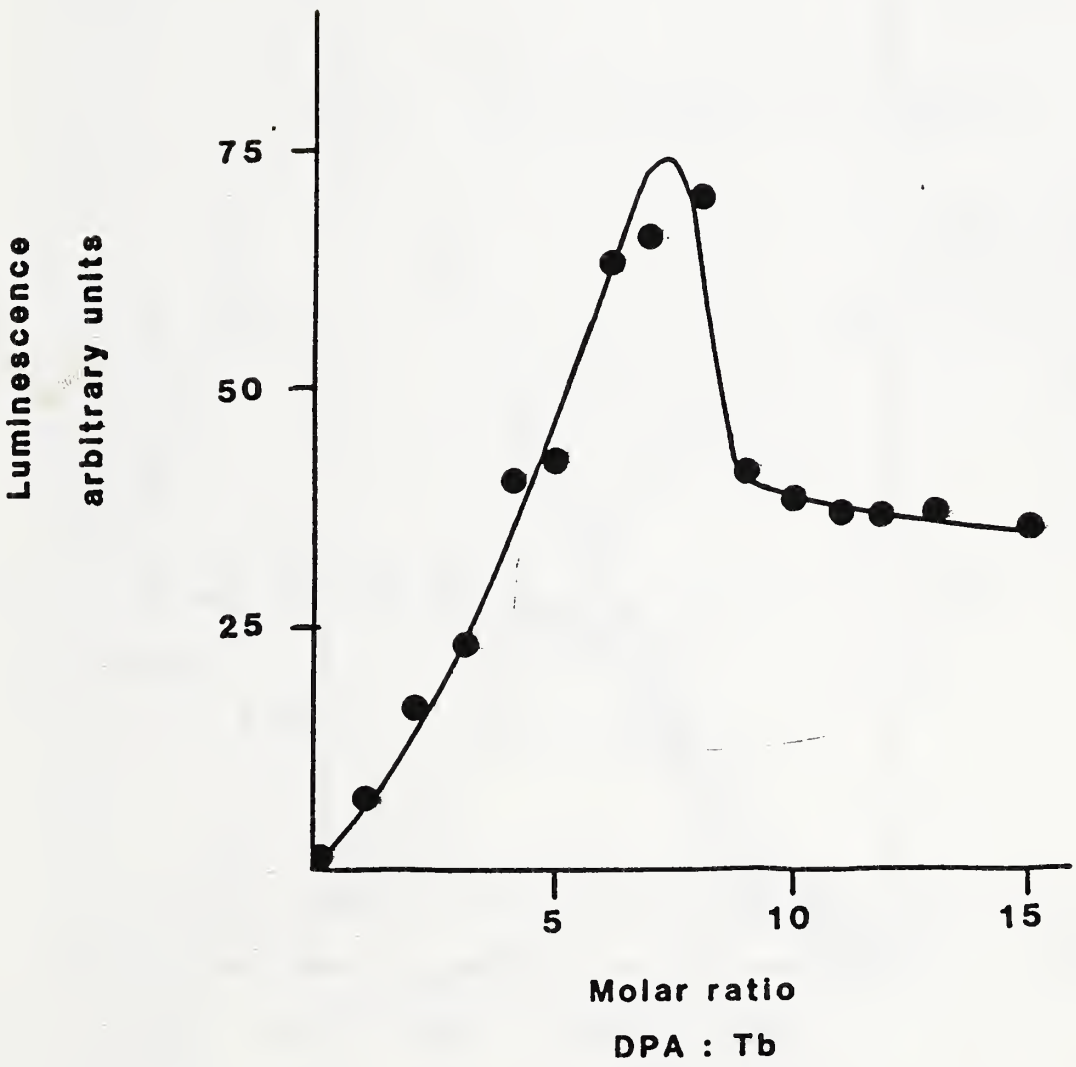

SCX chromatography of various DPA:Tb ratios in aqueous solution.

Eluant analysis shows luminescence maximum at 8:1.

FIGURE 29

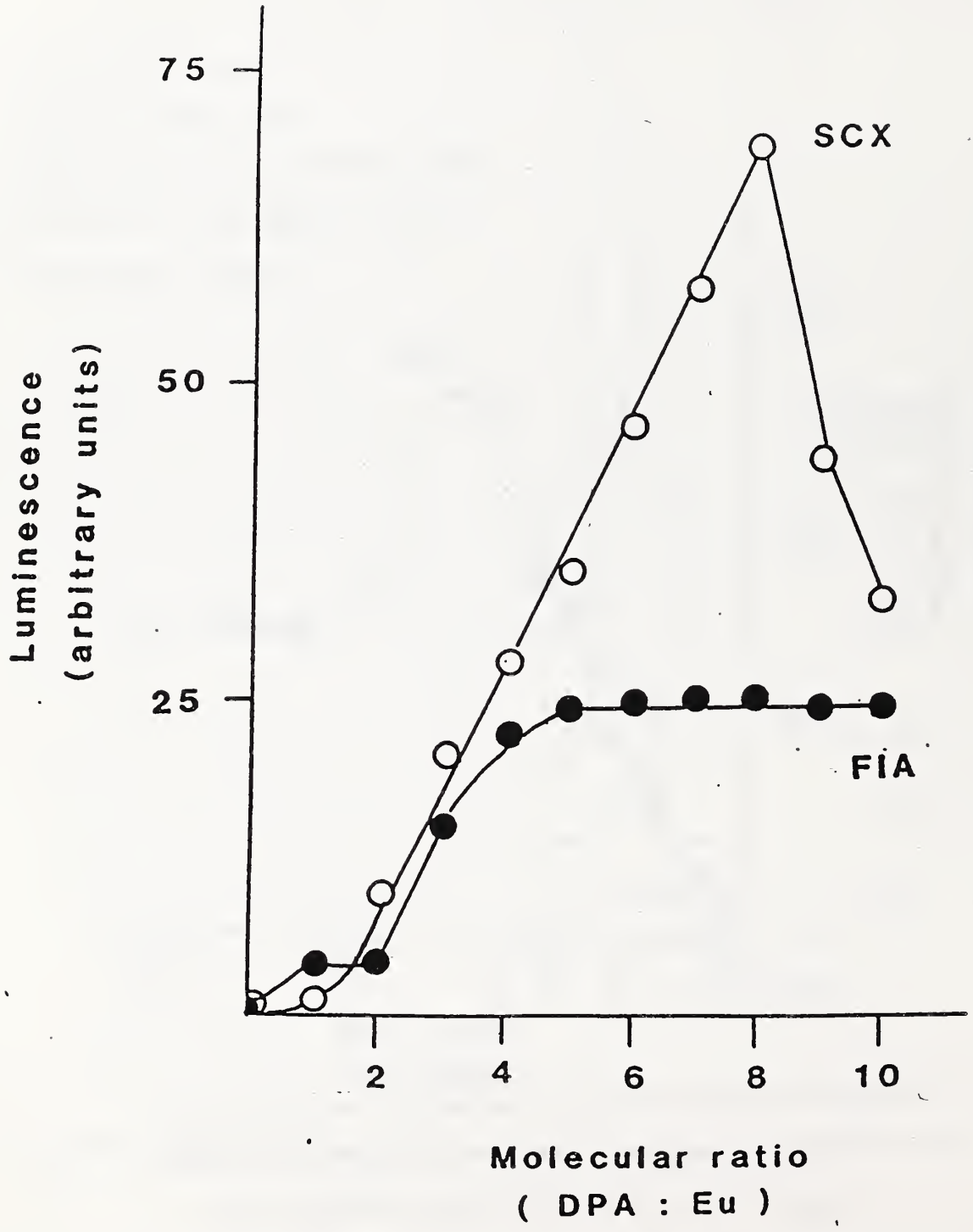

SCX (open circles) and flow injection analysis (closed circles) on aqueous solutions of varying DPA:Eu rations. Luminescence mole ratio.

Figure 30

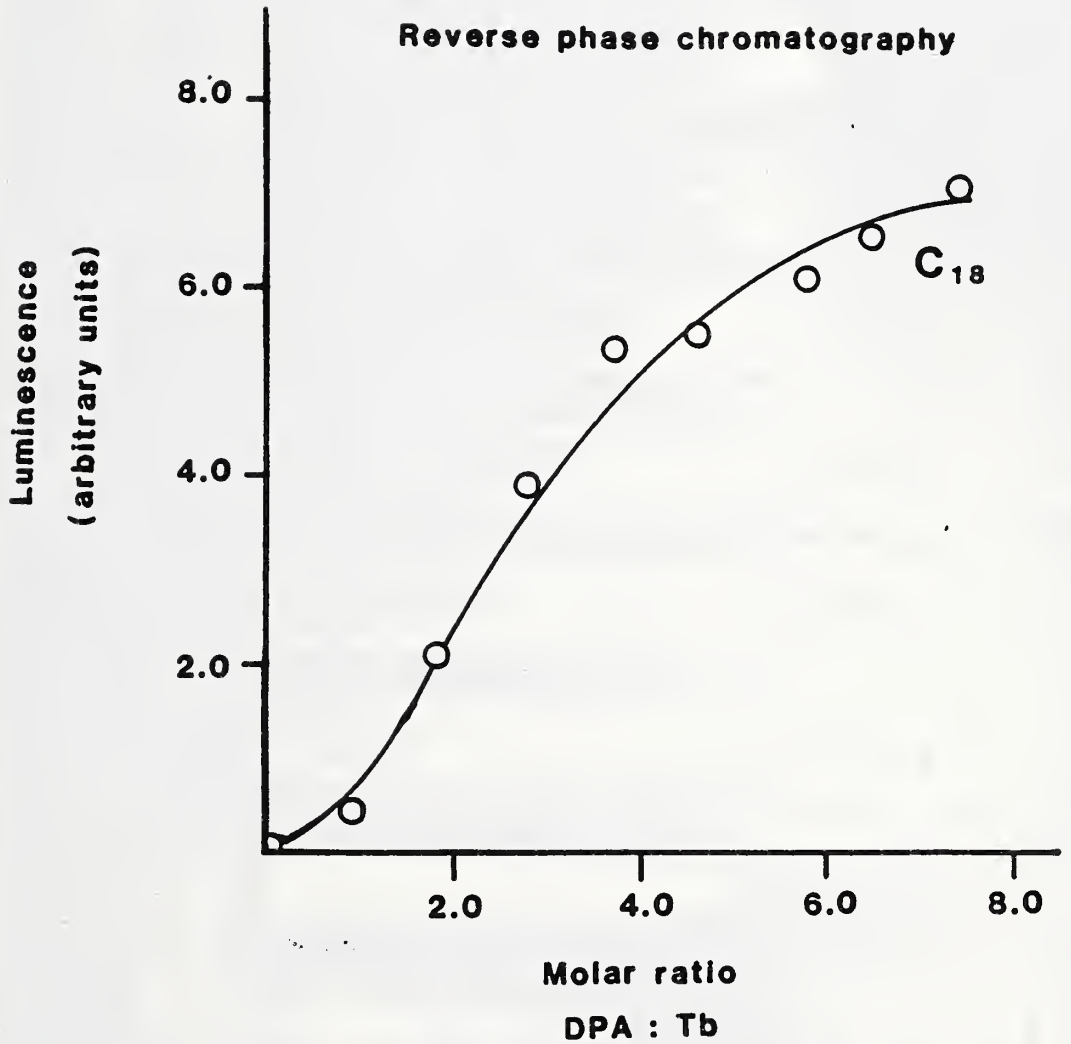

Reverse phase chromatographic results on aqueous solutions of varying DPA:Tb ratios. Luminescence vs mole ratio.

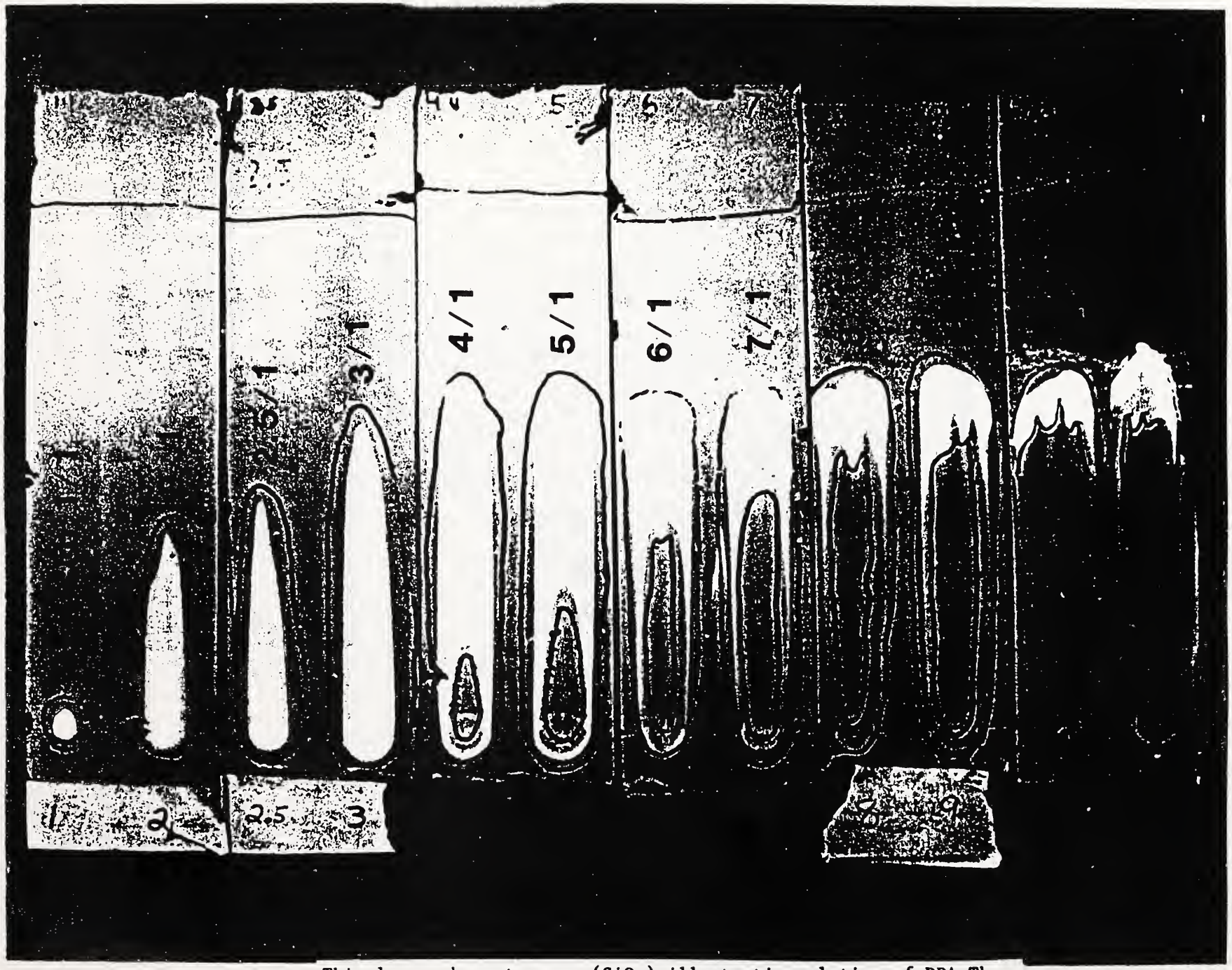

FIGURE 31

Thin layer chromatograms (SiO_2) illustrating elution of DPA-Tb complexes with water. Bright areas are due to luminescence excited at 254 nm.

FIGURE 32

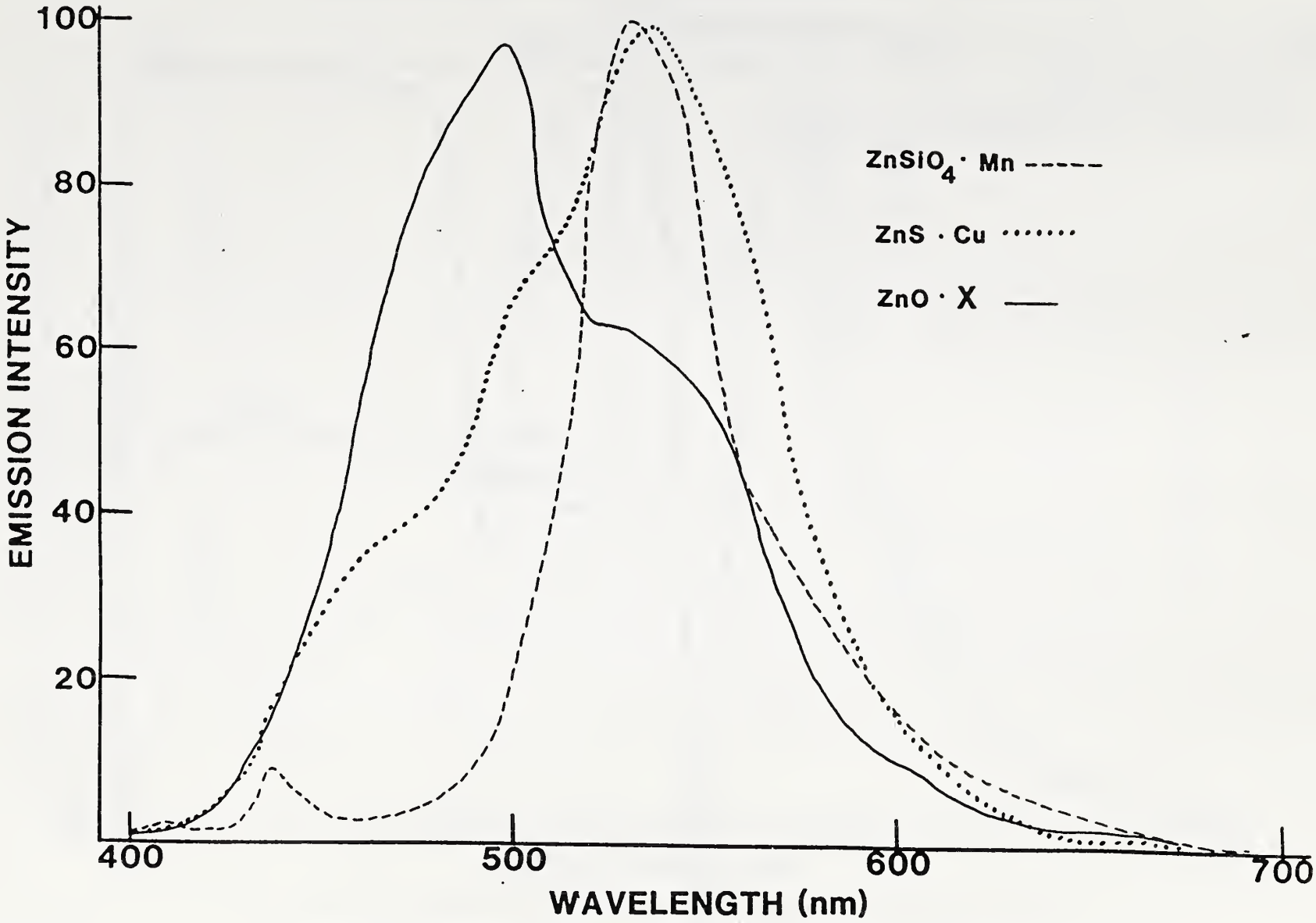

Normalized emission spectra of $ZnSiO_4 \cdot Mn$, $ZnS \cdot Cu$, and $ZnO \cdot X$ in the solid state. λ_{exc} = 254 nm.

FIGURE 33

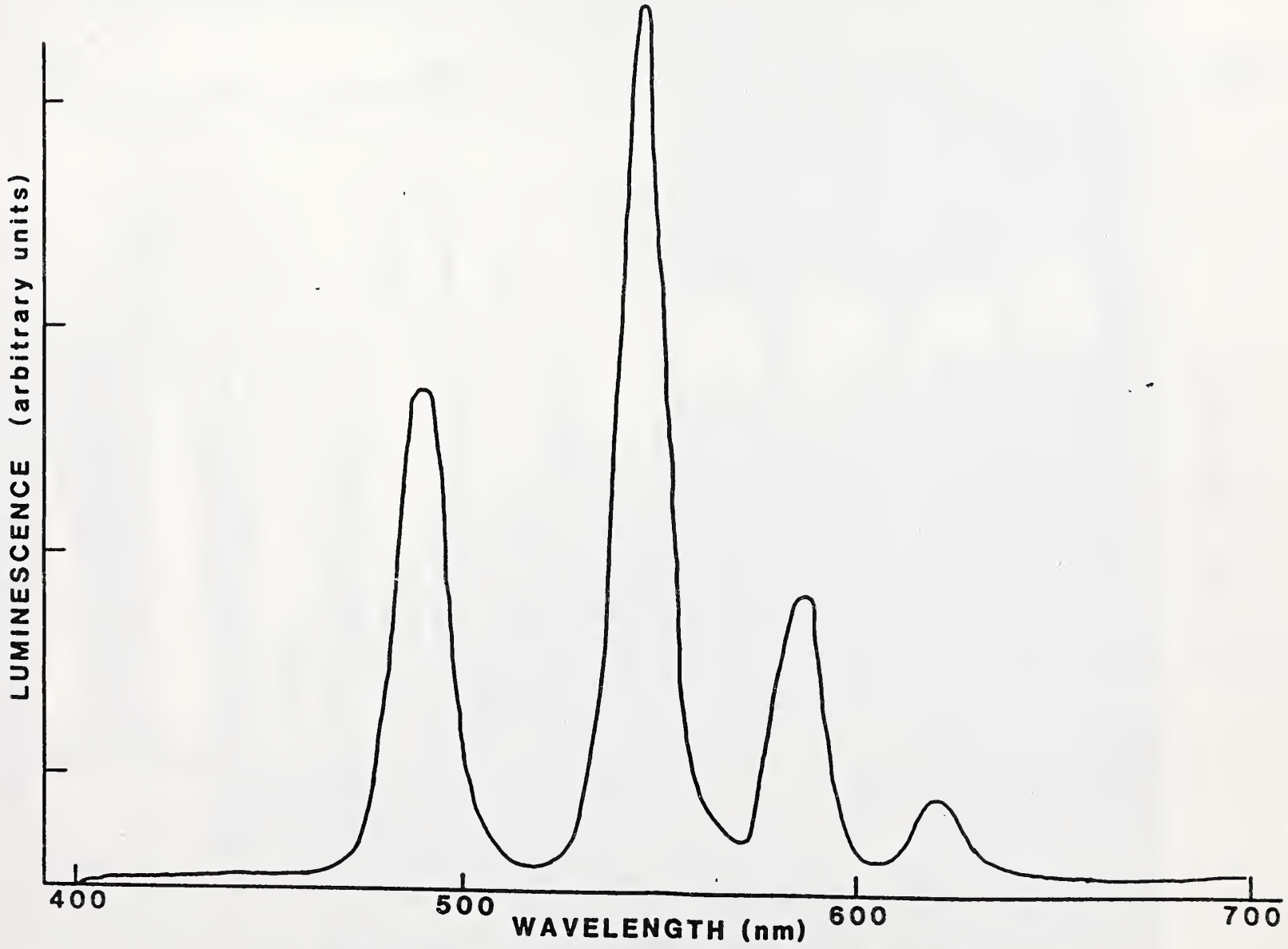

Emission spectrum of solid precipitated from aqueous mixtures of terbium nitrate and sodium tris(pyrazol-1-yl)borate. λ_{exc} = 254 nm.

FIGURE 34

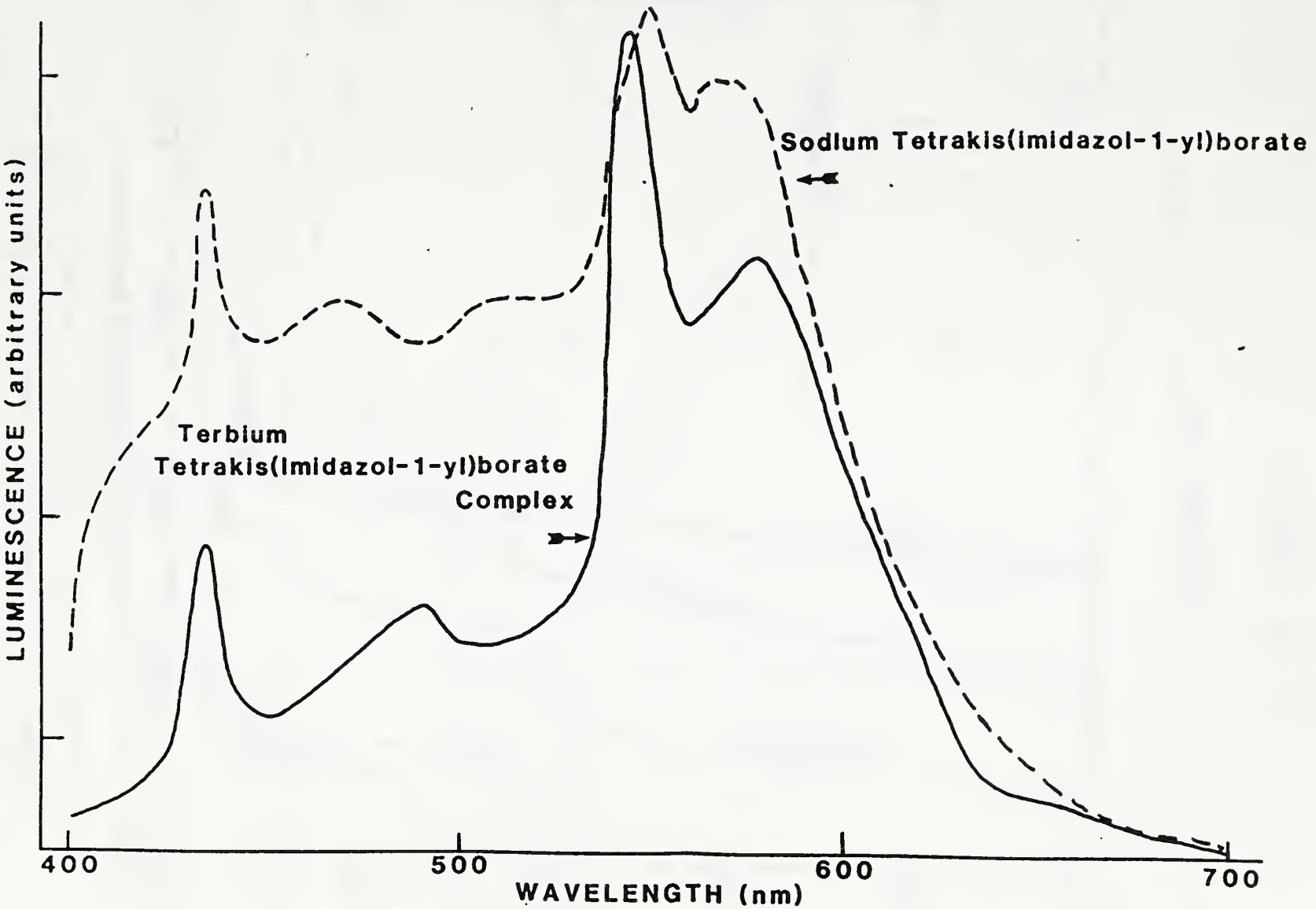

Emission spectra of sodium tetrakis(imidazol-1-yl)borate, and the complex formed between it and terbium nitrate. Solid state spectra. λ_{exc} = 254 nm.

FIGURE 35

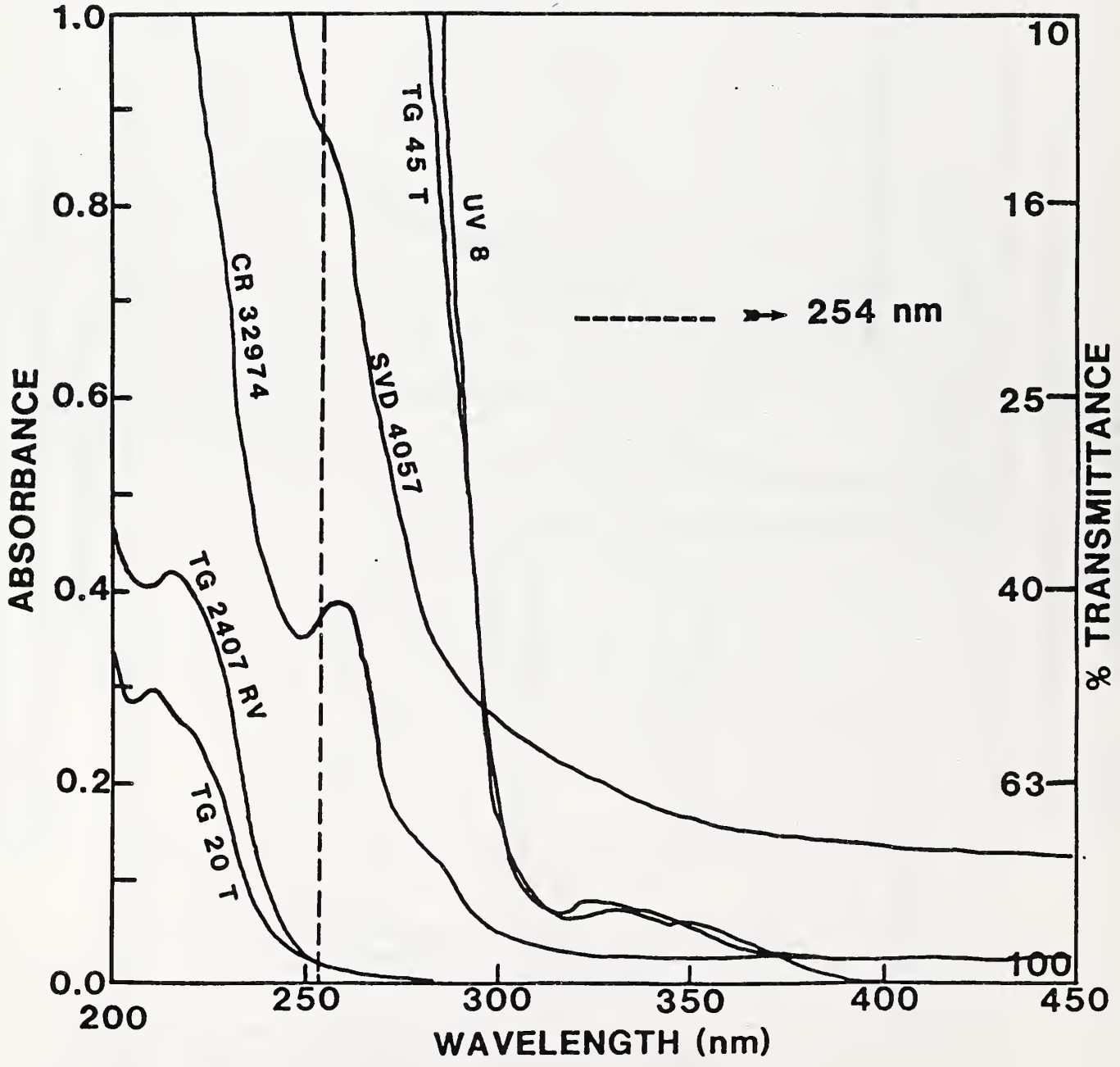

UV spectra of varnishes used by the Bureau of Engraving and Printing. Samples drawn down at 0.5 mil thickness and cured on a quartz cuvette.

FIGURE 36

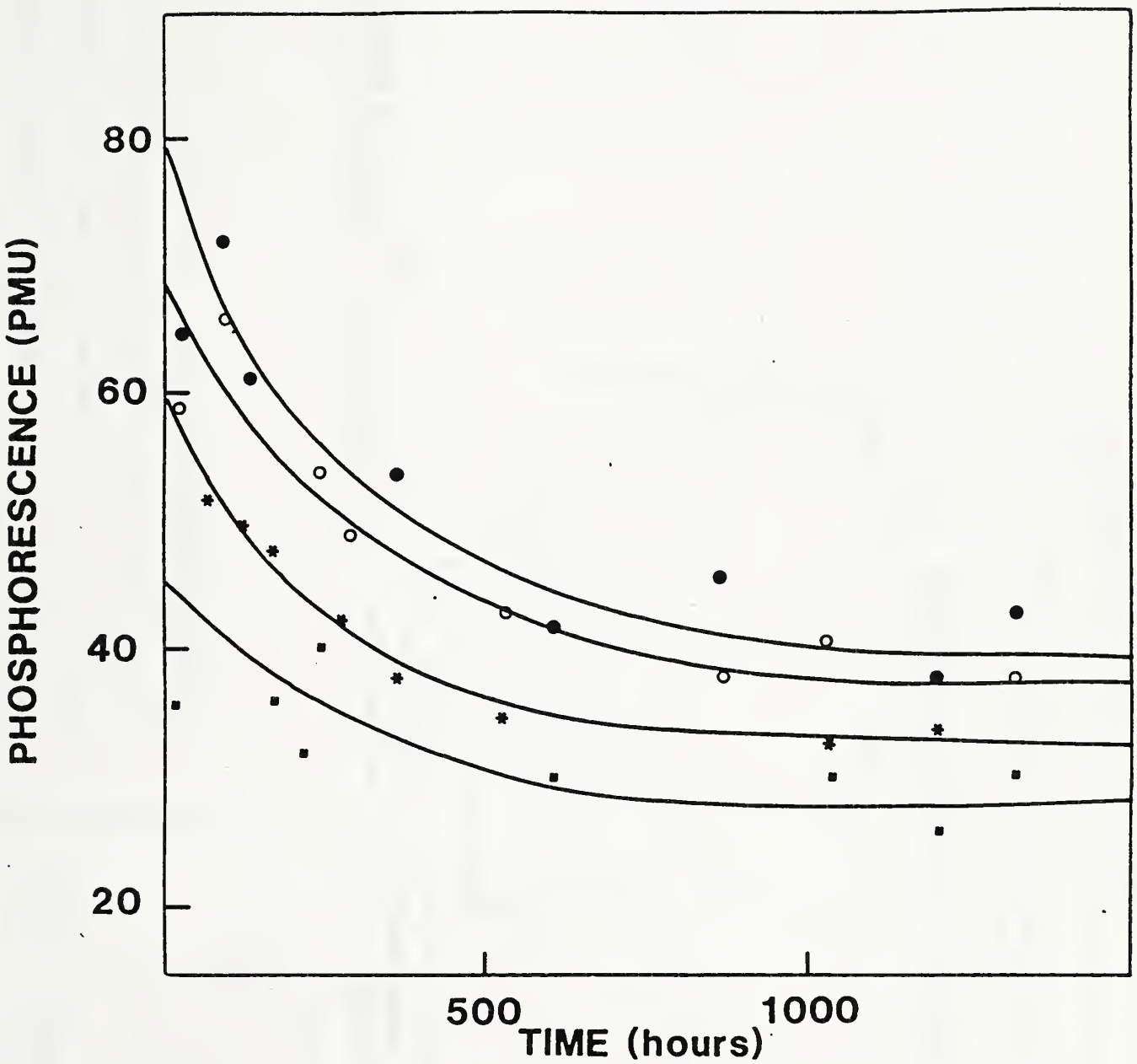

Phosphorescence vs time curves for Harrison and Sons terbium tagged "Showboat" trading stamps. Outdoor aging during June, July, 1986 in Montgomery County, MD. Principle colors: (·) = yellow, (o) = blue, (*) = green, (■) = red.

FIGURE 37

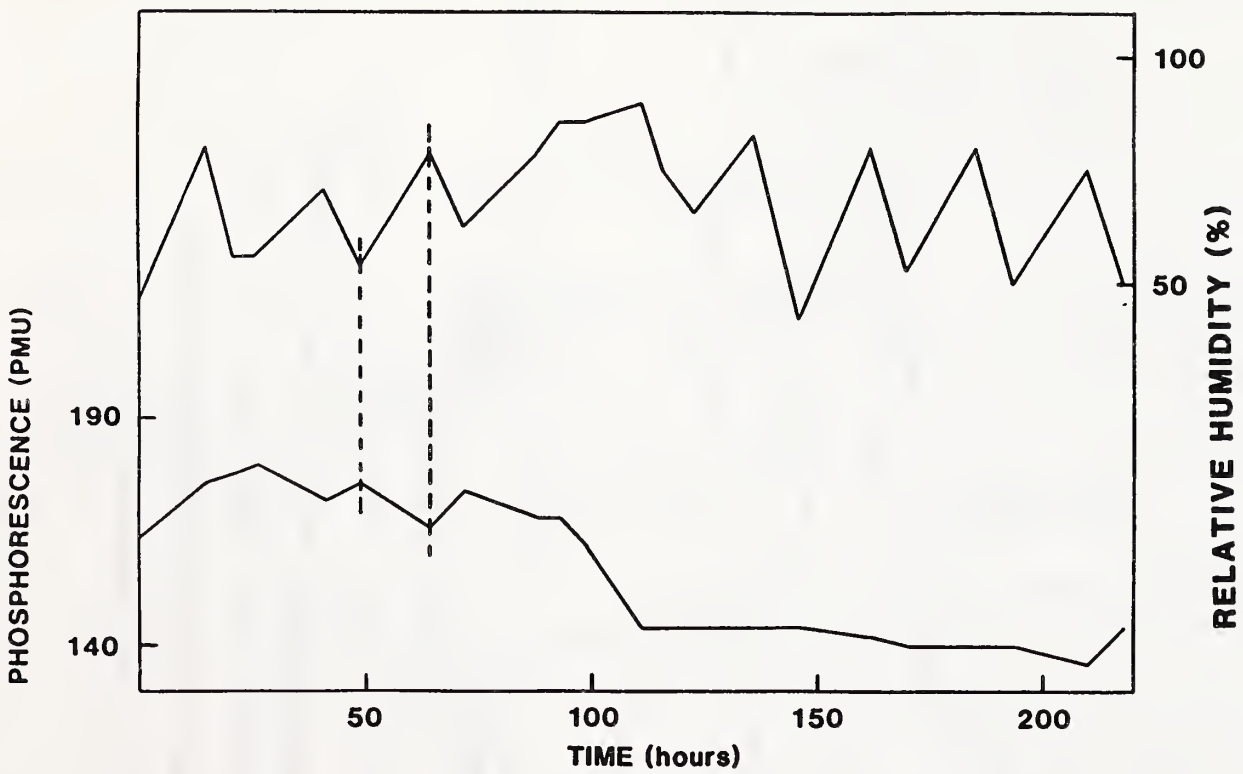

Phosphorescence (lower curve) and relative humidity (upper curve) vs time relations observed during outdoor aging (June, 1986; Montgomery Country, MD) of Harrison and Sons uninked Tb-tagged paper.

FIGURE 38

Attenuated total reflectance (ATR) FTIR spectrum (lower curve) of the reverse side of a Tb-tagged paper sample held in high relative humidity. Upper curve illustrates diffuse reflectance FTIR of genuine $Na_3Tb(DPA)_3 \cdot 6H_2O$ in KBr.

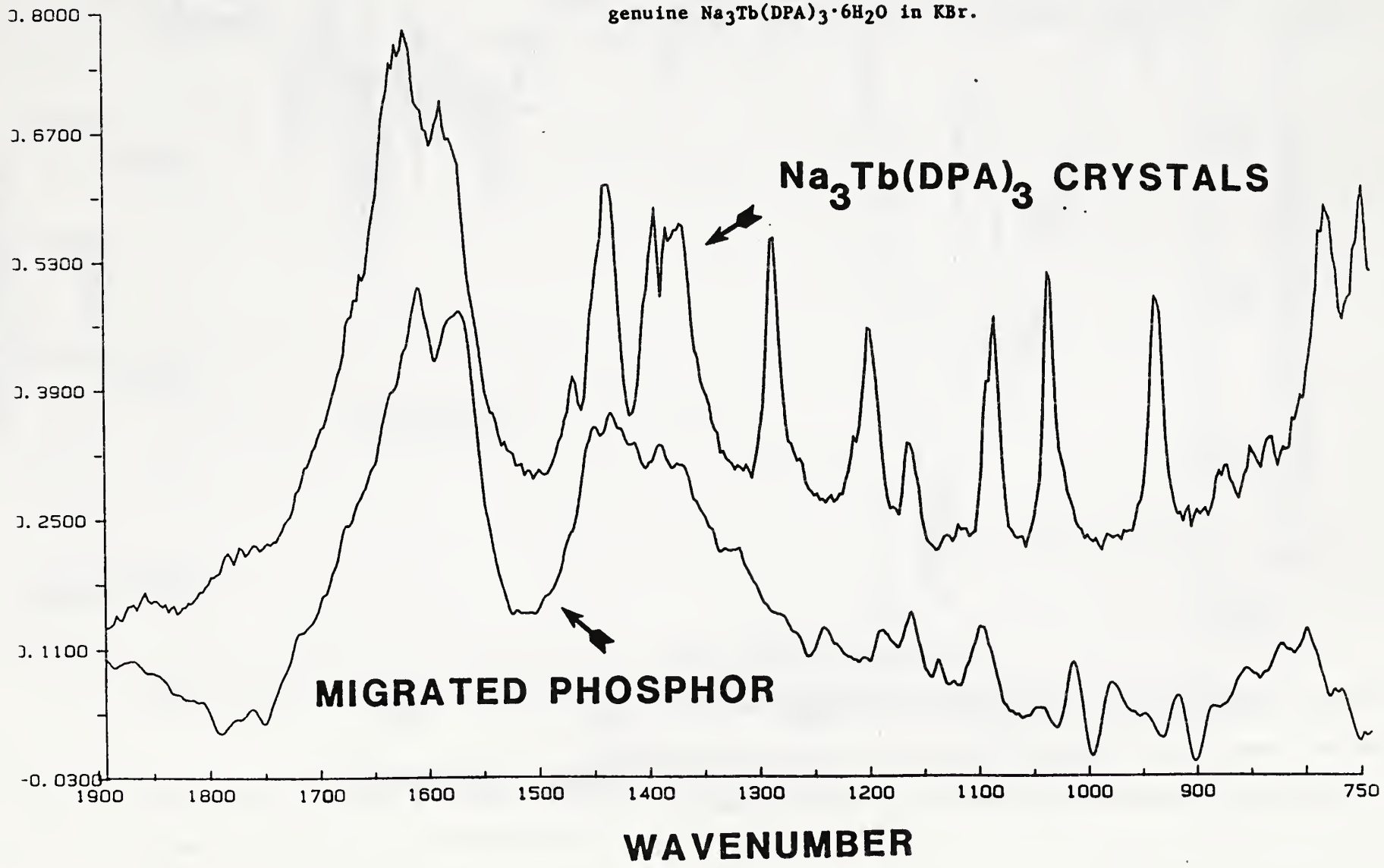

FIGURE 39

Attenuated total reflectance (ATR) FTIR spectrum of the non-exposed side of an unfilled paper floated for 16 hrs on an aqueous solution of $Na_3Tb(DPA)_3 \cdot 6H_2O$. (*) = strong carbonyl stretches due to migrated $Na_3Tb(DPA)_3$.

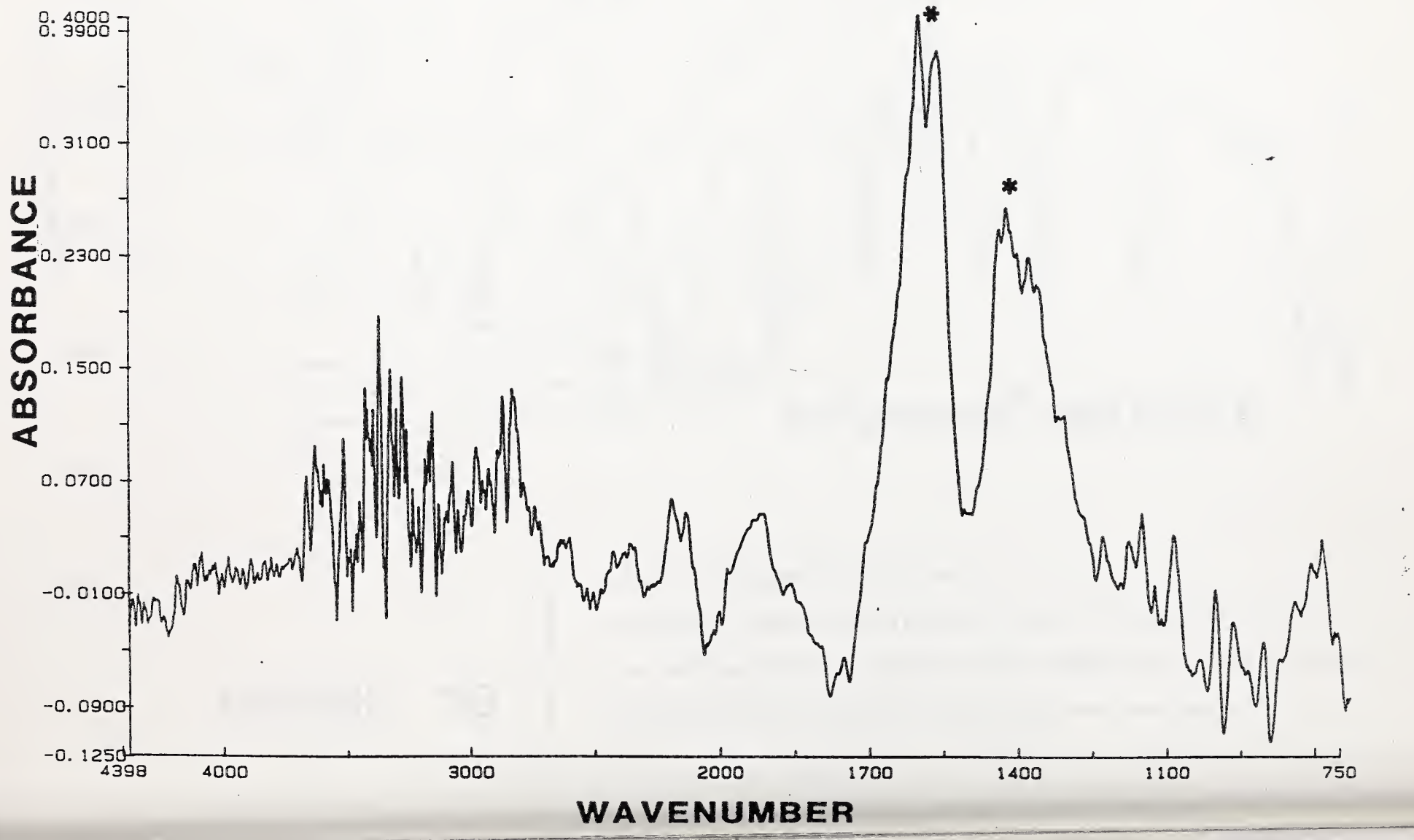

FIGURE 40

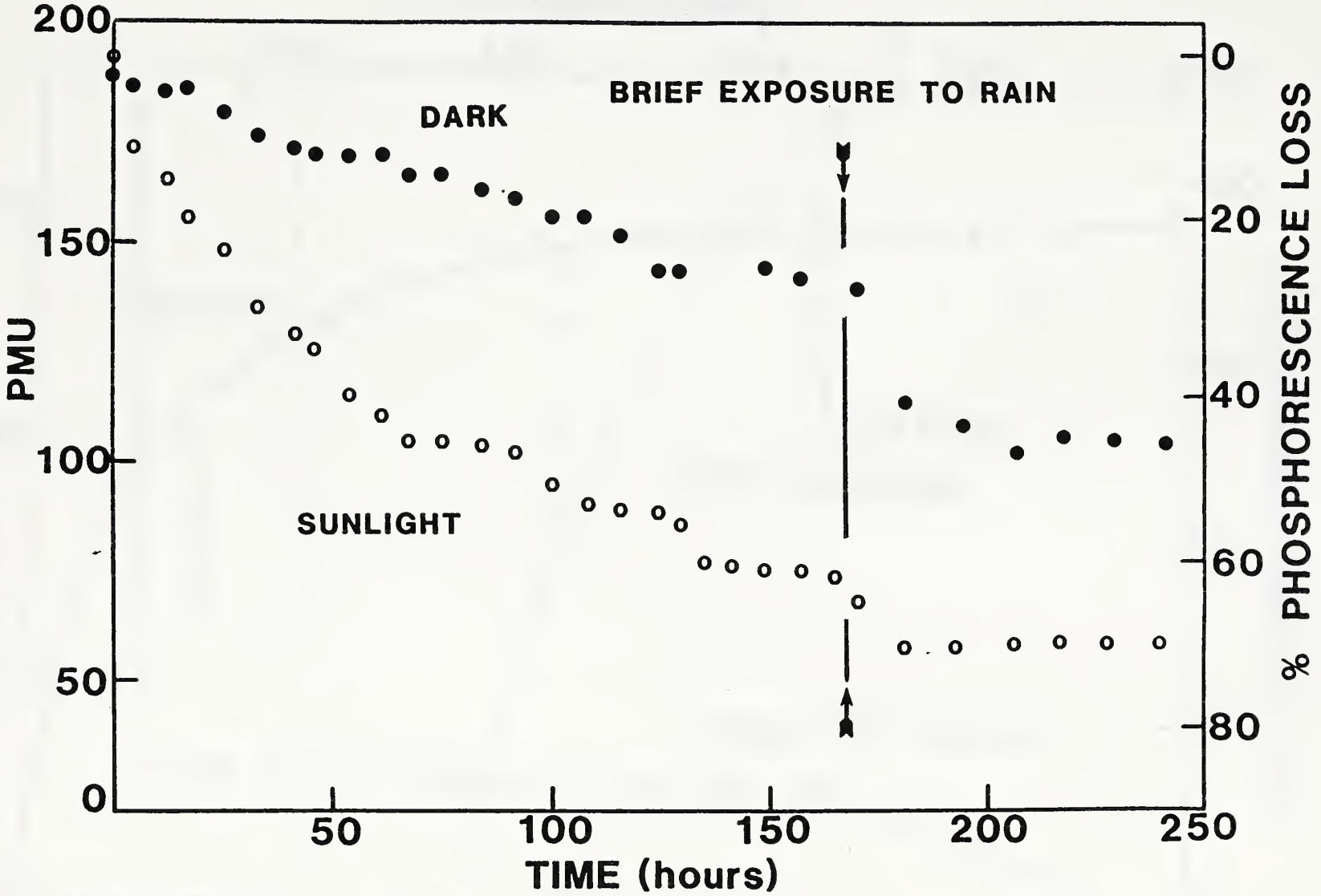

Phosphorescence and % phosphorescence loss vs time for outdoor exposure of Harrison and Sons uninked Tb paper (0.02% Tb).

Open circles = samples exposed to direct sunlight on NBS grounds in

Closed circles = samples outdoors but in the dark for the same time period.

FIGURE 41

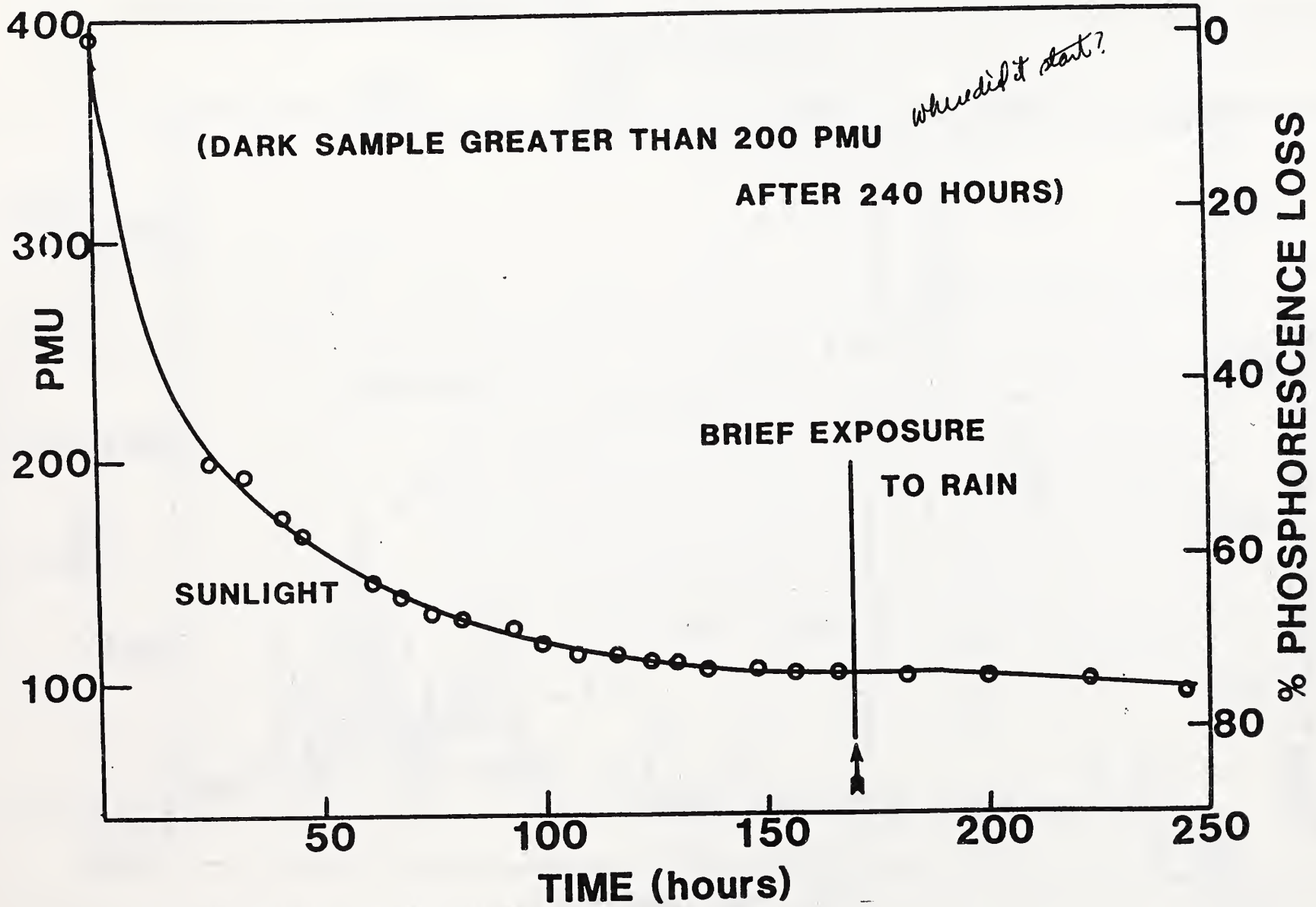

Phosphorescence and % phosphorescence loss vs time for outdoor exposure of Harrison and Sons uninked $ZnSiO_4$·Mn paper (4%).

Exposure to direct sunlight on NBS grounds in April-May, 1986.

FIGURE 42

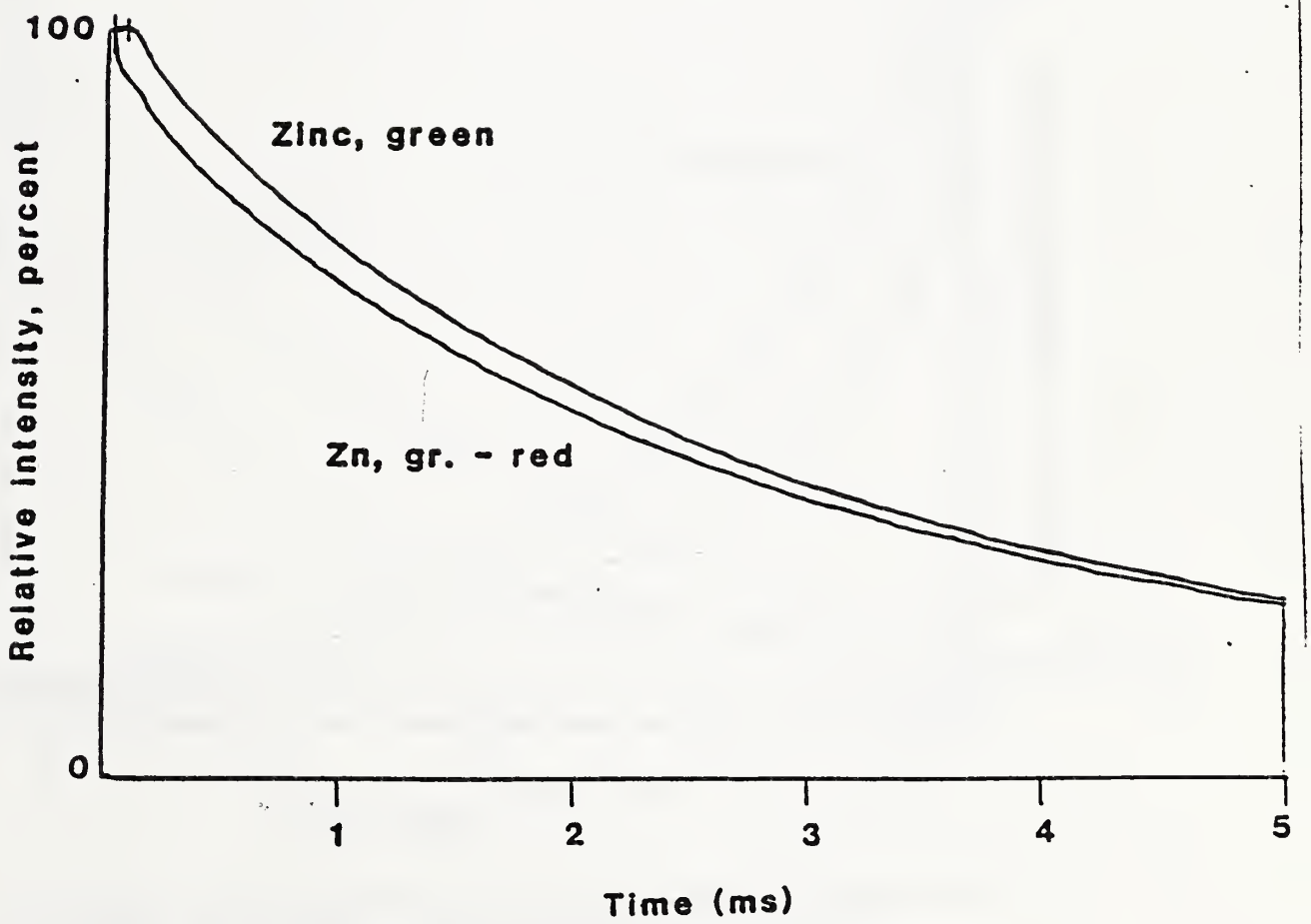

Phosphorescence decay curves for solid $ZnSiO_4 \cdot Mn$.

FIGURE 43

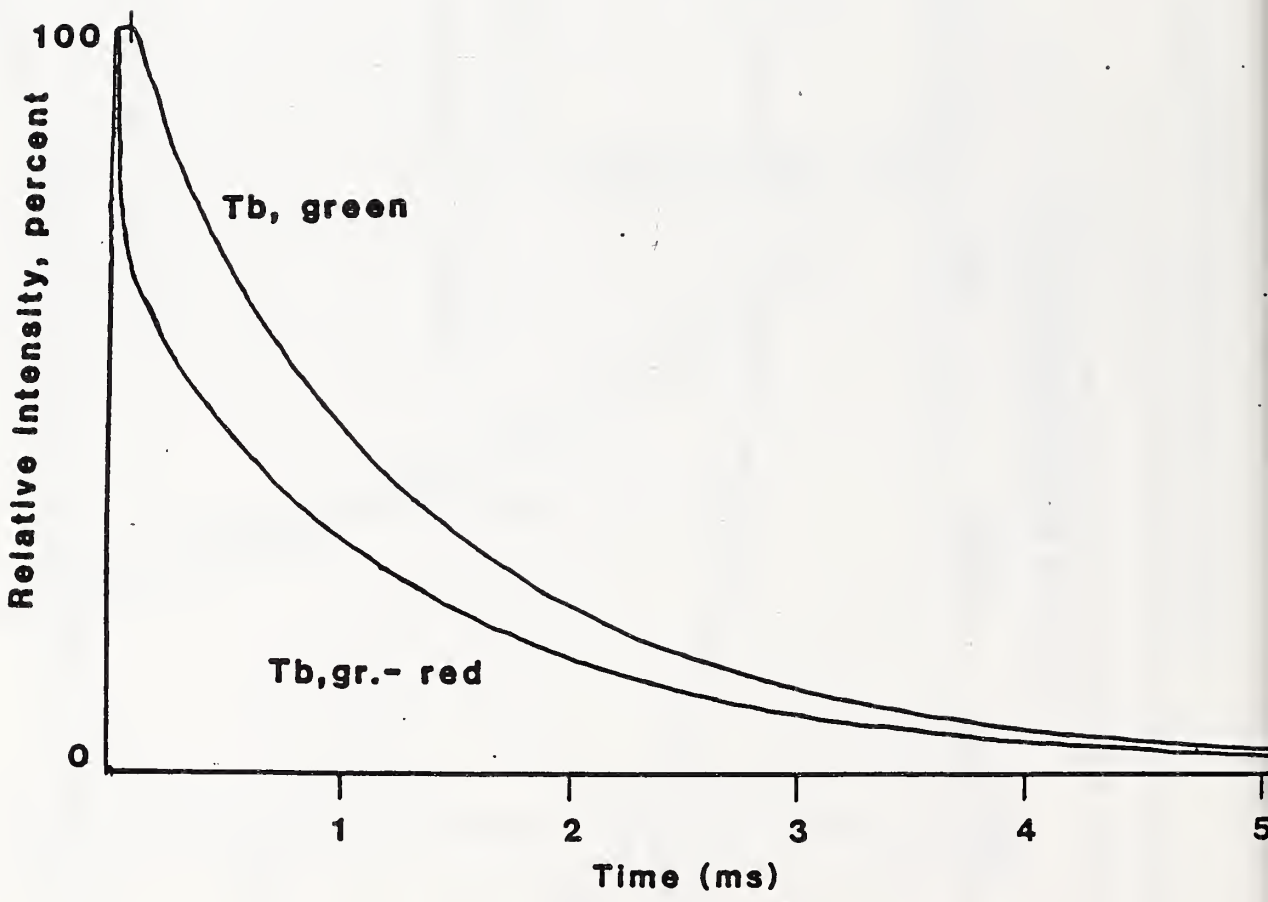

Phosphorescence decay curves for "Tb(DPA)(THF)" complex on unfilled paper.

FIGURE 44

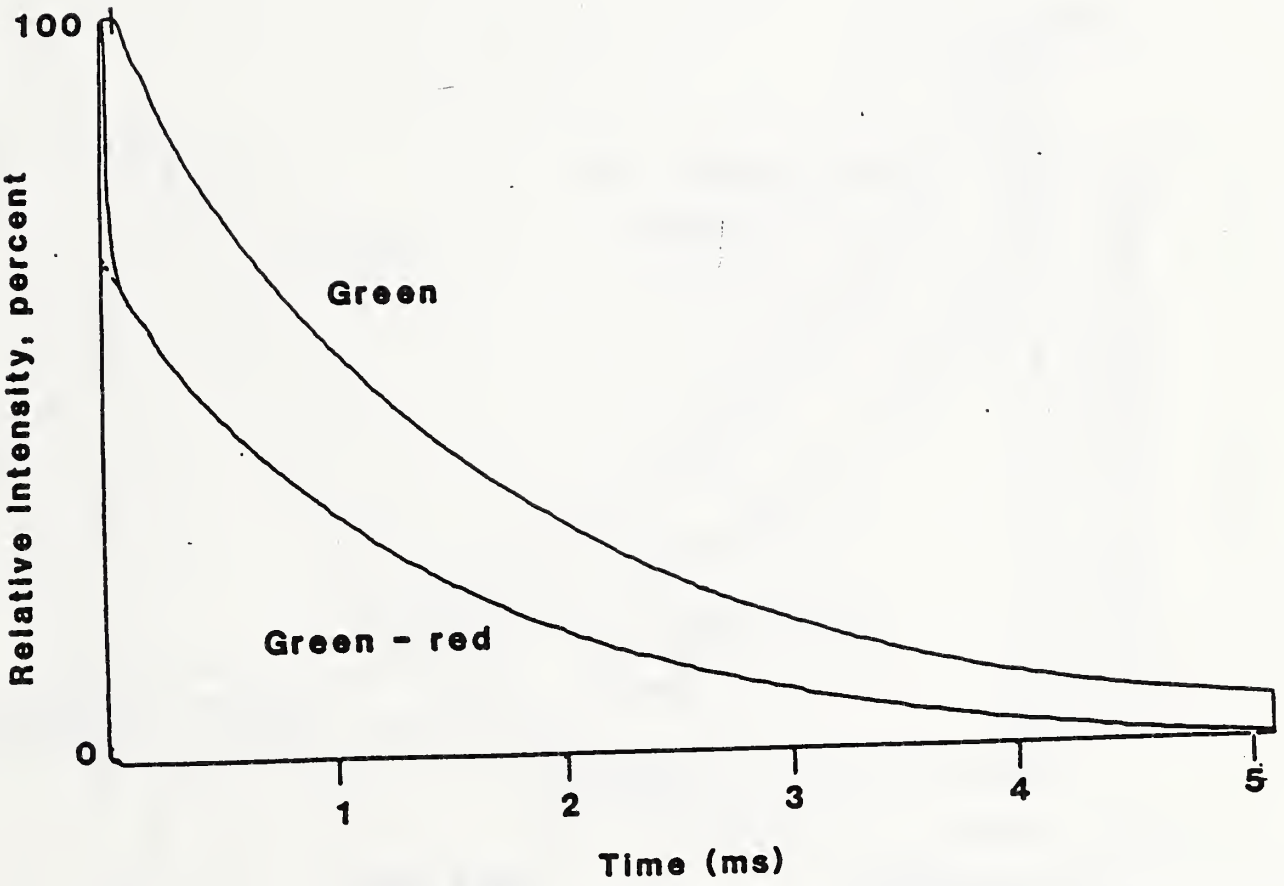

Phosphorescence decay curves for $Na_3Tb(DPA)_3 \cdot 6H_2O$ in varnish TG-2407-RV on unfilled paper.

FIGURE 45

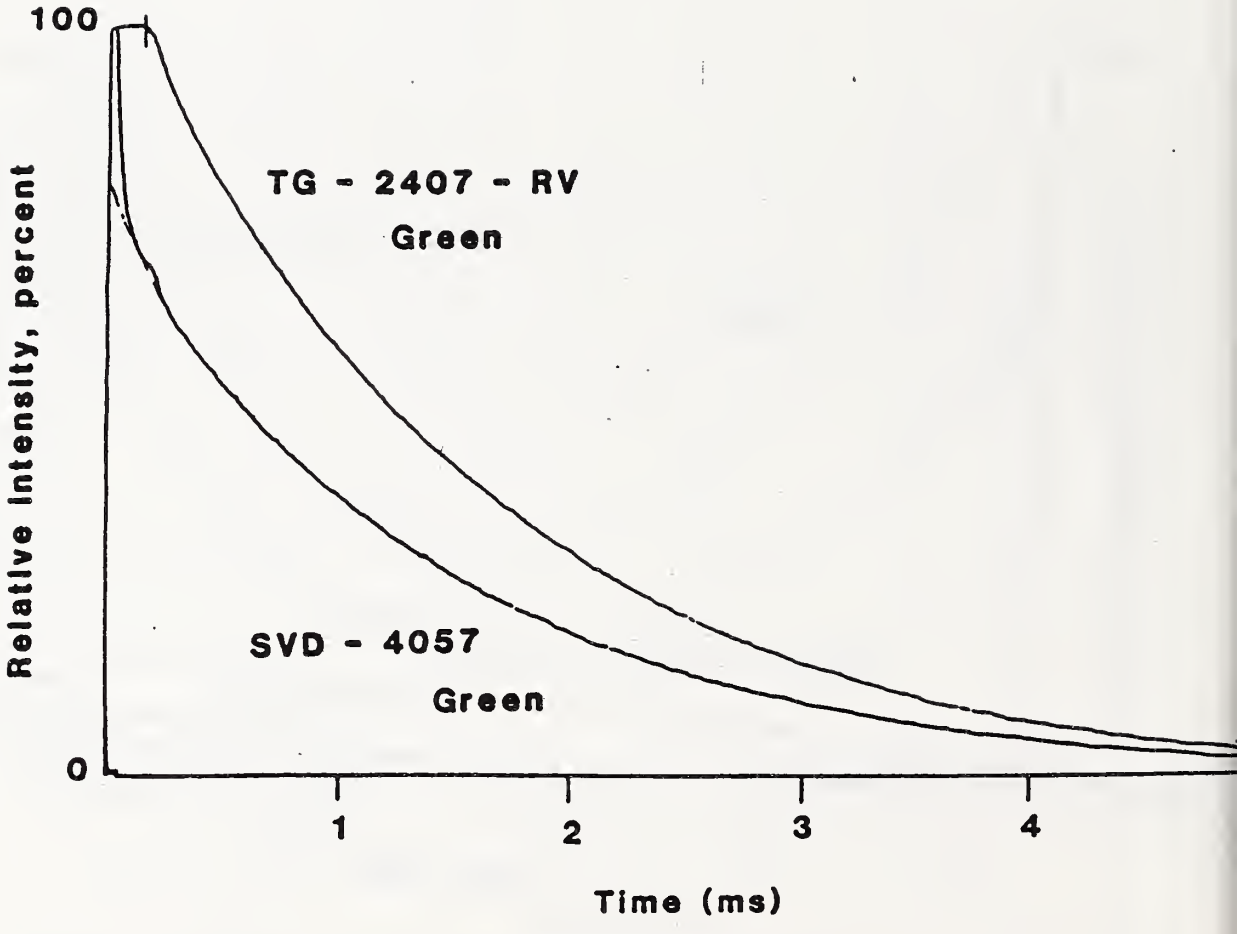

Comparative phosphorescence decay curves for $Na_3Tb(DPA)_3 \cdot 6H_2O$ in varnishes TG-2407-RV and SVD-4057 on unfilled papers.

FIGURE 46

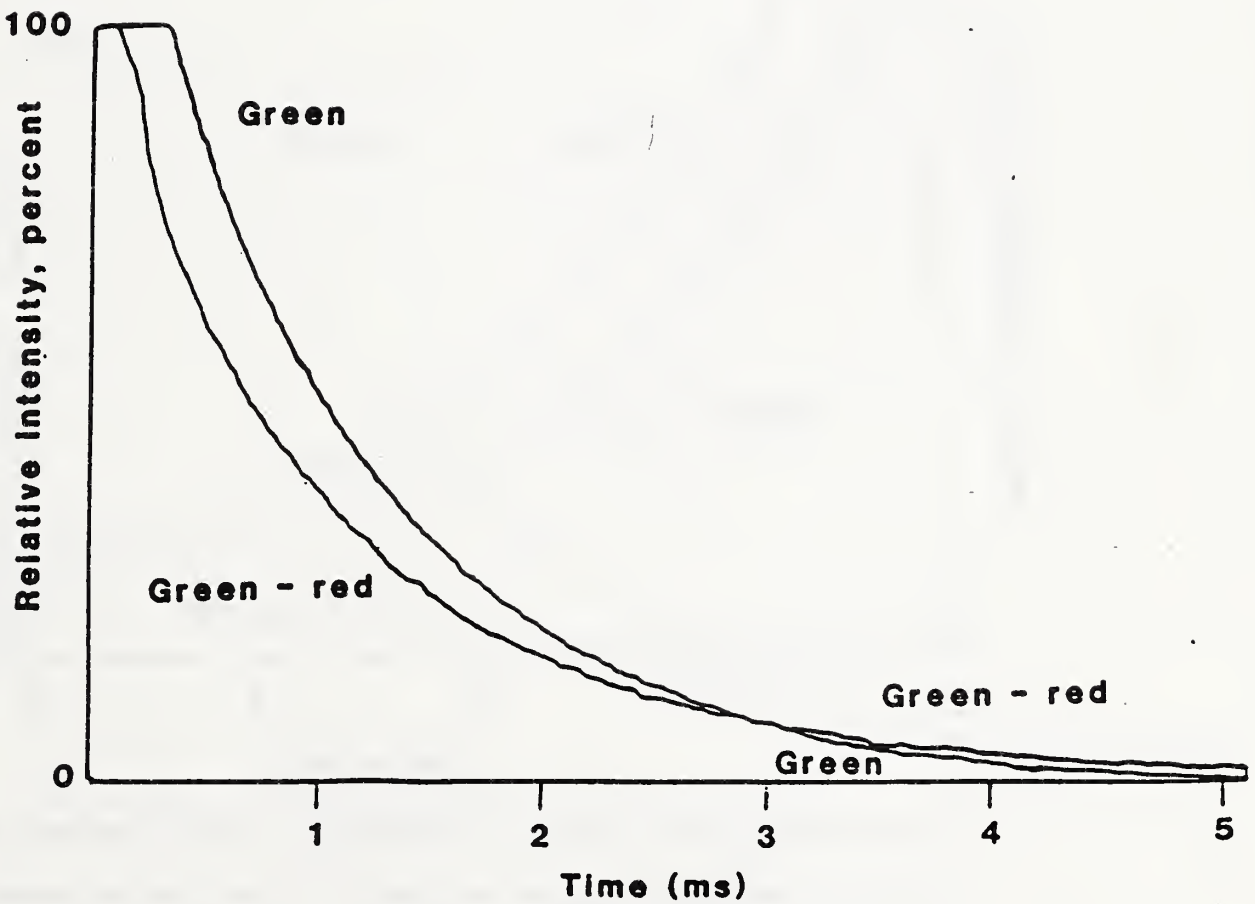

Phosphorescence decay curves for $Tb(acac)_3$ in varnish TG-2407-RV on unfilled paper after 6 months of aging in a south facing window.

FIGURE 47

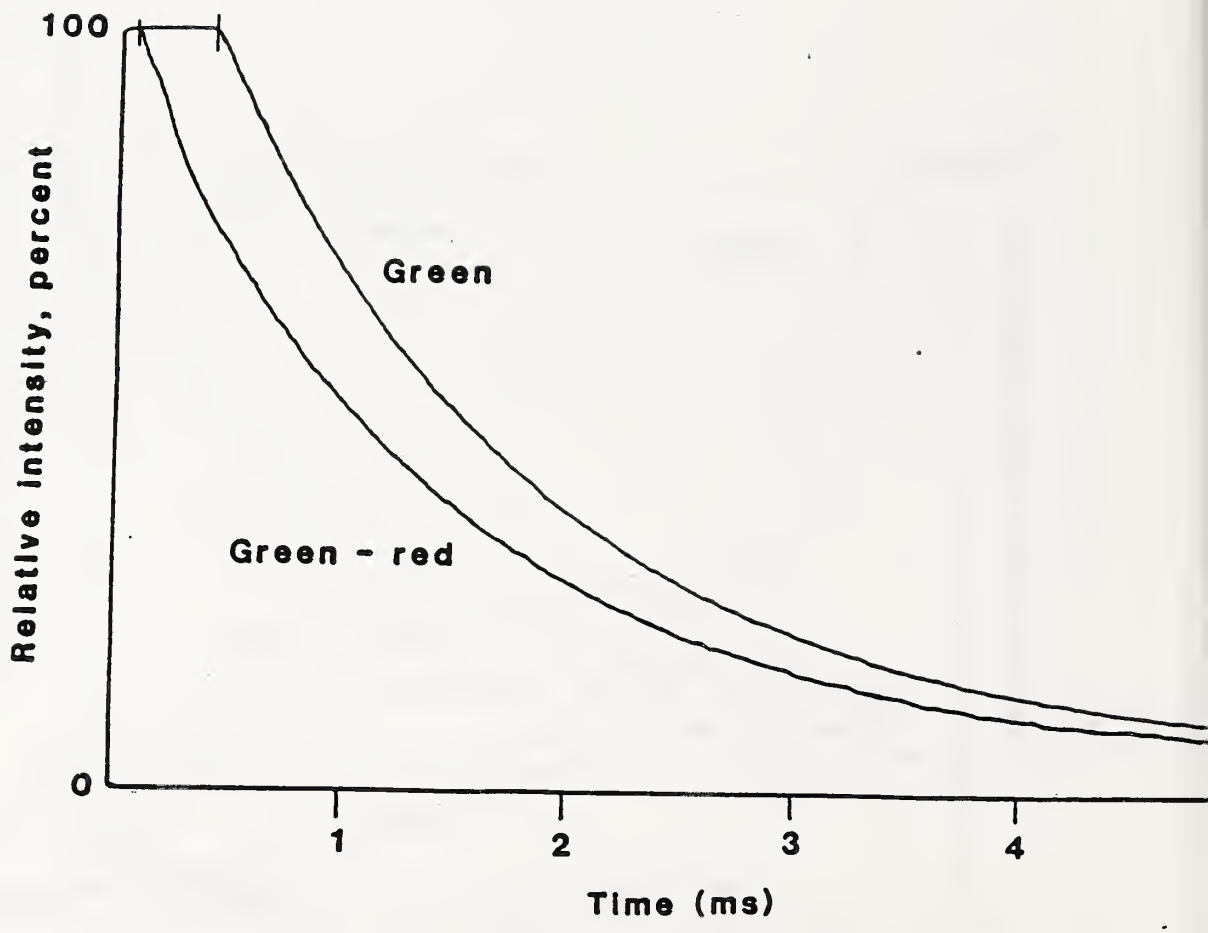

Phosphorescence decay curves for $Tb(acac)_3$ in varnish TG-20-T on unfilled paper after 6 months of aging in a south facing window.

FIGURE 48

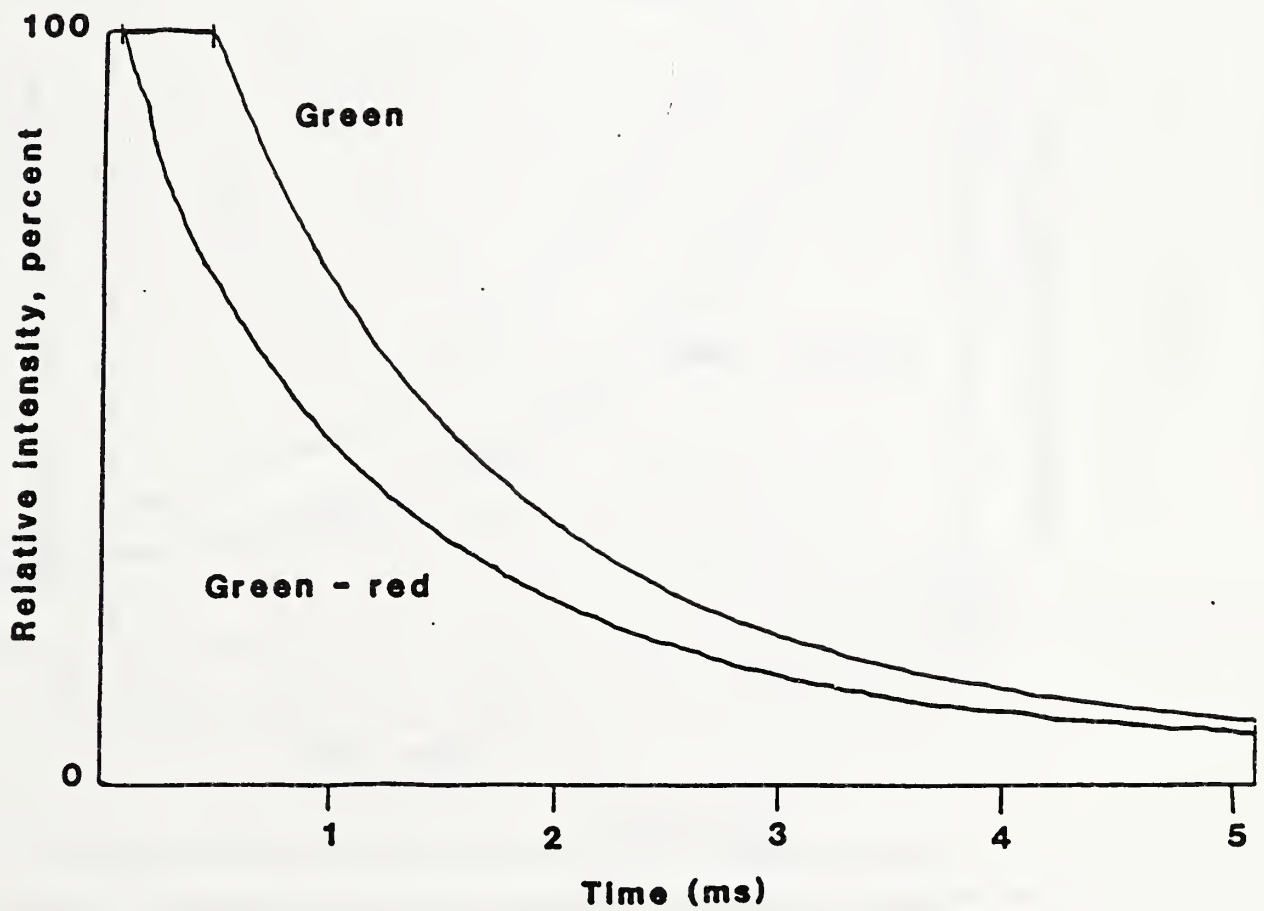

Phosphorescence decay curves for $Na_3Tb(DPA)_3 \cdot 6H_2O$ in varnish TG-2407-RV on unfilled paper after 6 months of aging in a south facing window.

FIGURE 49

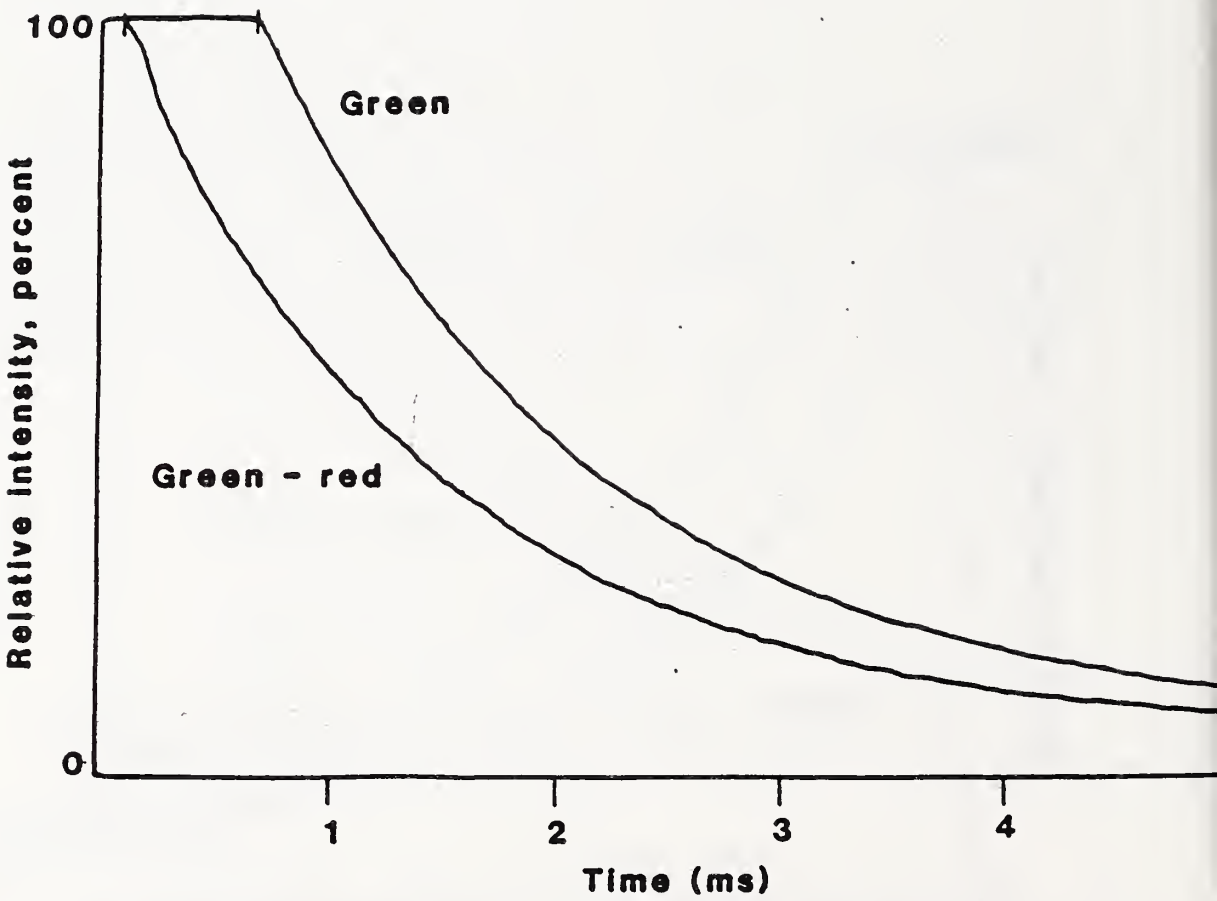

Phosphorescence decay curves for $Na_3Tb(DPA)_3 \cdot 6H_2O$ applied in aqueous solution to unfilled paper after 3 months of aging in a south facing window.

FIGURE 50

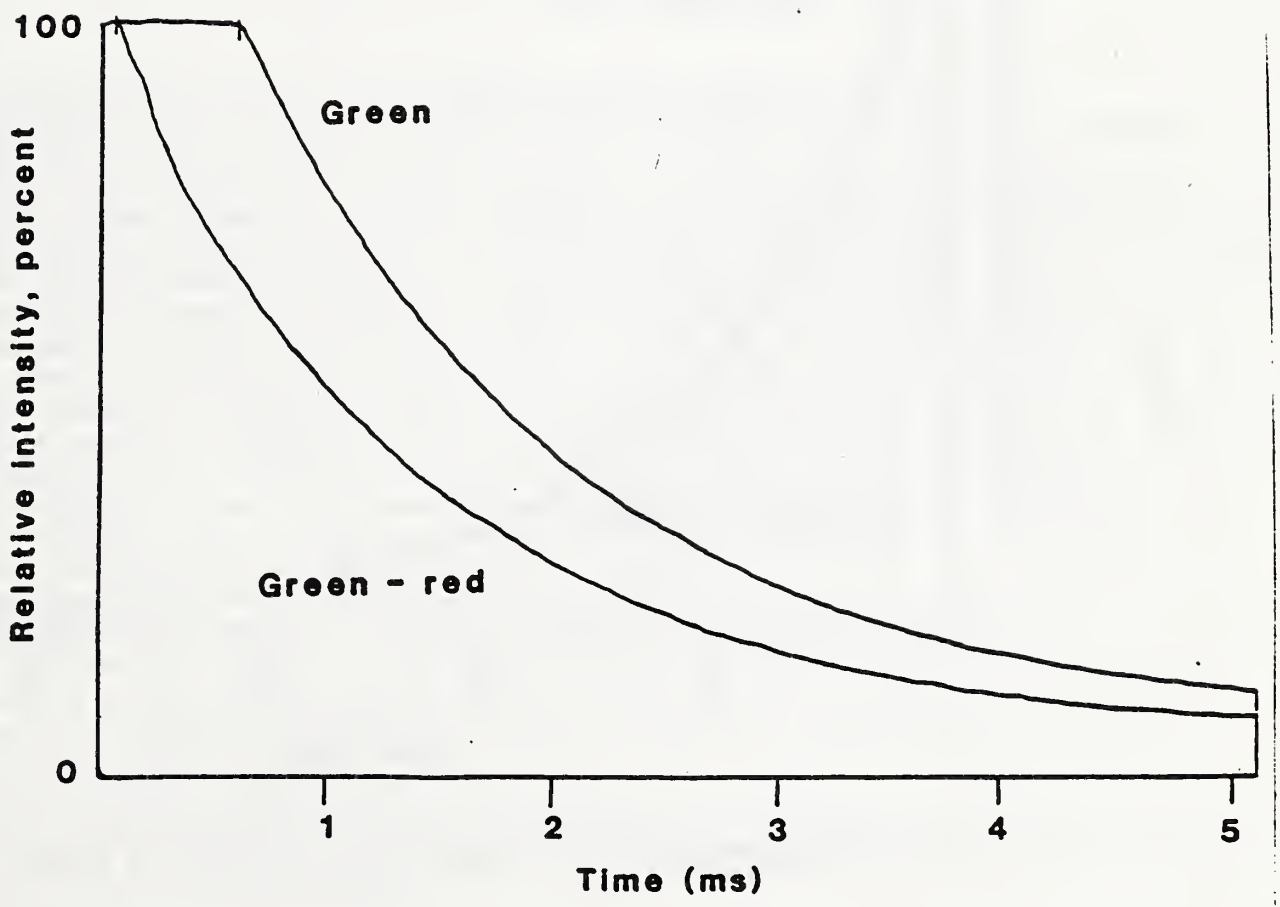

Phosphorescence decay curves for $Na_3Tb(DPA)_3 \cdot 6H_2O$ applied in aqueous solution to unfilled paper after 3 months indoors in the dark.

FIGURE 51

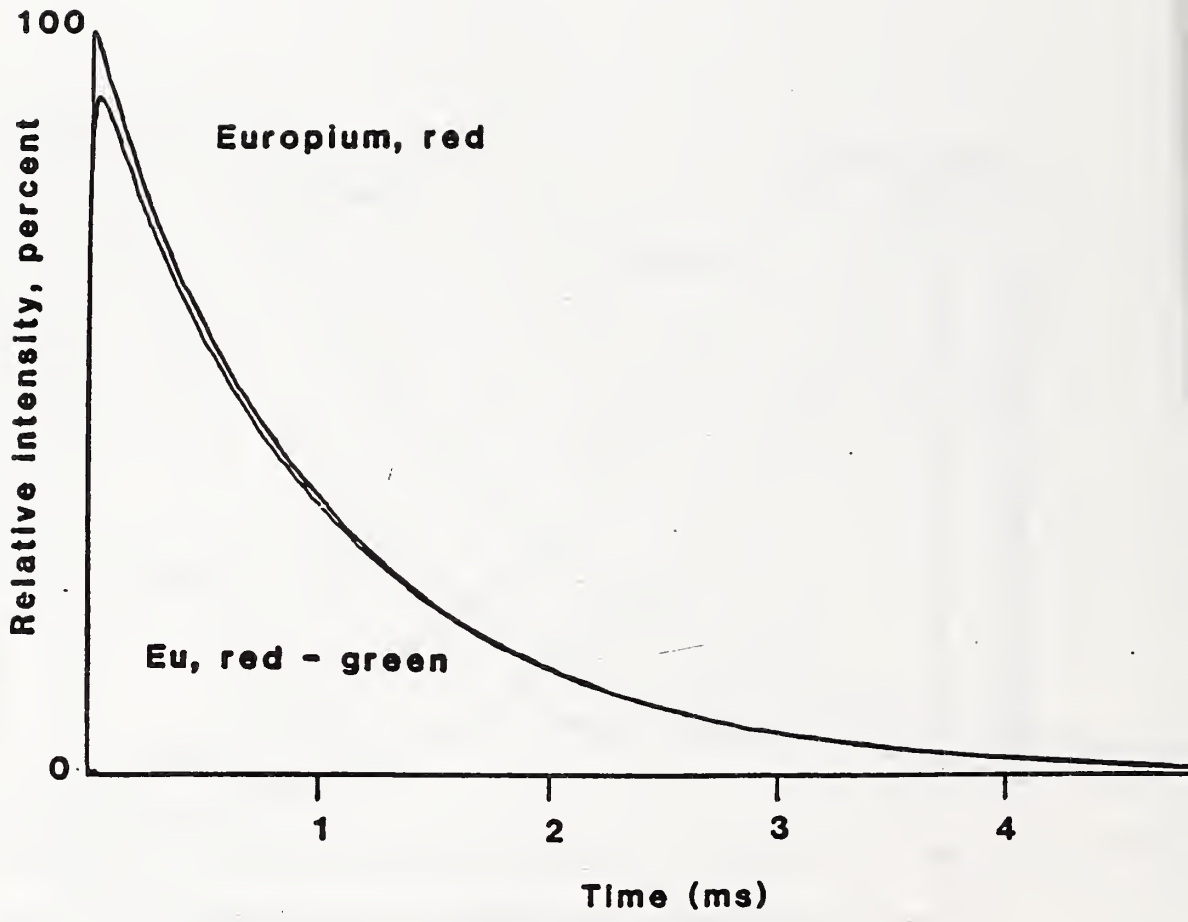

Phosphorescence decay curves for Eu_2O_3 solid on a ceramic plate.

NBS-114A (REV. 2-80)

U.S. DEPT. OF COMM. BIBLIOGRAPHIC DATA SHEET (See instructions)	1. PUBLICATION OR REPORT NO. NBSIR 87-3533	2. Performing Organ. Report No.	3. Publication Date JUNE 1987

4. TITLE AND SUBTITLE

Environmental Factors and Mechanisms Controlling Degradation of Terbium(III) Chelates; Development of Effective New Phosphors for Postage Stamp Use

5. AUTHOR(S)

E. J. Parks, R. A. Faltynek, and F. E. Brinckman

6. PERFORMING ORGANIZATION (If joint or other than NBS, see instructions)

NATIONAL BUREAU OF STANDARDS
DEPARTMENT OF COMMERCE
WASHINGTON, D.C. 20234

7. Contract/Grant No.

8. Type of Report & Period Covered

FINAL: Sept. 83-Dec. 86

9. SPONSORING ORGANIZATION NAME AND COMPLETE ADDRESS (Street, City, State, ZIP)

Research and Development Laboratories
U.S. Postal Service
11711 Parklawn Drive
Rockville, MD 20852

10. SUPPLEMENTARY NOTES

☐ Document describes a computer program; SF-185, FIPS Software Summary, is attached.

11. ABSTRACT (A 200-word or less factual summary of most significant information. If document includes a significant bibliography or literature survey, mention it here)

This final report details the evaluation of terbium coordination complexes as candidate stamp taggants to replace inorganic zincate complexes for the USPS high speed automated mail handling system. Zincate complexes are immiscible with carrier varnishes and are easily removed by abrasion. Terbium complexes are miscible in the same media. A chromogenic, hydrophobic ligand sheath is required to enhance the luminescence of terbium and to exclude water, which, bonded to the inner coordination sphere of the metal promotes radiationless deexcitation. The dianion of 2,6-dipicolinic acid (DPA) provides superior sensitization and sheathing of terbium centers to deliver a complex of high emission quantum yield that is coordinatively saturated and resistant toward quenching by water. Analysis by spectroscopic techniques shows the complex to be $Na_3Tb(DPA)_3 \cdot 6H_2O$. Neat or in varnish, the complex maintains its phosphorescence for months at high relative humidity. Carriers must be transparent to excitation and emission wavelengths, a failure of certain varnishes in current use. By weight, the terbium complex is 300 to 1500 times as bright as the best zincate phosphor. The complex applied varnish-free in water yields high initial brightness that fades under 90 to 100% relative humidity, due to migration into stamp paper. Future studies are recommended to render the complex or paper surface more hydrophobic. Phosphor excitation at 254 nm may be non-optimal, since the uncorrected excitation spectrum has a maximum at longer wavelengths.

12. KEY WORDS (Six to twelve entries; alphabetical order; capitalize only proper names; and separate key words by semicolons)

Analysis; epifluorescence microscopy; FTIR; humid air; luminescence; terbium coordination complex; microbore chromatography; molecular design; stamp phosphor; stability; synthesis; x-ray crystallography

13. AVAILABILITY

☐ Unlimited

☒ For Official Distribution. Do Not Release to NTIS

☐ Order From Superintendent of Documents, U.S. Government Printing Office, Washington, D.C. 20402.

☐ Order From National Technical Information Service (NTIS), Springfield, VA. 22161

14. NO. OF PRINTED PAGES

168

15. Price